An-Najah National University

Faculty of Graduate Studies

Extraction of Drugs Residuals from Aqueous Solution Using Three Types of Adsorbents

By

Yasmin Akram Khalid Thaher

Supervisor

Prof. Shehdeh Jodeh

Co-supervisor

Dr. Othman Hamed

This Thesis is Submitted in Partial Fulfillment of the Requirements for the Degree of Master of Chemistry, Faculty of Graduate Studies, An-Najah National University, Nablus, Palestine.

2018

Extraction of Drugs Residuals from Aqueous Solution Using Three Types of Adsorbents

By

Yasmin Akram Khalid Thaher

This Thesis was defended successfully on / /2018, and approved by:

Defense Committee Members	**Signature**
Prof. Shehdeh Jodeh/Supervisor	.....
Dr. Othman Hamed/Co-supervisor	.....
Prof. Ziad Abdeen /External Examiner	.....
Dr. Ibrahim Abu Shuqier / Internal Examiner	.....

Dedication

To my dear parents for being there for me and encouraging me at the toughest times, thank you for your endless support. To my great family. To dear Abed-alrahman Ganem whose encouragement make me able to get success. To my friends and teachers with all of love and respects to them.

Acknowledgments

Praise be to Allah, the lord of the worlds and peace and blessings of Allah be upon the noblest of the Prophets and Messengers, our Prophet Mohammad.

Foremost, I would like to express my sincere gratitude to my advisor Prof. Shehdeh Jodeh and Dr. Othman Hamed for their professional advice, guidance, and continued support throughout this project.

I would like to thank all the technicians and staff of the chemistry department at An-Najah National University, especially Mr. Nafiz Dweikat for his help.

Also warm thanks to all friends in the master program for the great and lovely time that we spent together.

Many thanks to Dr. Ziad Abdeen, Dr. Subhi Samhan and to the Ministry of Foreign Affairs, The Netherlands, North Africa and Middle East Department (DAM), The Hague, The Netherlands (NVHU 2016 01) for their financial support for this research

Last but not the least, I would like to thank my family: my parents Akram and Intisar Thaher, for giving birth to me at the first place and supporting me spiritually and financially throughout my life.

الإقرار

أنا الموقع أدناه مقدم الرسالة التي تحمل العنوان:

Extraction of Drugs Residuals from Aqueous Solution Using Three Types of Adsorbents

أقر بأن ما اشتملت عليه هذه الرسالة إنما هي نتاج جهدي الخاص، باستثناء ما تمت الإشارة إليه حيثما ورد، وأن هذه الرسالة ككل، أو أي جزء منها لم يُقدم لنيل أية درجة أو لقب علمي أو بحثي لدى أي مؤسسة تعليمية أو بحثية أخرى.

Declaration

The work provided in this thesis, unless otherwise referenced, is the researcher's own work, and has not been submitted elsewhere for any other degree or qualification.

Student's name: **اسم الطالب:**

Signature: **التوقيع:**

Date: **التاريخ:**

Table of contents

List of Tables

List of Figures

List of Abbreviations

Symbol	Abbreviation
IBP	Ibuprofen
C_e	The equilibrium concentration of the adsorbate (mg/L).
C_o	The initial concentration of the adsorbate (mg/L).
q_e	The amount of adsorbate per unit mass of adsorbent (mg/g).
K_L	Langmuir isotherm constant (L/mg).
Q_o	maximum monolayer coverage capacity at equilibrium (mg/g).
V	The volume of the solution (L).
M	The mass of the adsorbent (g).
R_L	Dimensionless constant separation factor
K_F	The Freundlich constant related to adsorption capacity (mg/g).
N	The heterogeneity coefficient that gives an indication of how favorable the adsorption process (g/L).
q_t	The mass of adsorbate per unit mass of adsorbent at time t (mg/g).
K_1	The rate constant of pseudo first-order adsorption model ($mg.g^{-1}.min^{-1}$).
K_2	The equilibrium rate constant of pseudo second-order adsorption model ($g.mg^{-1}.min^{-1}$).
K_{id}	The Intra-Particle diffusion rate constant ($mg/g.min^{1/2}$).
Z	Constant that gives an information about the thickness of the boundary layer (mg/g).
ΔG°	Standard Gibbs free energy change (J).
ΔH°	Standard Enthalpy change (J).
ΔS°	Standard Entropy change (J/K).
T	The absolute temperature (K).
R	The universal gas constant ($8.314\ J.mol^{-1}.K^{-1}$).
K_d	The thermodynamic equilibrium constant (L/g).
Cs	Cellulose
NCS	Nanocellulose
MNCs	Magnetic Nanocellulose
AgNCs	Silver Nanocellulose
CNF	Cellulose nanofibrils
CNC	Cellulose nanocrystals
CNFs	Cellulose nanofibers
CRG	Carrageenan

K-CRG	Kappa Carrageenan
CRG/NCs	Carrageenan composites with Nanocellulose
CD	Cyclodextrin
β-CD	Betacyclodextrin
Ac β-CD/NCs	Acetyl betacyclodextrin composites with nanocellulose
Bz β-CD/NCs	Benzoyl betacyclodextrin composites with nanocellulose
MB	methylene blue dye
SEM	Scanning Electron Microscopy
NSAID	Non Steroidal Anti-Inflammatory drugs
LC-MS/MS	Liquid Chromatography tandem mass
NMR	Nuclear Magnetic Resonance
XRD	X-Ray Diffraction
FTIR	Fourier Transform Infrared
HPLC	High Performance Liquid Chromatography
PAD	Photodiode Array Detector
APMP	Alkaline peroxide mechanical pump
AgNPs	Silver Nanoparticles
CNCs	Cellulose nanocrystals
MFC	Microfibrillated cellulose
FeNP	Iron nanoparticles
AC	Activated Carbon
SPE	Solid Phase Extraction
ppm	Part per million
AAS	Atomic Absorption Spectroscopy
TGA	Thermal Gravimetric Analysis
UV	Ultra-Violet

Extraction of Drugs Residuals from Aqueous Solution Using Three Types of Adsorbents

By
Yasmin Akram Khalid Thaher
Supervisor
Prof. Shehdeh Jodeh
Co- Supervisor
Dr. Othman Hamed

Abstract

Large number of emergent pollutants from pharmaceutical industries leach every day to soil and ground waters without treatment. This will lead to different health problems to both human beings and living organisms. The major problem is try to remove this pollutant like Ibuprofen (IBP) using adsorption.

Many treatment options were inspected for extract or remove the pharmaceuticals, include both conventional (e.g., biodegradation, adsorption, activated sludge) and advanced (e.g., membrane, microfiltration, ozonation) processes [1] .

In our study we prepared three types of adsorbents to extract the emergent drug (Ibuprofen) from aqueous solution, the first type is cellulose derivatives (Cellulose Nanocrystalline (CNC), Magnetic Cellulose Nanocrystalline (MNCs), and Silver Cellulose Nanocrystalline(AgNCs)). The cellulose was converted to CNC, and then it was converted to MNCs and AgNCs. The second adsorbents are Carrageenan (CRG) material compared with CRG composites with CNC. Final adsorbents were prepared using beta-cyclodextrin (β-CD), it was converted to Acetyl β-CD and Benzoyl β-CD. These two prepared adsorbents were then composites with CNC. The

Cellulose Nanocrystalline, Acetyl β-CD and Benzoyl β-CD were analyzed by using IR. That was the first objective of my work.

A second one was adsorption of the Ibuprofen from aqueous solution, using these prepared materials as an adsorbent. However, the NCs, AgNCs, CRG/NCs Benzoyl β-CD/NCs showed excellent extraction efficiency toward IBP relative to MNCs and CRG, but the Acetyl β-CD/NCs showed good efficiency. Five variables were monitored and evaluated during the extraction process: time, pH, temperature, dosage, and IBP concentrations. The adsorption thermodynamics of the adsorbents were evaluated, all of them followed Langmuir isotherm model and pseudo second order. The negative ΔG° values indicate that the adsorption is favorable and spontaneous at different temperatures. The positive values of ΔH° reflect an endothermic adsorption and that the adsorption is favored at high temperature. While ΔS^0 values were positive indicating the disorder at the solid/solution interface increased during adsorption process.

Chapter One

1.1 Introduction and Background

Water pollution considered as one of the global environmental challenges in the 21st century due to discharges of toxic substances from anthropogenic activities. Many new chemicals and their byproduct were detected in waste water all over the world [2].

Toxic water pollution affects more than 200 million people worldwide, according to Pure Earth organization (a non-profit environmental organization). In some of the world's worst polluted places, babies are born with birth defects, children have lost 30 to 40 IQ points, and life expectancy may be as low as 45 years because of cancers and other diseases [3].

In the last three decades the influence of the chemical pollution has almost exclusively on the conventional pollutants. However, the grow of uses of pharmaceuticals worldwide, called emerging contaminants, has become a huge environmental problem [4].

Pharmaceuticals emerging contaminants have high presence in environment, and they are known to give side effects on the human and other living organisms [5].

The exposure to pharmaceutical residues is inevitable, they are present in all ecosystems, particularly Non Steroidal Anti-Inflammatory Drugs (NSAID) and their mixtures. In fact, the impact studies of these compounds on microorganisms are infrequent such as IBP [6]

The IBP used for relief of symptoms of arthritis, primary dysmenorrheal, and fever and as an analgesic. Ibuprofen is known to have blood-thinning effect [7]. The removing of IBP from water is an important issue to process in all analysis research and the development of effective technologies for removal. The biological treatment such as activated sludge and biological filters are unable to remove this emerging contaminants completely, so most of these contaminants remains soluble like IBP [8-10].

Adsorption has become a popular and widely used technique for the removal of different pollutants.

Of the more common adsorbents, activated carbon continues to be the most widely used adsorbent for the purification of water with low pollutant concentration [11].

19 drugs were Investigated using LC-MS in Almadinah Almunawarah, Saudi Arabia in municipal wastewater before and after treatment [12].

Highly sensitive and selective analysis technique used for quantified different pharmaceutical (such as Ibuprofen, paracetamol, etc.) compounds in sewage effluents and surface waters using LC-MS/MS technique, after simultaneous extraction and pre-concentration has developed [13].

1.2 Adsorption and Adsorbent

To the best of our knowledge, that the use of the natural cellulose from cotton for adsorption based on many derivatives such as (Nanocellulose, Magnetic nanocellulose, Silver nanocellulose) and other different materials such as (Carrageenan, Acetyl beta-cyclodextrin, Benzoyl beta-cyclodextrin)

composites with NCs as an adsorbent toward removal of Ibuprofen (IBP) have not been investigated yet.

Adsorption is a potential method for the removal of pharmaceuticals and personal care products, considering the mild operation conditions [14], in contrast to the other methods which have the disadvantages of high energy consumption and the formation of residual byproducts such as Ozonation [15-16].

The surface accumulation of adsorbate on adsorbent is called adsorption. Adsorbate may be liquid, gas, or dissolved solids. While adsorbent may be a solid or a liquid material [17].

Various modification methods have been used and discussed to prepare modified cellulose-based adsorbents for their subsequent application in water treatment [18].

Pill Won Seo studied the adsorption of typical pharmaceuticals and personal care products such as naproxen, ibuprofen and oxybenzone from aqueous solutions, by using the highly porous metal organic framework with and without functionalization [14].

1.3 Cellulose as natural adsorbents (Cs), cellulose Nanocrystalline (CNC), magnetic nanocellulose(MNCs) and silver nanocellulose (AgNCs):

In this study, cotton as natural cellulose (Cs) was used for making nanocellulose (NCs) and magnetic nanocellulose (MNCs) and silver nanocellulose (AgNCs), and composite of nanocellulose with other

materials. These materials were used for the removal of Ibuprofen (IBP) from wastewater treatment plants.

When discuss about the cellulose-based adsorption materials you always talk about the “Lowest cost and environmentally friendly” materials.

Cellulose is the most abundant biopolymer resource in the world. It is widely recognized as a renewable and biodegradable raw material with applicable advantages and properties. Cellulose consisted of β-1,4-linked anhydro-D-glucose units with the formula $(C_6H_{10}O_5)_n$, in which the glucoses are 6-carbon rings linked by single oxygen between C1 and C4 . Each glucose is corkscrewed 180° to its neighbors thus two glucoses are usually taken as one unit (Figure 1). The polymerization degree on each chain more than 20,000 (dependent on the source) [19-22].

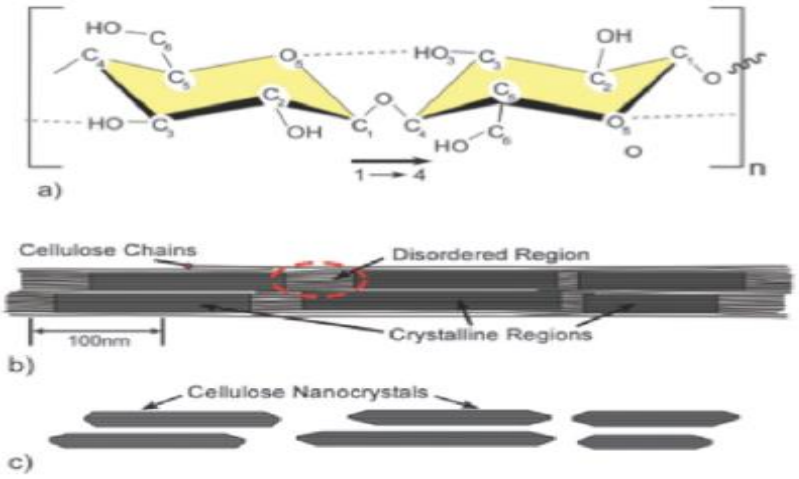

Figure 1: (a) Structure of single cellulose chain repeat unit, the direction of 1-4 linkage and intra chain hydrogen bonding are shown; (b) Schematic of cellulose microfibers with crystalline and amorphous regions; (c) Schematic of cellulose nanocrystals after amorphous regions are dissolved by acid hydrolysis [21].

The hydrogen bonds between the cellulose chains and van der Waals forces between the glucose units lead to the formation of crystalline regions in cellulose [23].

Cotton represents an excellent model system to investigate the structure of cellulose in plant. The structure of cellulose microfibrils in mature cotton fibres have been studied by multitechnique, present a I_{β}-rich crystalline structure with limited surface disorder [24].

Only a small amount of cellulose used is used to produce textile fibers, films and a larger number of cellulose derivatives, such as cellulose ethers and esters [25-28].

Large specific surface area, high specific strength and modulus, low density, reactive hydroxyl groups that can facilitate grafting chemical species to tailor the surface properties, non-toxic character, biocompatibility and biodegradable properties are some useful features of the CNCs [29-32,25].

1.3.1 Nanotechnology

Nanotechnology and applications may play an important role in resolving issues relating to water quality, due to the large surface areas and their size- and shape-dependent catalytic properties [33].

Nanotechnology is the understanding and controlling matter at dimensions about 1-100 nm may used in many novel applications.

Nanomaterials from cellulose and lignocelluloses are very important in the nanotechnology field [34]. Nanomaterials and its derivatives with various

different chemical groups increase their affinity toward a given compound, also have a high capacity and selectivity for organic, inorganic solutes, toxic metal ions and inorganic anions in aqueous solutions [33].

1.3.1.1 Cellulose Nanocrystalline (CNC)

Cellulose nanocrystals are derived from acid hydrolysis of wood fiber, plant fiber, microfibrillated cellulose, microcrystalline cellulose or nanofibrillated cellulose [35-37].

The main sources of CNC are wood, cotton, tunicate, bacterial, ramie and sisal cellulose. CNC are mostly produced from wood and cotton due to their abundant supply, high cellulose content and uniformity [38].

Nanocellulose, can also referred as crystallites, nanocrystals, whiskers, nanofibrils, and nanofibers, has been the subject of extensive research covering the isolation, characterization, and applications of various forms of cellulose, so it’s classified as in table 1.1.

Table 1.1: Classification of Nanocellulose [39]

Type of Cellulose	Microfibrillated cellulose (MFC)	Cellulose nanocrystals (CNC)	Cellulose nanofibrils (CNF)	Bacterial nanocellulose (BNC)
Synonyms	Microfibrillated cellulose nanofibrils and microfibrils nanofibrillated cellulose	Nanocrystalline cellulose, whiskers,rod like cellulose microcrystals	Nanofibrillated cellulose	Bacterial cellulose, microbial cellulose, biocellulose
Sources	Wood, sugar beet, potato tuber, hemp, flax delamination of wood pulp	Wood, cotton, hemp, flax, wheat straw,mulberry bark, ramie, Avicel, tunicin	Wood, cotton, hemp, flax, wheat straw, ramie, sugar beet, potato tuber, tunicin, algae, certain bacteria	Low-molecular-weight sugars and alcohols
Formation and size	Mechanical pressure before and/or after chemical or enzymatic treatment, diameter: 5-60 nm	Cellulose from algae and bacteria acid hydrolysis of cellulose from many sources diameter: 5-70 nm length: 100-250 nm (from plant celluloses); 100 nm to several micrometers	Isolated either through homogenization of cellulose feedstocks or directly produced by bacteria diameter: 5-100 nm length: several microns	Synthesis using bacterial diameter: 20-100 nm; different types of nanofiber networks

Cellulose nanocrystals (CNC) and cellulose nanofibrils (CNF) (see figure 2) are rod-like nanoparticles, with lengths varying between 100 and 2000 nm, and diameters ranging between 2 and 20 nm. Preparation processes usually involve acid hydrolysis using hydrochloric or sulfuric acid [40].

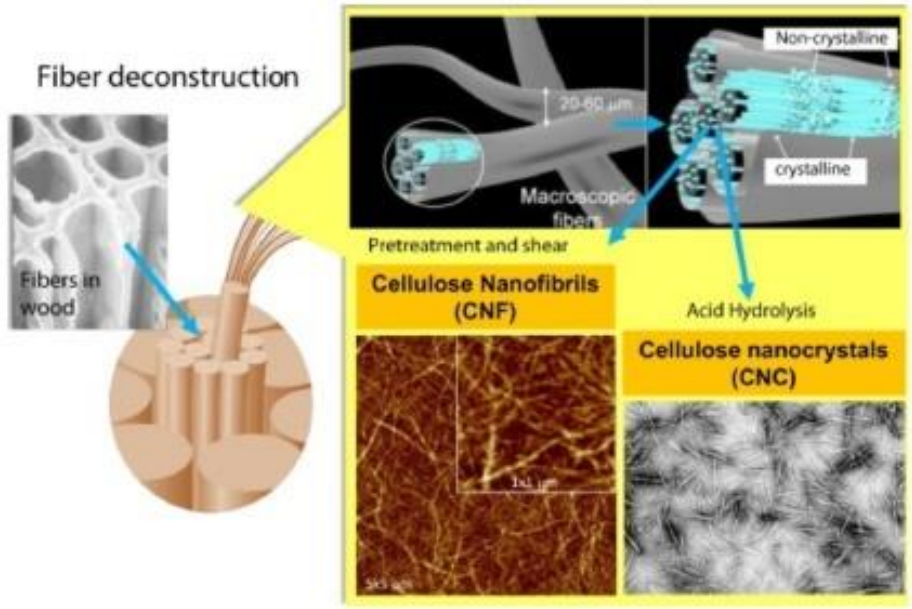

Figure 2: Schematic illustration for cellulose Nanofibrils (CNF) and Cellulose Nanocrystals (CNC) which produced from fiber cell walls by mechanical and chemical treatments [40-41].

Cellulose Nanocrystals (CNCs) and Cellulose Nanofibers (CNFs) were synthesized from absorbent cotton, characterized using FTIR, XRD, SEM, BET, and zeta potential. Surface charges of the celluloses were highly negative and the CNCs had higher negativity than CNFs [42].

CNCs have been successfully added to a wide variety of natural and synthetic polymers [43] and have been shown to modify composite properties. CNCs are a particularly attractive nanoparticle because they have low environmental, health, and safety risks, are inherently renewable, sustainable, and carbon-neutral like the sources from which they are extracted, and have the potential to be processed in industrial-scale quantities at low costs [44].

NCFs constructed as a kind of longer and entangled network with diameter of 20–90 nm from poplar Alkaline peroxide mechanical pump (APMP) by using high intensity ultrasonication [45].

Nanocellulose was extracted from cotton (Gossypiumhirsutum) linters and characterized and subjected to electronic microscopy, thermal analysis, X-ray diffractometry, light scattering, and contact angle [46].

Jindrayani studied the use of nanocellulose and its modified forms for the wastewater treatment [47].

1.3.2 Magnetic nanocomposites

A composite is a combination of two or more materials with diverse physical and chemical properties. Nanocomposite materials are composed of two phases: the continuous phase known as matrix and the dispersed phase known as reinforced materials [48,49].

A few studies have been carried out on nanocomposites applied to wastewater treatment. Mahdavian et al. investigated the ability of magnetite nanoparticles functionalized with APTES ((3-aminopropyl) triethoxysilane) and acryloyl chloride (AC) to adsorb heavy metal cations such as Cd^{2+}, Pb^{2+}; Ni^{2+} and Cu^{2+} [50].

Ozmen et al. studied the capacity of magnetite nanoparticles functionalized with APTES and glutaraldehyde (GA) to remove Cu (II) from water [51].

1.3.2.1Magnetic nanocellulose

Nanocellulose, Fe_3O_4, (magnetic- nanocellulose) were synthesized, and characterized by XRD, TEM, PSD, SEM, EDX, VSM and FTIR. The Hg (II) uptake on Fe_3O_4-nanocellulose and investigated by 14 isotherm models, 12 kinetic models, adsorption activation energy and thermodynamic of adsorption [52].

Precipitation of nano-sized ferrite (Fe_3O_4 and $CoFe_2O_4$) particles with the presence of cellulose fibers has also been used to produce films with good magnetic properties [53].

Arsenate (As(V)) removal from aqueous solutions by novel adsorbent, magnetic iron nanoparticles modified microfibrillated cellulose(MFC) , Iron nanoparticle modified MFC have a magnetic properties so it was considered as an excellent adsorbent material due to high surface area and good adsorption capacity [54].

Magnetic Nanocellulose (MNCs) have been used for adsorption of inorganic [55] and organic analytes, because they have a wide range of applications [56,57].

The determination of Sudan dyes (Sudan I, Sudan II, Sudan III and Sudan IV) in food samples by using two methods, both methods use nano adsorbent for the adsorption which is Nanocellulose (NCs) extracted from bleached argan press cake (APC), one of the methods involves NCs was modified by magnetic nanoparticles before the adsorption of Sudan dyes [56].

It should be noted that some of emerging pollutants such as Paracetamol (PAR), Ibuprofen (IBU), Naproxen (NAP) and Diclofenac (DIC) have been adsorbed

from natural waters by using the Magnetic Nanocellulose (MNCs) coated with 1-butyl-3-methylimidazolium hexafluoro phosphate ionic liquid [58].

1.3.3 Silver - Cellulose nanocomposites

1.3.3.1 Silver Nanoparticles

Silver nanoparticles has attracted scientific 59 interest due to bacterial resistance to antibiotics, and many applications of Ag-NPs in water-, air- and surface- disinfection were described [59].

Silver considered as antimicrobial agent in which could be biologically transferred into silver nanoparticles and used as antimicrobial agent against multidrug resistant microbes [60-63].

The research on silver composites is still focused on medical applications [64].

Silver nanomaterials exhibit a broad spectrum biocides activity toward bacteria, fungi, viruses, and algae [65].

The silver nanoparticles damaging the bacterial membranes when it forms a free radical [66,67].

1.3.3.2 Silver Nanocellulose

Nanocomposites of surfactant modified cellulose nanocrystals (s-CNCs) with silver nanoparticles (AgNPs) in the polylactic acid (PLA) matrix has been investigated in terms of morphological, mechanical, thermal and antibacterial response [68]. This combination of (s-CNC) with (AgNPs) produced an efficient barrier effect due to the well dispersion of the fillers

[69]. So it would be an efficient compound for food packaging applications which requires an antibacterial effect constant.

H. Liu Studied the AgNPs composite with carboxylated CNC for employed as the labeled DNA probe for the identification of the complementary target DNA sequence by a selective and sensitive method [70].

Arcot R. Lokanathan studied the CNC composite with silver nanoparticle synthesis and elucidate the effect of CNC surface chemistry in nanoparticle formation and nucleation in the presence of borohydride reduction [71].

Cellulose nanofibers (CNFs) coated with silver nanoparticles (AgNPs) were developed. The flexible CNF-AgNPs films are effective substrates for SERS analysis. The CNF-AgNP films can be used to rapidly detect pesticides in fruits [72].

The production of silver nanoparticles composite with bacterial cellulose (BC) synthesized and the properties were studied, and reported as very effective for antibacterial activity specially Gram-positive and Gram-negative bacteria [73].

Moreover, the influence of the combination of the CNC structures with silver nanoparticles for the drugs adsorption represents the novelty of this research.

1.4 Carrageenan

The main source of Carrageenan is the “alga Chondrus crispus”. This alga is also known as carrageenin, “Irish moss” or “carragheen moss” from Carragheen (Waterford, Ireland) where it grows abundantly which prepared by alkaline extraction (and modification) from red seaweed [74,75].

The structures of Carrageenan are generally based on linear chains of alternating 3-linked b-D-galactopyranosyl and 4-linked a-galactopyranosyl residues [76]. There are three forms of Carrageenan, Iota (ι)-, Kappa (κ)-, Lambda (λ)-, Mu (μ)-, Nu (ν)- and Theta (θ)- carrageenan Carrageenan which identified based on the modification of the disaccharide repeating unit depending on the occurrence of ester sulphate, or anhydride formation in the 4-linked residue [77].

All of these forms of carrageenan have anti-human immunodeficiency virus (HIV) activity [78], inflammation and inflammatory pain [79].It should be known that carrageenan biopolymers have such properties of non-toxicity, biodegradability, and biocompatibility which give research an efforts to provide new carrageenan-based materials [80]. ι- and κ- carrageenan microparticles were synthesized by using glutaraldehyde as cross-linking agent and successfully applied as biosorbents for removal of the beta blocker metoprolol from aqueous solutions [81].

Carrageenans are versatile, and used in a variety of commercial food and industrials applications such as pharmaceutical, cosmetics and other applications [82-84].

The total market of carrageenans estimated as US $300 million/year [85].

1.4.1 κ-Carrageenan properties

κ-Carrageenan is 3-linked b-D-galactopyranosyl 4-sulfate alternating 4-linked 3,6-anhydro-a-Dgalactopyranosyl (see figure 3) [86,87]. κ-CRG are well known as their gel-forming ability in the food technology.

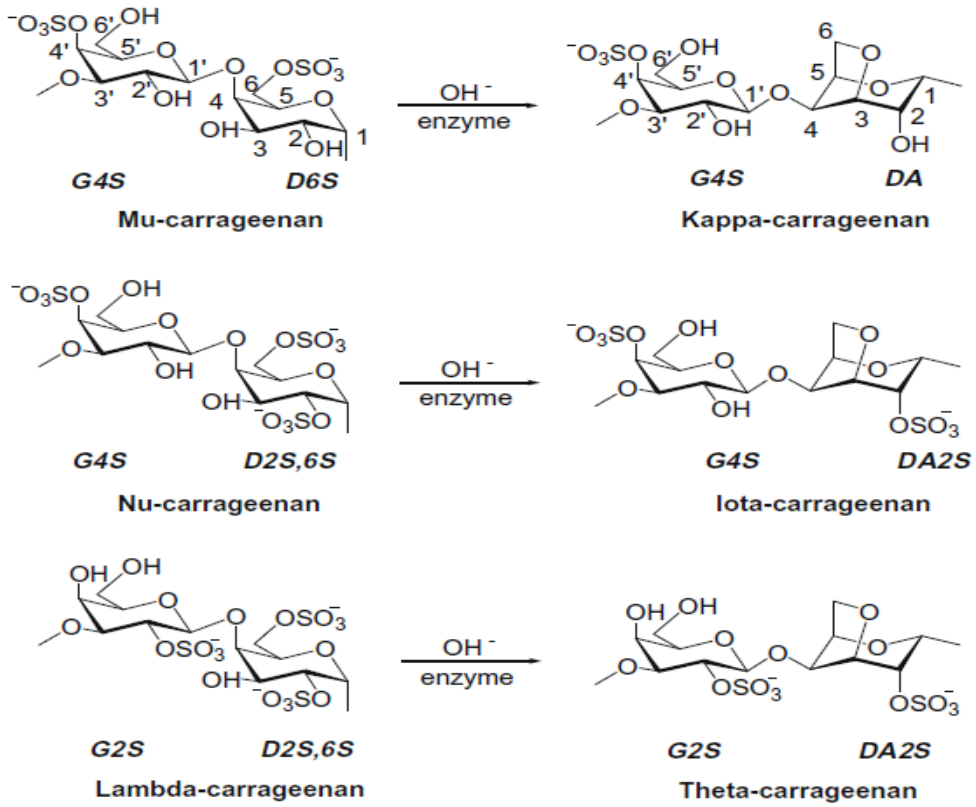

Figure 3: Schematic represent different structures of the repeating dimeric units of the commercial carrageenans.

Carrageenans have been widely used by food industry and consider as a valuable and low cost source of new drugs.

The gelation process of κ-CRG involves two separate and successive steps; coil-to-helix transition upon cooling and subsequent cation-dependent aggregation between helices [87].

Tari and Pekcan [88] have studied the association of κ-CRG with $CaCl_2$ which can change the swelling properties of carrageenan gels, make emphasizing the commercial relevance of carrageenans chemical modifications.

High-performance liquid chromatography (HPLC) analysis of carrageenans has been performed after various depolymerization methods, either directly on commercial products or for their detection in a food matrix [89,90].

Carrageenans almost may contain additional substituents. O-methyl groups considered as the most common substituent in the position 6 of D unity, as occurs with κ-CRG and several others polysaccharides [91].

1.4.2 Application of Carrageenan with different composites

Cellulose nanoparticles composites with carrageenan have effective applications in tissue engineering and regenerative medicine [92,93], also it is widely used as drug delivery, for increase drug loading, releasing and drug solubility [94,95], as it can composite with CNC for making plant based hard capsules [96].

A novel isocyanate-modified carrageenan polymers used as sorbent materials for pre-concentration and removal of drugs (diclofenac and carbamazepine) in different aqueous matrices (surface waters and wastewaters) [97].

Removal of wastewater nutrients N and P have been achieved by using CRG and Alginate immobilized with Chlorella Vulgaris [98].

Many studies and characterization of κ-CRG composites with CNC as it forms biodegradable film and soft material structure [99], in which the properties of κ-CRG influenced by the presence of CNC [100], and the mechanical strength also studied [101].

κ-CRG nanosilica biocomposite film were prepared and characterized for mechanical, thermal, barrier, contact angle and crystallinity properties [102]. Magnetic κ-CRG-g-poly(methacrylic acid) have been used for adsorb crystal violet dye [103], where the malachite green dye were adsorbed by novel nanocomposite of κ-CRG -g-polyacrylic acid/TiO_2–NH_2 hydrogel [104], also the Magnetic κ-CRG and κ-CRG Biopolymer-Based Nanocomposite used for the removal of Methylene Blue Dye (MB) [105,106,107].

Furthermore the preparation of O-maleoyl low molecular weight κ-carrageenan has been achieved [86].

1.5 Cyclodextrin and its modifications composites with CNC

1.5.1 Cyclodextrin

Cyclodextrins are cyclic oligosaccharides composed of six, seven or eight α-D-glucose units linked by α-(1,4) bonds, which are called α, β and γ-cyclodextrin respectively (figure 4,5) [108,109].

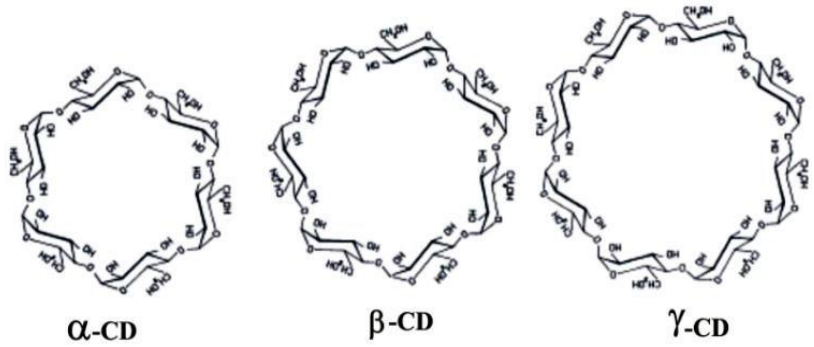

Figure 4: Chemical structure of α-cyclodextrin, β-cyclodextrin and γ-cyclodextrin respectively.

Interesting to know that the first cyclodextrins were discovered and reported in 1891 [110]. In 1903, the Austrian microbiologist Franz Schardinger, who considered to be founder of cyclodextrin chemistry, identified two crystalline compounds (A, B) similar to cellulosine from bacterial digest of potato starch and then he named these two cellulosine "α-dextrin and β-dextrin" [111].

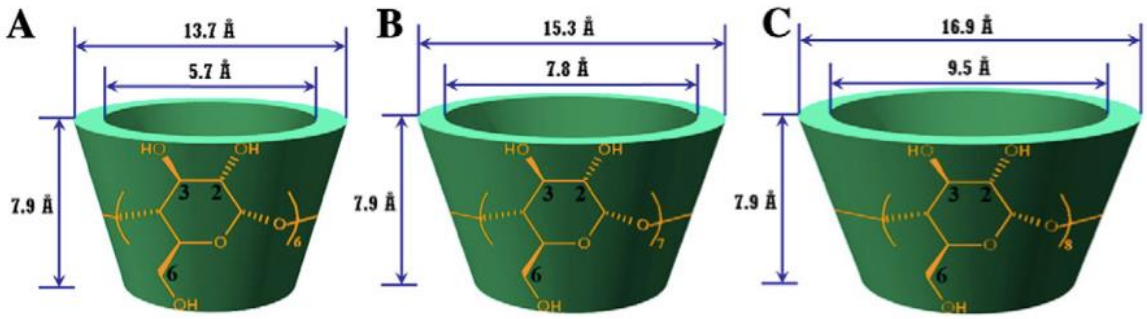

Figure 5: Schematic structure of A: α-cyclodextrin, B: β-cyclodextrin and C: γ-cyclodextrin

The properties of the three major kinds of cyclodextrins are α, β and γ cyclodextrins are summarized in Table 1.2 [112].

Table 1.2: properties of α, β and γ cyclodextrins

Property	α-cyclodextrin	β-cyclodextrin	γ-cyclodextrin
Number of glucose units	6	7	8
Molecular weight (g/mol)	972	1135	1297
Solubility in water at 25°C (%, w/v)	14.5	1.85	23.2
Outer diameter (Å)	14.6	15.4	17.5
Cavity diameter (Å)	4.7-5.3	6.0-6.5	7.5-8.3
Height of torus (Å)	7.9	7.9	7.9
Hydrate water molecules	2	6	8.8

β-cyclodextrin is the most widely abundant, lowest priced, most widely studied and also considered to be the most useful. β-cyclodextrin is found to be less irritating than α-cyclodextrin after injection.

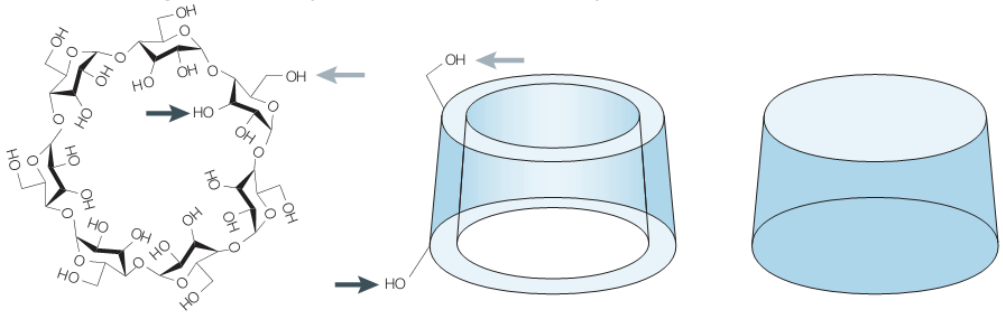

Figure 6: Schematic represent the chemical structure of β-cyclodextrin.

CDs are widely used in many applications such as enhancement of solubility of materials with low solubility in water [113], controlled release of drugs [114], protection of materials against oxidation and UV-degradation during storage or processing, catalytic action in chemical reaction, conversion of liquid materials to dry form, stabilization of flavors and spices and masking of bitterness and unpleasant odor of foods and drugs [115].

Cyclodextrins are extensively used in drug delivery, specially with different nanoparticles (NPs), also E.V. López used the blend of ethyl cellulose and pectin as film-coating material for cyclodextrin pellets for controlled drug release.

Furthermore L.A. Hergert, [116] prepared the inclusion complexes of β-cyclodextrin with ibuprofen and determined the presence of ibuprofen in pharmaceutical preparations and serum by using of spectrofluorimetry at both acid and alkaline pH.

Ibuprofen adsorbed by using modified cyclodextrin containing nanofilters from municipal wastewater [117], it’s also used for adsorb toluene from

aqueous solution by functionalized it with cellulose nanofiber composites [118], while D. Shi, [119] prepared and studied the adsorption of Laponite-cyclodextrin complex which considered great for wastewater treatment.

Cyclodextrins and its modifications were used to adsorb different types of dyes [120].

Acetylated β-cyclodextrin (Ac βCD) and γ-cyclodextrin (Ac γCD) were prepared and studied the interaction with naproxen in the solid and liquid state [121], meanwhile synthesized of substituted Benzoyl modified β-cyclodextrin and their inclusion properties were studied by using fluorescence spectroscopy [122].

1.6 Water pollutants,

1.6.1 Water pollutants from pharmaceutical

In fact, every day, industries, agriculture and the general population used to use water and releasing many compounds into wastewater. Agriculture practices, industrial discharges and the human being play an important role of causing pollutants in wastewater. All of these have generated various pollutants which impact on wild life human health and all living organisms. The removal of pharmaceuticals and personal care products residues from water is one of the major environmental concerns nowadays. It is estimated that 10–20 million people die every year due to waterborne and nonfatal infection which causes death of more than 200 million people every year [123]. Furthermore, thousands of children die every day due to the water

pollution problems of diarrhea. For knowledge, 4000km^3 from 15000km3/year considered as the total freshwater which may used for industrial and domestic purposes [124], and may it increases to nearly 5000km^3 per year in 2025 [125].

An activated carbon, oxidation, activated sludge, nanofiltration (NF), and reverse osmosis (RO) membranes which considered as traditional materials and treatment technologies which are not effective to treat complex and complicated polluted waters including pharmaceuticals, personal care products, surfactants, various industrial additives [126].

The pharmaceuticals are grouped into different types: hormones, anti inflammatory, anti epileptic, statins, antidepressants, beta blockers, antibiotics, products of contrasts, etc. [127]. And there are numerous studies have demonstrated the presence of human drugs in the urban wastewater, sewage from hospitals and surface waters, groundwater and drinking water, also may reach the soil due to irrigation [128].

Pharmaceuticals and Personal Care Products (PPCPs) contamination levels have been detected up to the μg/L-level in municipal sewage and surface waters, and may presence in sludge, sediments, and soil in the range of ng g^{-1} to μg g^{-1} [129]. In fact, a very little is known about the long-term effect and behavior of pharmaceutical residues in the aquatic environment, and particularly in groundwater [130].

To the best of our knowledge, a large number of analytical methodologies, mainly using liquid chromatography tandem mass spectrometry (LC–MS/MS) which allowed the detection of extremely low concentrations

(ng/L), without using solid phase extraction (SPE) for purification; are already available for pharmaceutical detection in environment and wastewaters [131], but nowadays, there is increasing efforts for going to use more fast and cost-effective method for purification and extraction the samples by using on-line SPE followed by LC-MS/MS for analyze trace emerging contaminants in wastewaters, such as drugs, pesticides, and hormones [132,133]. For example [134], a simultaneous determination of 74 pharmaceuticals in environmental waters (groundwater and superficial water) and wastewater treatment plants (effluent and influent) has been developed, validated and applied to the samples.

1.6.2. Emerging pollutants

Large number of emergent pollutants from different sources leach every day to soil and ground waters without treatment. An emergent pollutant is a material or chemical product which can be considered a potential hazard for the mammals or the environment. A pollutant is classified as emergent when associated to a new way of interaction with mammals and required a new method of detection or a recently developed technology [134].

There is a lack of knowledge of the impact of emerging pollutants in the middle or long-term effect on human health, the environment and aquatic environments [135]. They are considered as emerging pollutants in water bodies because they still remain unregulated or are currently undergoing a regularization process, although the directives and legal frameworks are not set-up yet [136].

There are 47 different pharmaceutical emergent organics considered as pollutants in waste water, summarized in Table 1.3.

Table 1.3: Selected emerging pollutants for analysis [137].

N#	Name	N#	Name
1	Chloramphenicol	2	Ketoprofen
3	Chlortetracycline	4	Naproxen
5	Doxycycline	6	Gemfibrozil
7	Oxytetracycline	8	Ibuprofen
9	Tetracycline	10	Indometacin
11	Clarithromycin	12	Carbamazepine
13	Erythromycin	14	Diazepam
15	Roxithromycin	16	Ethofibrate
17	Sulfadiazine	18	Fenofibrate
19	Sulfadimidine	20	Pentoxifylline
21	Sulfamethoxazol	22	Phenacetin
23	Trimetazidine	24	Phenazone
25	DL-Atenolol	26	β-Sitosterol
27	Betaxolol	28	β-Estradiol
29	Bisoprolol	30	Estriol
31	Metoprolol	32	Estrone
33	Pindolol	34	Mestranol
35	Propanolol	36	Ethinylestradiol
37	Sotalol	38	Diatrizoicacid
39	Aspirin	40	Iohexol
41	Bezafibrato	42	Iopamidol
43	Clofibricacid	44	Iopromide
45	Diclofenac	46	EDTA
47	Fenoprofen		

The residues of an emerging pharmaceuticals pollutant causes huge problems, such as a decline of vulture population in Pakistan from diclofenac, also have adverse effects on wildlife population decline [138].

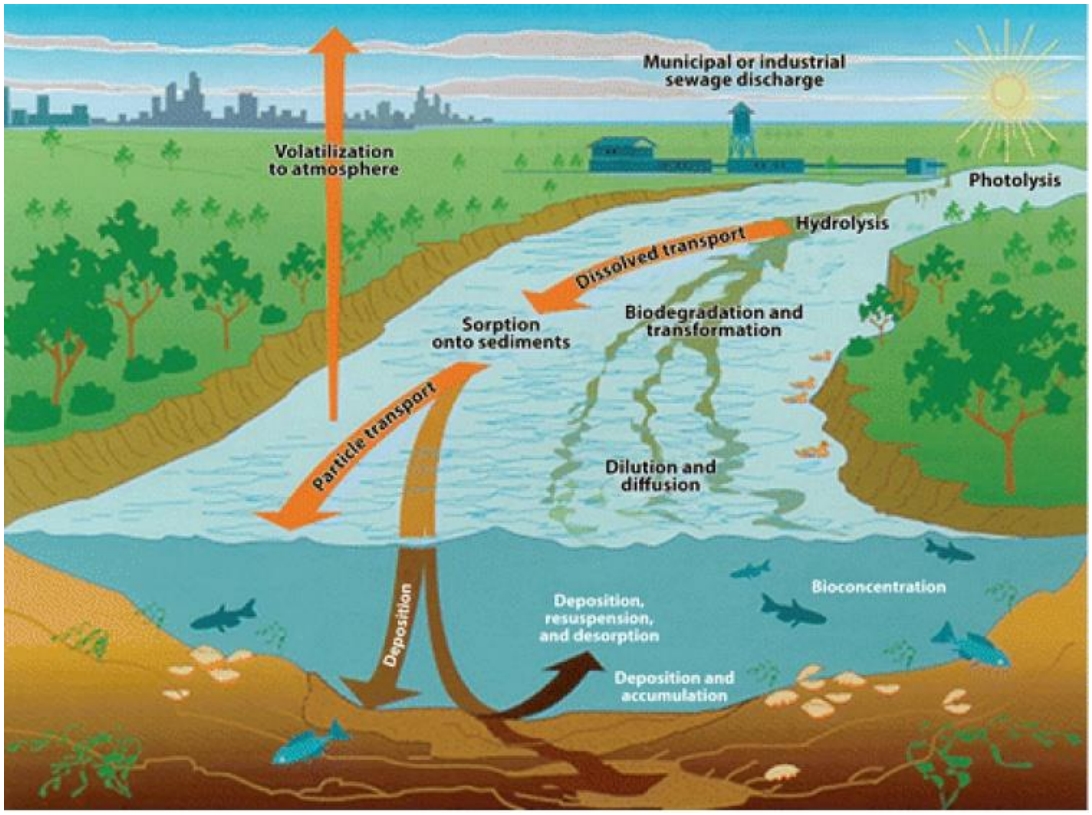

Figure 7: Pharmaceuticals Entering Water [139]

1.6.2.1. Ibuprofen

Ibuprofen is one of the most popular consumed pharmaceuticals, because it is widely used all over the world. It is a nonsteroidal anti-inflammatory (NSAID) analgesic and antipyretic compound, which has become worldwide used for the treatment of rheumatic disorders, pain, fever and inflammation [140]. It is slightly soluble in water, readily soluble in organic solvents, and so it has high mobility in the aquatic environment, that's the reason to be selected. Figure 8 shows the chemical structure of ibuprofen.

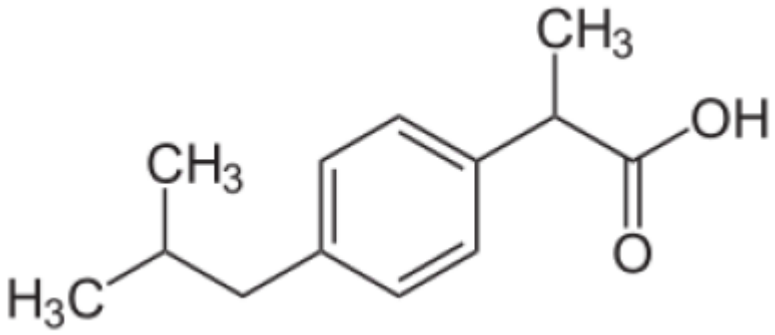

Figure 8: Chemical Structure of Ibuprofen [141]

1.6.2.2 Ibuprofen in the Environment

Over the past several decades, the implementation of environmental laws, which control the chemicals released into the environment by industries, companies and households, have been continually reformed in an attempt to keep any dangerous chemicals out of water supplies, where it can easily reach animals and humans.

There are many studies shows the occurrence of Ibuprofen in different areas, for example, In the U.S., a study was done and found 0.90 – 2.11 μg/L of ibuprofen in raw and reclaimed water sources and nearly 1.35 μg/L in drinking water [142].

1.6.2.2.1 Resistance and Risk of Ibuprofen

Nowadays, as concentrations of ibuprofen are being found in the environment, the thought of how the chemicals might affect organisms in aquatic ecosystems is becoming a concern.

Several studies have been conducted on aquatic life looking for how concentrations of ibuprofen might affect these species. A cyanobacterium,

Synechocystis sp. PCC6803, was specifically looked at along with a species of water plant called duckweed, Lemna minor [143]. Looking for unnatural growth in the two organisms, they tested the ability to grow at different concentrations. The Synechocystis exhibited a strong and rapid growth at all concentrations of ibuprofen. Lemna on the other hand showed a declined ability to grow in an exponential decreasing manner. The effects on Lemna have been the most severe recorded to date.

The impact on the ecosystem of losing one species like Lemna minor could be detrimental. In a small ecosystem the loss of one organism could mean disaster for most all other organisms in the ecosystem. In the case of humans there is a growing concern with prolonged use of ibuprofen [144]. Many health specialists are concerned that ibuprofen can cause gastrointestinal, cardiovascular, kidney, and brain conditions.

Despite current research in ibuprofen removal, little has been done to look at the effectiveness of adsorption methods. There have been successes in removal with biological processes but there is a need for research in different types of adsorption. Biological treatments are secondary treatments common in wastewater treatment facilities, but not in drinking water facilities. Adsorption methods may be more effective for removing ibuprofen as this processes show promise on a smaller scale in applications.

1.7 Adsorption Types and Definition

1.7.1 Equilibrium Isotherm Models

Adsorption phenomenon is generally described by an invaluable non-linear curve known as adsorption isotherm. Which represents the amount of the Adsorbate on the adsorbent as a function of its concentration (if liquid) or pressure (if gas) at constant temperature and pH. The mathematical correlation that drawn by the adsorption modeling analysis is important for applicable practice and operational design of large scale adsorption systems [145].

Adsorption equilibrium is confirmed when an adsorbate become in contact with the adsorbent for certain period of time, and in the presence of adsorbate concentration in the bulk solution that allows a dynamic equilibrium with the interface concentration [146].

Analysis of the isotherm data is important to develop an equation that exactly explain the observed results. The most known isotherms which are applied in liquid /solid systems are the theoretical equilibrium isotherm models, including Langmuir and Freundlich isotherms [147].

1.7.1.1 Langmuir Adsorption Isotherm

After the formation of a monolayer adsorbate on the outer surface of the adsorbent, no more adsorption occurs [148],so it is called the ideal localized monolayer model; it was developed to represent chemisorption. Adsorption is limited to monolayer coverage, and so the adsorbed molecule cannot

migrate across the surface or interact with neighboring molecules. Furthermore, the surface of the adsorbent is uniform, and so all the adsorption sites are energy equivalent [149].

The Langmuir equation relates the coverage of molecules on a solid surface to the concentration of a medium above the solid surface at a fixed temperature. This equation can be written as:

$$\frac{1}{q_e} = \frac{1}{q_0} + \frac{1}{q_e K_{LC_e}} \quad (2.1)$$

Where:

C_e = the equilibrium concentration of adsorbate (mg/L)

q_o = maximum monolayer coverage capacity (mg/g)

K_L = Langmuir isotherm constant (L/mg).

q_e is the amount of adsorbate per unit mass of adsorbent (mg/g) [150], and it can be calculated using the following relation:

$q_e = (C_o - C_e) \frac{V}{m}$ (2.2)

Where:

C_o is the initial concentration of the adsorbate (mg/L).

V is the volume of the solution (L).

m is the mass of the adsorbent (g).

($C_o - C_e$) represents the adsorbed amount (ppm). A graph of (C_e/q_e) values versus C_e is used to find the Langmuir parameters. That are, ($1/K_L Q_o$) as y-intercept and ($1/q_o$) as slope [151].

The essential features of the Langmuir isotherm can be expressed in terms ofa dimensionless constant separation factor $R_L$which is given by the following equation :

$$R_L = \frac{1}{1 + K_L C_0} \quad (2.3)$$

Where:

C_0 = initial concentration.

K_L = the constant related to the energy of adsorption (Langmuir Constant). R_L value indicates the isotherm shape to be unfavorable if (R_L >1) Linear if (R_L = 1), favorable if (0 <R_L <1), or irreversible if (R_L = 0) [152].

1.7.1.2 Freundlich Adsorption Isotherm

This adsorption to surfaces supporting sites depends on different affinities or to heterogeneous surfaces. Freundlich isotherm supposes that stronger binding sites are occupied first, so; the binding strength reduces with increasing degree of site occupation. Related to this articulation, the adsorbed mass per mass of adsorbent can be represents this equation [153].

$$\ln q_e = \ln K_F + \frac{1}{n} \ln C_e \quad (2.4)$$

Where:

K_F is the Freundlich constant which indicates the adsorption capacity of the sorbent (mg/g).

n is the heterogeneity coefficient that gives an indication of the Favorable way

of the adsorption process (g/L)m if the value of 1/n is less than one then the adsorption is normal ,and if n is between one and 10, the sorption process is favorable [154].

A plot of lnqe values versus lnCe is used to find Freundlich parameters. That are, lnK_F as y-intercept and (1/n) as a slope.

1.7.2 Adsorption Kinetic Models

The kinetic of adsorption is the process which represents the transportation of the adsorbate molecules from bulk solution to a boundary layer of the water surrounding of the adsorbent particle by molecular diffusion through the stationary layer of water. So, the adsorbate particles are transported into an available site. And formation of an adsorption bond will occur between the adsorbateand the adsorbent [155].

There are many adsorption kinetic models that describe adsorption kinetics and rate-limiting step. These models give information about the adsorption system behavior and determine whether the adsorption process is a chemical or a physical one, and also which is the rate determining step. These adsorption kinetic models include, external mass transfer model, pseudo first-order and pseudo second-order rate models, Adam–Bohart–Thomas relation, Weber and Morris sorption kinetics, first-order reversible reaction model, first-order equation of Bhattacharya and Venkobachar and Elovich's model [156].

1.7.2.1 Pseudo First–Order Kinetics

This kinetic model is the first model developed to describe adsorption kinetics.

The rate equation for pseudo first-order kinetic model can be written as:

$$\ln(q_e - q_t) = \ln q_e - K_1 t \quad (2.5)$$

Where:

q_e and q_t are the amounts of adsorbate adsorbed per unit mass of adsorbent at equilibrium, and at time t respectively (mg/g).

k_1 is the pseudo first-order rate constant for adsorption (min^{-1}).

A plot of $Ln(q_e - q_t)$ versus t should give a linear relationship that allows the computation of a first-order rate constants, k2 and qe [157].

1.7.2.2 Pseudo Second–Order Kinetics

This kinetic model assumes that the rate-determining step may be chemical adsorption which involve valence forces through sharing or exchange of electrons between the adsorbate and the adsorbent.

The final integrated equation for this kinetic model is:

$$\frac{t}{q_t} = \frac{1}{K_{2q_e^2}} = \frac{t}{q_e} \quad (2.6)$$

Where;

k_2 is the pseudo second-order rate constant for adsorption ($g.mg^{-1}.min^{1}$).

The plot of t/q_t versus t will give a straight line for the pseudo second order adsorption with $(1/ K_2 q_e^2)$as y-intercept and $(1 /q_e)$ as the slope of the graph [158].

1.7.2.3 Intra-Particle Diffusion Kinetic Model

This model is established on the theory suggested by Weber and Morris. The final equation of this adsorption kinetic model can be written as:

$$q_t = K_{id}\, t^{1/2} + Z \qquad (2.7)$$

Where;

K_{id} is the Intra-Particle diffusion rate constant ($mg/g.min^{1/2}$).

Z is a constant that gives an information about the thickness of the boundary layer (mg/g) [159].

A plot of q_t versus $t^{1/2}$ will give a linear relationship for intra-particle diffusion kinetic model with constant Z as a y-intercept and K_{id} as a slope.

1.7.3 Adsorption Thermodynamics

Adsorption thermodynamics of a process are necessary to determine whether the process is favorable or not. The adsorption characteristics of a material can be expressed in terms of thermodynamic parameters such as the change in Gibbs free energy (ΔG), enthalpy change (ΔH) and the change in entropy (ΔS). Where; ΔG and ΔH are in (J) and the unit of ΔS is (J/K).

The general equation which connects between the adsorption parameters can be written as: [160]

$$\Delta G = \Delta H - T\,\Delta S \qquad (2.8)$$

Where:

T is the absolute temperature (K).

The change in Gibbs free energy can be also calculated by the following equation:

$$\Delta G = -R\ T \ln K_d \quad (2.9)$$

Where:

R is the universal gas constant that equals 8.314 $J.mol^{-1}.K^{-1}$.

K_d is the thermodynamic equilibrium constant that equals (q_e/C_e) with a unit of mol or (L/g).

The combination of the previous two equations will give the following equation:

$$\ln K_d = \frac{\Delta S}{R} - \frac{\Delta H}{RT} \quad (2.10)$$

The plot of LnK_d versus (1/T) will give a straight line with ($-\Delta H/R$) as slope and ($\Delta S/R$) as y-intercept. The resulting graph is known as Van't Hoff plot.

1.7.4 Adsorption as an effective method for removing IBP from wastewater

Emerging pollutants can be removed from wastewater using several treatment methods, Which can be classified as chemical, physical, and biological methods. According to the different methods, adsorption is an effective separation process for many applications. Economically it is suitable for removal of both organic and inorganic pollutents from wastewater [17].

Adsorption is a common technique used to remove dyes from aqueous solution, this is because of many advantages of this method such as low in cost, simple, and environmentally friendly [161].

1.8 Research Objectives

1.8.1 General Objectives

1. Convert the cellulose to Nano Crystalline Cellulose (NCs)
2. Prepare Magnetic Nanocellulose (MNCs) and Silver Nanocellulose (AgNCs) from NCs.
3. Prepare Acetyl β-CD and Benzoyl β-CD
4. Prepare a composite of Carrageenan, Acetyl and Benzoyl β-CD with NCs.
5. Develop a method for removal of IBP from wastewater using these adsorbents

1.8.2 Specific Objectives

1. Make a comparison of the efficiencies between the all adsorbents toward adsorption of Ibuprofen from an aqueous solution.
2. Study the effect of pH, temperature, amount of adsorbent, concentration and contact time on the adsorption of Ibuprofen.

Chapter Two

Experimental Part

2.1 Chemicals and Materials

In this study, all reagents were purchased from Aldrich Company, and confidentially used without any further cleaning unless otherwise specified. All chemicals like H_3PO_4, NH_4OH, NaOH, $FeCl_3.6H_2O$, $FeSO_4.7H_2O$, $AgNO_3$, $NaBH_4$, Benzoyl chloride, Triethyl amine, Acetyl chloride, H_3PO_4 were of analytical grade. HPLC grade Water for HPLC solvent, Methanol and Acetonitrile. β-Cyclodextrin (β-CD; purity ≥ 99.3) was purchased from Sigma-Aldrich, κ-Carrageenan were kindly supplied by KEVIN, China. Ibuprofen standard was of high purity grade (IBP; purity ≥ 99.5%) was purchased from IOL (IOL Chemicals and pharmaceuticals L.T.D, India). Ibuprofen was used as Adsorbate. Distilled water was used for all solutions.

2.2 Instrumentation

For this work, the required instrumentations includes the following: shaking water bath (DaihanLabtech, reach to 250 rpm Digital Speed Control), thermometer, pH meter (model: 3510, JENWAY), Centrifuge (5000 rpm, Universal 320R, Hettich, Canada), FTIR Spectrometer (Nicolet iS5, iD3 ATR, from Thermo Scientific), HPLC (Waters 1525 Binary HPLC Pump, Waters, Singapore) with Photodiode Array Detector (PAD) Waters 2998.

2.3 Preparation of adsorbents

2.3.1 Preparation of (NCs, MNCs and AgNCs)

- **Cellulose Nanocrystalline(CNC)**

The extracted cellulose powder from OISW using a process developed previously at our laboratory were used in this work [161]. Extracted cellulose was then well-converted to CNC as following procedure: cellulose (5.0 gram) was added to a beaker containing distilled water (180 mL) and stirred magnetically for 30 min. To the beaker content was added 20g of concentrated H_2SO_4 to produce a solution with 10 wt% of sulphuric acid. Then stirring the mixture for 20 min at 60 ºC. Then dilute the hot mixture with ice cold DW. Make centrifuge for the colloidal suspension carefully at 5,000 rpm and decanted. To the residue was added water, mixed then centrifuged and decanted. This process was repeated for five times to remove any suspension from hydrolysis product and sulphuric acid completely. The NCs residue was left to dry for 2 days at room temperature.

- **Magnetic cellulose Nanocomposite**

Cellulose nanocrystalline was then converted to magnetic cellulose. 1.5 g of NCs were added to 500 mL beaker containing 200 mL distilled water and stirred for 20 min. Then add the $FeSO_4.7H_2O$ (0.75 g) and $FeCl_3.6H_2O$ (1.49 g) to CNC in the beaker and heated with stirring to 60ºC for another 20 min. MNCs was precipitated by adding 8M ammonium hydroxide drop wise with stirring until reached 10 of pH value. At this pH the color of the precipitate observed to be black. The mixture was centrifuged and left to dry overnight [162].

- **Silver Nanocellulose**

A 300 ppm of $AgNO_3$ solution was prepared in 500 mL beaker. 50 mL water solution containing 1.5 g of CNC was mixed with 25 mL of $AgNO_3$ solution. 0.3 g of $NaBH_4$ were carefully added to 7 g of ice water, then mixed with the mixture by stirring for an hour. The mixture was centrifuged and left to dry for 24 hours.

2.3.2. Preparation of (Acetyl β-Cyclodextrin, Benzoyl β-Cyclodextrin)

- **Acetyl β-Cyclodextrin**

  1.0 g of β-Cyclodextrin was weighed accurately. 10 mL triethyl amine was added on it and stirring for 20 minutes. then 1.5 mL drop wise of acetyl chloride was added carefully while stirring for half an hour. Wash the precipitate with water to get rid of access acetyl for 3 times, and let it to dry overnight.

- **Benzoyl β-Cyclodextrin**

  β-Cyclodextrin was converted to Benzoyl β-CD by dissolve 0.5 g of β-CD in 2-3mL of triethyl amine. 0.28 mL benzoyl chloride was added and mixed for 30 minutes. Wash it with water and let it to dry overnight.

2.3.3 Preparation of CRG/NCs, Acetyl β-CD/NCs and Benzoyl β-CD/NCs

5 g of each one was putted with 5 g of NCs into beaker with 3 mL of distilled water and shaking for 30 min, then let it to dry before use.

2.4. Characterization of adsorbents

Some desired matrix of NCs, Acetyl β-CD and Benzoyl β-CD was examined by FT-IR spectroscopy.

2.5. Statistical Analysis

In this work, the experiments were done in duplicate. At first, for each duplicate the mean was calculated. The coefficient of variance often less than 1%. Determination of the error range by using a certainty interval of 96% which were used for the data analysis using Excel Microsoft software. The collected data were analyzed using t-test. Also, all the variations were statistically as the value of $p < 0.05$.

2.6 Preparation of Ibuprofen solutions

Ibuprofen stock solution with a concentration of 1000 ppm IBP was prepared by 0.1 g of IBP dissolved into 100 mL of Acetonitrile in a volumetric flask. A set of solutions of IBP with various concentrations: 0.1 to 100 mg/L were prepared by dilution in methanol.

2.7 Chromatographic Conditions:

Here, in this work a High Performance Liquid Chromatography system (HPLC) (Waters, Waters 1525 Binary HPLC Pump) with PA Detector (Waters 2998), were used for the analysis of this experiment, where the data was saved by using Breeze software. The determination was performed by using a column of 250 mm cartridge long, 4.6 mm internal diameter (X

TERRA C18, 5µm , 250 mm x 4.6 mm), with the mobile phase included (A) methanol: water (80: 20 v v^{-1}) which adjusted to pH 3 by drop wise addition of H_3PO_4 and (B) 100% methanol in gradient ratio (50:50) at normal temperature. The elution was monitored at 254 nm while the flow rate was recorded at 1ml/min. All the samples were filtered using 0.45µm filter before inject to the HPLC.

2.8 Calibration Curve

The absorbance of the prepared solutions in section 2.6 were measured by HPLC method. The absorbance was plotted versus concentration, a linear calibration curve between peak areas and concentrations was obtained with IBP concentrations in the range 0.1-50 mg/L (R^2 = 0.991) as shown in Figure 9 (a) and in the range 2-100 mg/L (R^2 = 0.999) as shown in Figure 9 (b).

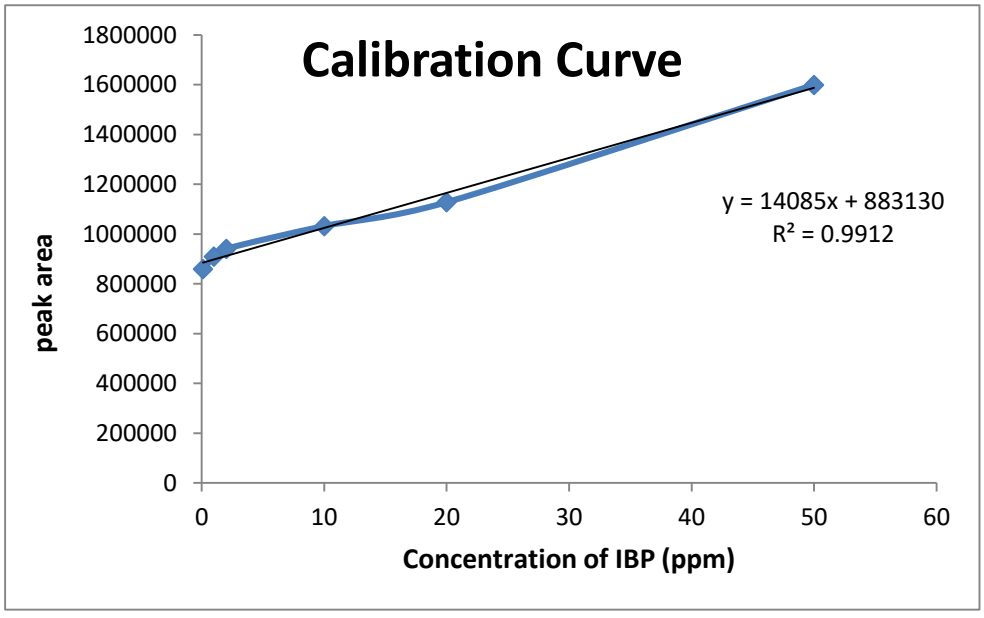

Figure 9 (a): Linear calibration curve between peak area and IBP concentration in the range 0.1- 50 mg/L

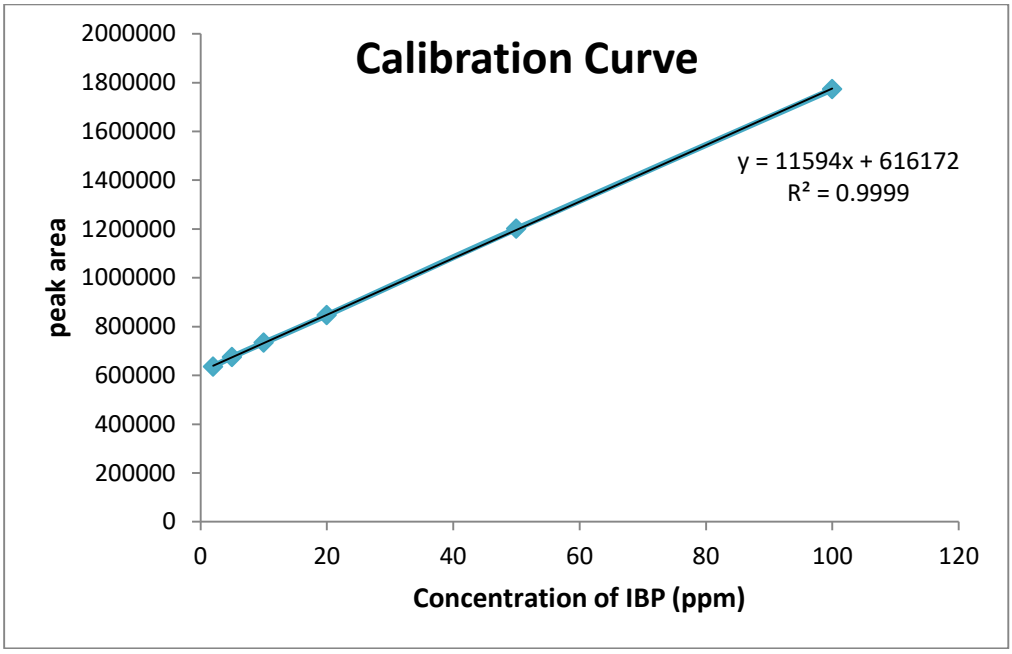

Figure 9 (b): Linear calibration curve between peak area and IBP concentration in the range 2-100 mg/L

2.9 Adsorption Experiments

The experimental parts were performed using different concentrations of Ibuprofen in 50 mL solutions using different weight of adsorbent samples depending on the experiment. The pH of solutions was adjusted using 0.1 M NaOH and diluted H_3PO_4 solutions. All the measurement of adsorption were performed HPLC-PAD method as showed in section 2.7 at different temperatures depending on the experiment like effect of contact time of IBP, the pH value, adsorbent dosage, adsorption isotherm, kinetic and thermodynamics. A calibration curve made before the adsorbate concentration was measured in solution by using a range from 2 to 100 ppm. All of the concentrations were made from a stock solution of 1000 ppm by

dilute it into Acetonitrile (ACN), and then dilute it in methanol for the diluted IBP to make calibration curve solutions.

Here, removal ratio percentage (E %) is well-defined as the ratio of Ibuprofen concentration differences before and after adsorption (C_0-C_f) to the initial concentration of IBP in the aqueous solution (C_0) and was studied by using the following Eq. (3.1):

$$E\ (\%) = \frac{C_0 - C_f}{C_0} * 100\% \qquad (3.1)$$

Where C_0 was defined by the initial concentration of IBP and C_f was the final IBP concentration. All of the experiments were done twice and the means were taken unless there are presence of difference more than 6%, and for enhance the experiments, then a third measurement was taken.

For the experiment of effect of contact time which was carried at 298 K and different concentrations (5, 10,15, 20, 50 mg/L) and time range from 5 to 360 min the adsorption capacity was calculated using Eq. (3.2):

$$q_t = \frac{C_0 - C_t}{m} \text{x } V \qquad (3.2)$$

Where q_t (mg/g) the adsorbed amount of the Ibuprofen at time t. Meanwhile, m is the mass of adsorbent (g), the C_t was Ibuprofen concentration at time t, and the volume of solution was expressed by V (L).

In working on this study a replicate experiments were conducted on the whole experimental part. The mean was taken for each duplicate. In our study the coefficient of variance was mostly less than 1%. We determined the margin of error using a confidence interval of 95% for the data of

experiment using Excel Microsoft software and the data were analyzed using t – test. All the differences was considered statistically at $p < 0.05$ for the results of t- test.

2.9.1. Optimization of time and the initial Ibuprofen concentration

The Ibuprofen adsorption on the adsorbent was studied as a function of shaking time at 25^{o}C. A sample of 50 mL of different IBP concentrations (5 ppm, 10 ppm, 15 ppm, 20 ppm and 50 ppm) solution at normal pH added to 50 mL a beaker with 0.05 g of adsorbent. At different time intervals the supernatant was carefully removed by a thin plastic dropper and the adsorption was measured by using HPLC- PAD.

2.9.2 Effect of pH

Effect of initial pH on adsorption was investigated in the pH range 2-10. The pH was adjusted using roughly concentrations of 0.1 M HCl and 0.1 M NaOH. 0.05 g adsorbent samples were added to 50 mL of IBP solutions with concentration 20 ppm. The solutions were putted in Shaking Water Bath instrument at normal temperature (25°C) at optimized time for each adsorbent depending on the results of experiment in section 2.9.1. At the end of intervals of time, the solution was filtered and supernatant was analyzed for the residual IBP particles.

2.9.3 The effect of adsorbent dosage

To discuss the effect of dose of these adsorbents (NCs, MNCs, AgNCs, κ-CRG, Acetyl β-CD and Benzoyl β-CD) on the removal of IBP on these surfaces, different experiment were done using different dose of adsorbent substrates ranging between 5–75 mg. This experiment was studied using 20ppm solution of IBP and pH 10 at 25 ºC. The samples were putted in Shaking Water Bath at normal temperature (25°C) at optimized time for each adsorbent depending on the results of experiment in section 2.9.1. The absorbance of supernatant was measured by HPLC-PAD for the residual concentration of IBP.

2.9.4 Effect of temperature

The effect of temperature on adsorption is also an important issue to be evaluated, constant amount of adsorbent samples (depending on the previous experiment) were added to 50 mL of Ibuprofen solutions with a concentration of 20 ppm at pH 10. Each mixture was shaken in a water bath at desired temperature (the range was 10.7-50°C) at optimized time for each adsorbent depending on the results of experiment in section 2.9.1. At the end of intervals of time, the solution was filtered and supernatant was analyzed for the residual IBP by HPLC-PAD for the residual concentration of IBP.

2.10 Thermodynamics and Kinetics of Adsorption

The removal of emergent pollutant such as Ibuprofen were studied by adsorption methods using the prepared adsorbents (NCs, MNCs, AgNCs, κ-

CRG, Acetyl β-CD and Benzoyl β-CD). The batch technique was adopted under the optimize condition of adsorbent dosage, initial concentration of IBP, contact time, pH and temperature. By using HPLC-PAD (Waters 1525 Binary HPLC Pump, Waters), concentrations of Ibuprofen were measured before and after operating the adsorption. Langmuir and Freundlich adsorption isotherm equations were studied. The values of their uniform parameters were calculated and discussed. The thermodynamic parameters such as the standard free energy (ΔG°), entropy (ΔS°) and enthalpy (ΔH°) of the systems were determined by using Van't Hoff's plot. The percent of removal efficiency values and K_d for IBP were determined at various temperatures ranging (10.7 – 50^{o}C).

Adsorbent (0.05 g) was added to 50 mL of (5,10,15, 20 and 50 mg/L) of IBP solution at normal pH. The mixture was putted in Shaking Water Bath at constant temperature (25°C). We adjust the adsorption rate by studying the contact time for about 6h and contrast to theoretical models. The two known models, pseudo first and pseudo second orders kinetic models have been examined and the experimental data obtained were used different time. The pseudo first order and pseudo second order kinetic model parameters (K, Q_e and R^2) for Ibuprofen adsorption on NCs, MNCs, AgNCs, κ-CRG, Acetyl β-CD and Benzoyl β-CD were determined. The values of the calculated and experimental Q_e were compared.

Chapter Three

Results and Discussion

3.1 Characterization of Adsorbents

3.1.1 NCs FT-IR Characterization

FT-IR of cellulose is shown in Fig.4.3. The spectrum shows a broad band at 3293.09 cm^{-1} which corresponds to the OH-stretching vibration. The band at 1427.05 cm^{-1} corresponds to the CH_2 bending vibration, The peak at 2895.17 cm^{-1} corresponds to the C–H stretching vibration, meanwhile the band at 1314.38 cm^{-1} corresponds to the C-O,C-H stretching. 1159.62 cm^{-1} band corresponds to the O-C-O,C-O stretching.

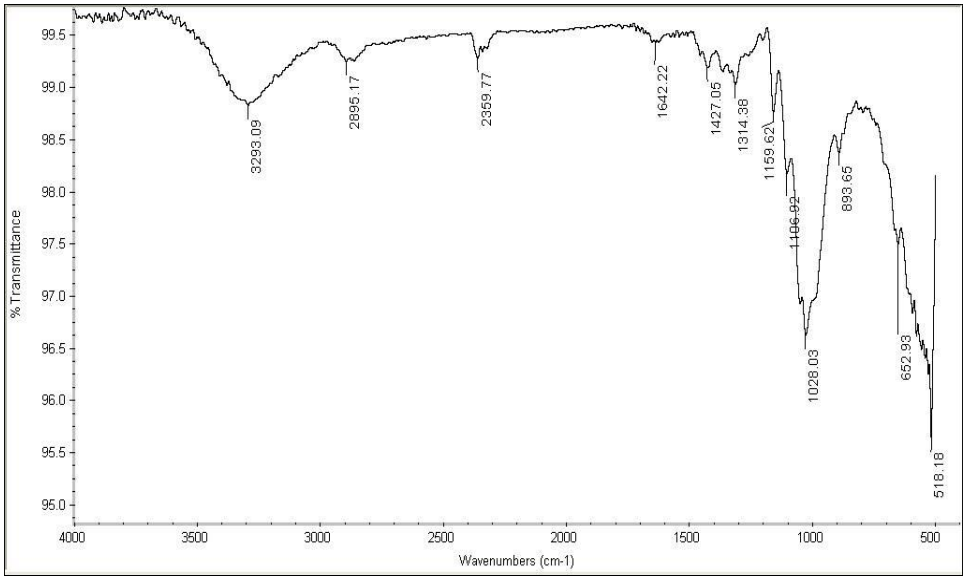

Figure10: Schematic of FT-IR for the nanocellulose used for Adsorption

Acetyl β-CD FT-IR Characterization

Acetyl cyclodextrin cm-1 (neat): 3391 (O-H, stretching), 1746.35 (C=O, stretching of ester, external), 1651 (C=O, ester, internal), 1028 (C-O, ether stretching)

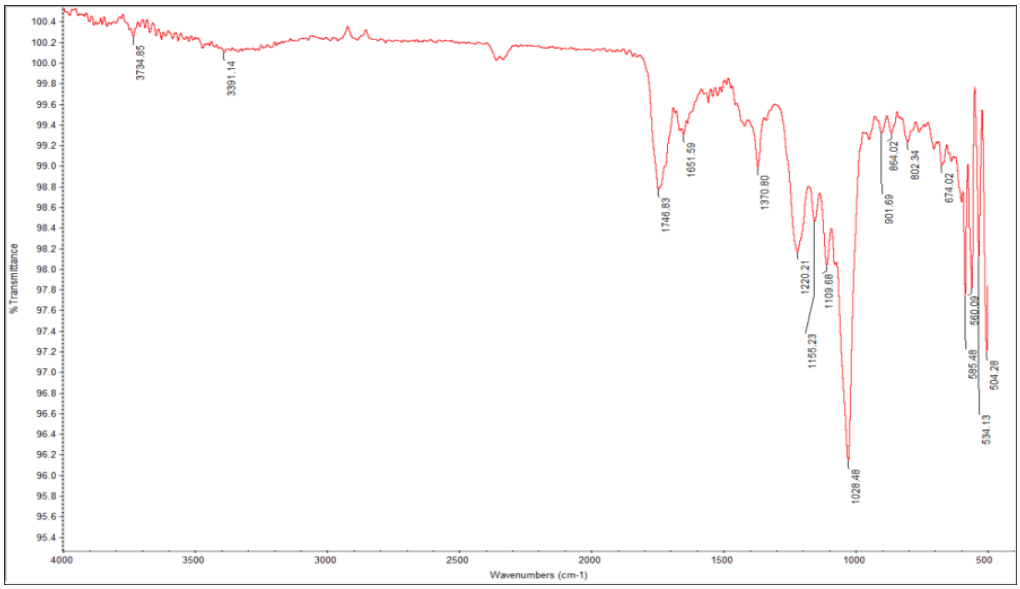

Figure 11: Schematic of FT-IR for the Ac β-CD used for Adsorption

5.1.2. Benzoyl β-CD FT-IR Characterization

Benzoyl cyclodextrin cm-1 (neat): 3331 (O-H, stretching broad), 3050 (=C-H, aromatic), 2095 (-C-H, aliphatic), 1748.6 (C=O. ester external), 1723 (C=O, ester, internal), 1599 (C=C, aromatic), 1212 (C-O, ester) 1050 (C-O ether), 700 (monosubstituted benzene ring)

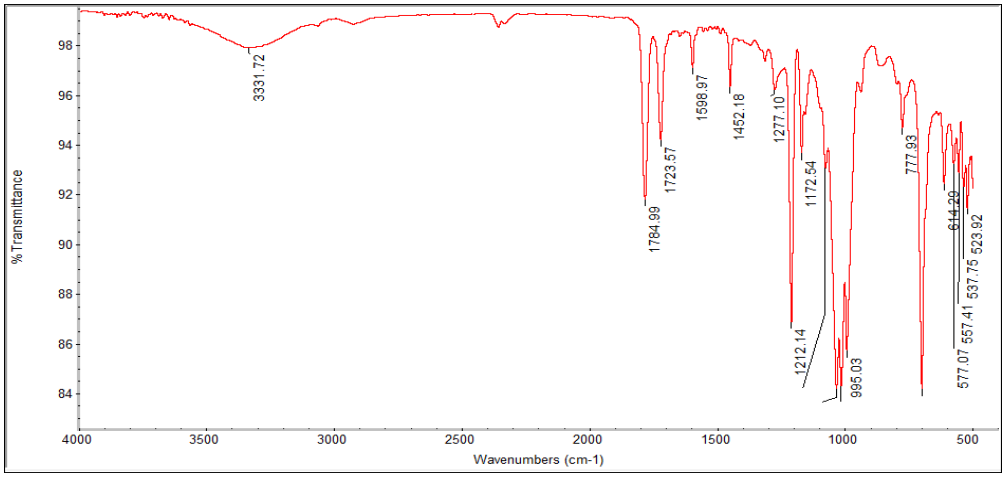

Figure 12: Schematic of FT-IR for the Benzoyl β-CD used for Adsorption

3.2 Investigation of adsorption parameters

3.2.1 Effect of contact time with IBP

The amount of Ibuprofen adsorbed (q_t) at different times (5 -360 minutes), the concentration (20 mg/L) were studied at pH 7 and 25°C as follows:

- **NCs, MNCs and AgNCs**

  Results of cellulose adsorption of IBP are shown in Fig.13(a), the adsorption capacity (q_t) of IBP on the cellulose samples were very fast in the interval time between 40 min to 180 min and it was faster specially in both the nanocellulose and magnetic nanocellulose and reached more than 75 , 27%, respectively, and reach more than 57% in AgNCs.

  The slow subsequent step (5 -40 min) was due to the rearrangement of IBP to find available adsorption sites on the cellulose.

  In our study we used 180 min as a contact time of NCs, MNCs and AgNCs when we studied IBP concentrations, pH and dose effect, etc.

- **Carrageenan and Carrageenan composites with NCs**

  As shown bellow in Fig.13 (b), the absorbance of Ibuprofen by using Carrageenan and Carrageenan composites with NCs was completely effective in the first 5 min of the adsorption which reached about 98%, 98.1% respectively, and it became decreasing after 5 min.

  For these adsorbents, 5 min is the time we used in the other adsorption experiments (IBP concentrations, pH, etc).

- **Acetyl β-CD/NCs and Benzoyl β-CD/NCs**

  For these adsorbents, the Benzoyl β-CD/NCs showed the higher amount of adsorption capacity (q_t) from the first 5 min which reached more than 87%, see Fig.13 (c), then it became decreasing slowly at the other intervals time. Meanwhile, the Acetyl β-CD/NCs give a good adsorption after 40 min from contact with IBP, It give 35% of removal efficiency which is not as high as Benzoyl β-CD/NCs did.

  For Acetyl β-CD/NCs 40 min is the time we used in the other adsorption experiments (IBP concentrations, pH, etc), and for Benzoyl β-CD/NCs we chose 5 min as best contact time.

  The decreasing of the adsorption capacity (q_t) may happened due to after filling of some or all surface sites of adsorbents by IBP which named by fill-pores mechanism, the other molecules of IBP may compete with these IBP molecules in the adsorbent sites and cause a random movement of molecules with the passage of time which lead to decreasing of the amount of adsorption capacity with increasing of contact time.

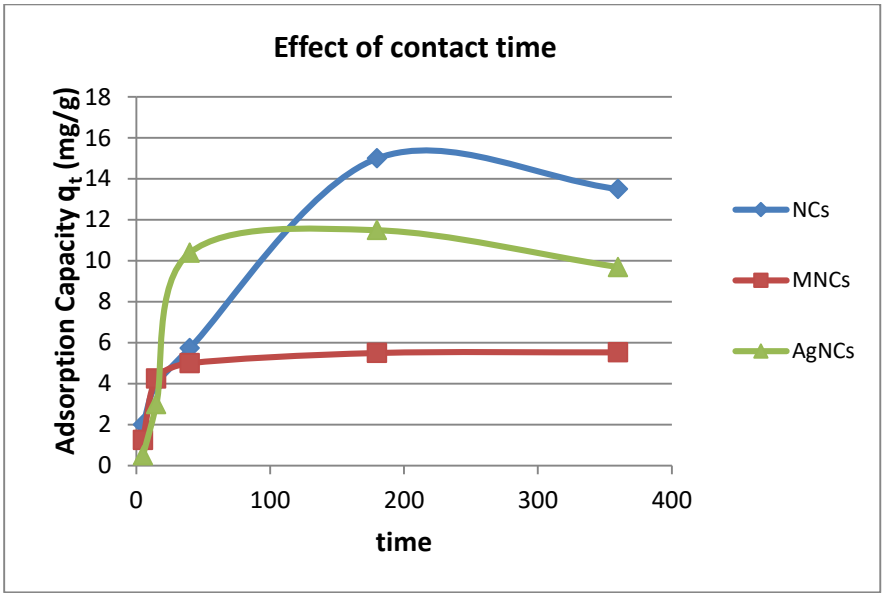

Figure 13(a): Effect of contact time to determine the time of maximum adsorption of Ibuprofen by using NCs, MNCs and AgNCs. (Temperature= 25°C, pH= 7, Concentration of IBP= 20 mg/L, Volume= 50 mL, adsorbent dose= 50 mg).

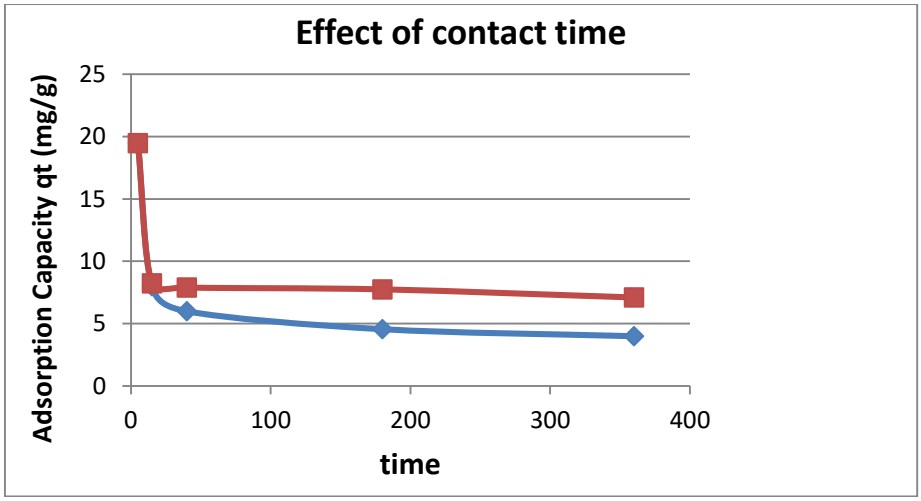

Figure 13(b): Effect of contact time to determine the time of maximum adsorption of Ibuprofen by Carrageenan and Carrageenan composite with NCs. (Temperature= 25°C, pH= 7, IBP Concentration= 20 mg/L, Volume= 50 mL, adsorbent dose= 50 mg CRG, 50mg CRG-NCs).

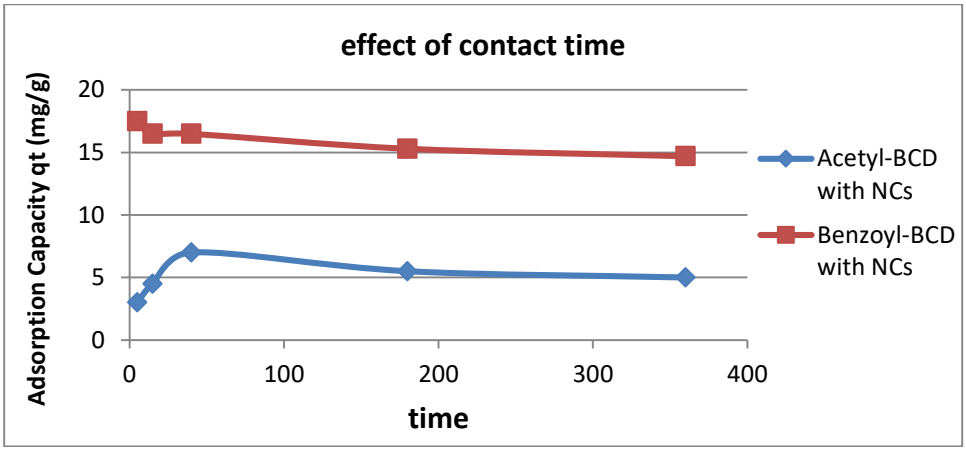

Figure13(c): Effect of contact time to determine the time of maximum adsorption of Ibuprofen by using Acetyl β-Cyclodextrin/NCs and Benzoyl β-Cyclodextrin/NCs. (Temperature= 25°C, pH= 7, Concentration of IBP= 20 mg/L, Volume= 50 mL, adsorbent dose= 50 mg Acetyl β-CD/NCs, 50 mg Benzoyl β-CD/NCs).

3.2.2 Effect of Ibuprofen Concentration

The amount of adsorption (q_t) at different Ibuprofen concentrations range between (5-50mg/L) at constant time for each adsorbent as discussed in section 3.2.1, were studied at pH 7 and 25°C as follows:

- **NCs, MNCs and AgNCs**

  The amount of IBP adsorbed are shown in Fig.14(a), the adsorption capacity (q_t) of IBP on the cellulose samples were increased as the IBP concentrations increased till reach 20 ppm and then it become steady. So, when we increased the initial concentration, the mass transfer driving force will then speed up the Ibuprofen ions diffusion from the bulk solution to cellulose surfaces, so this will increase the amount of equilibrium adsorption [163]. and it was specially in both the

nanocellulose and silver nanocellulose and reached more than 75, 57%, respectively, and reach more than 27% in magnetic NCs.

So, here we have chose to use 20 ppm as a IBP concentration when we studied pH, dose and temperature effect.

- **Carrageenan and Carrageenan composites with NCs**

  These adsorbents give high response of the adsorption capacity of Ibuprofen as shown bellow in Fig.14(b), the absorbance of Ibuprofen by using both of adsorbents increased very fast at concentration 20 mg/l as it reach about 98% and 98.1% removal efficiency of the IBP and it became steady.

  For these adsorbents, 20 ppm is the concentration we used in the other adsorption experiments (pH, dose, temperature effect).

- **Acetyl β-CD/NCs and Benzoyl β-CD/NCs**

  For these adsorbents, the Benzoyl β-CD/NCs gave us higher amount of the equilibrium adsorption capacity (q_t) than Acetyl β-CD/NCs for all Ibuprofen concentrations as it reached more than 17 mg/g of adsorption capacity, meanwhile the Acetyl β-CD/NCs reached not more than 7mg/g, see Fig.14(c).

  So, for Acetyl β-CD/NCs and Benzoyl β-CD/NCs the concentration of Ibuprofen used is 20 mg/L in the other adsorption experiments (pH, dose, temperature effects).

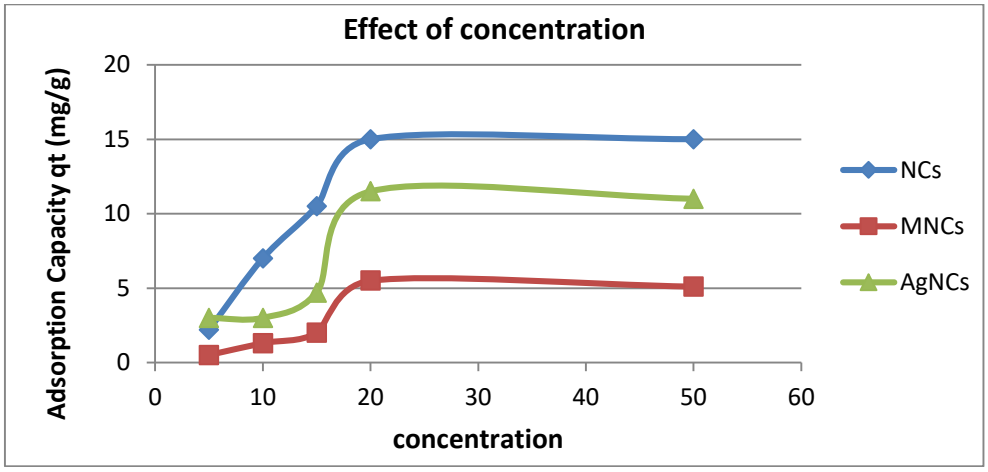

Figure 14(a): Effect of Ibuprofen concentrations to determine better concentration give high adsorption by using NCs, MNCs and AgNCs. (Temperature= 25°C, pH= 7, Contact time= 180min, Volume= 50 mL, adsorbent dose= 50 mg for each one).

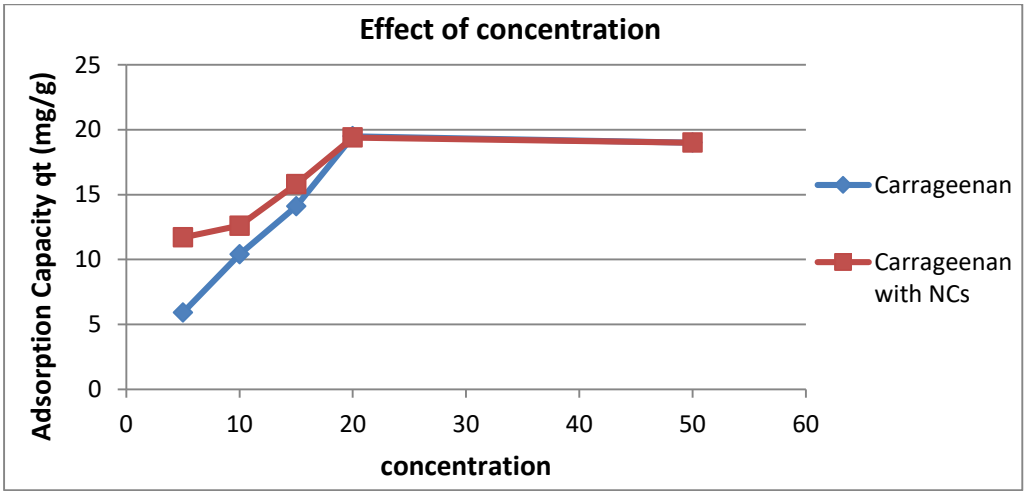

Figure 14(b): Effect of Ibuprofen concentrations to determine better concentration give high adsorption by Carrageenan and Carrageenan composite with NCs. (Temperature= 25°C, pH= 7, Contact time= 5 min, Volume= 50 mL, adsorbent dose= 50 mg for both).

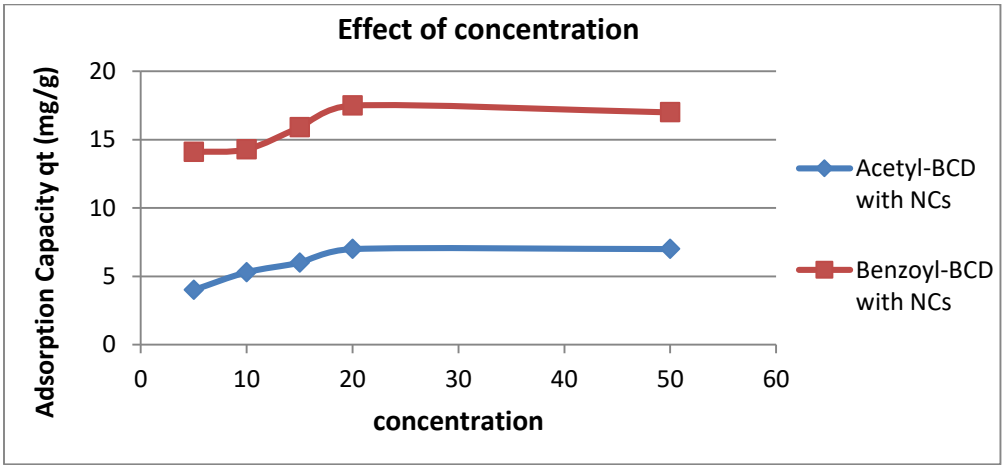

Figure 14(c): Effect of Ibuprofen concentrations to determine better concentration give high adsorption by Acetyl β-Cyclodextrin/NCs and Benzoyl β-Cyclodextrin/NCs. (Temperature= 25°C, pH= 7, Contact time= 40 min, 5 min respectively, Volume= 50 mL, adsorbent dose= 50 mg for both).

3.2.3 Effect of pH on Ibuprofen

The adsorption experiment of the pH effect on the IBP adsorption on the adsorbents surface showed dramatic effect. That effect was studied over a range of 2.0 – 10 at constant time for each adsorbent as discussed in section 3.2.1, were studied at concentration 20 ppm and 25°C as shown below:

- **NCs, MNCs and AgNCs**

  The results are shown in Fig.15(a). The cellulose substrates showed best removal of IBP at high pH (10). The amount of adsorption reached almost 16.1, 9.9, 13.6 mg/g for the NCs, MNCs and AgNCs respectively at basic pH value (10). The active sites of cellulose compounds were almost empty at the beginning and then by the removal of IBP starts filling those sites. Also, it depends on the chemistry of solutes in the solution.

To evaluate the pH effect on the adsorption capacity of the nanocellulose, MNCs and AgNCs, the experiments were carried out in the solutions having different pH values . The results show that as pH increased, an increase of Ibuprofen uptake is increased. The uptake reached the maximum value when pH =10. And at lower pH values show low uptake capacity, this is mainly caused by protonation of alcohol oxygen atoms on Cs.

For these adsorbents, pH 10 is the pH we used in the other adsorption experiments (Adsorbents dose and temperature effect).

- **Carrageenan and Carrageenan composites with NCs**

These adsorbents show very high adsorption capacity of Ibuprofen as shown in Fig.15(b), the absorbance of Ibuprofen by using CRG and CRG composites with NCs increased very fast from 5.3, 6.1 mg/g to 19.4, 19.5 mg/g respectively as increasing of pH from pH 4 to pH 7 which consider best removal efficiency of the IBP and then it return to decrease at high pH.

The binding of IBP onto CRG and CRG/NCs is properly controlled by H-bond interaction between hydrogen bonding donor group and O-donor group, here H-bonding between phenolic OH in CRG and carbonyl group (-C=O) in IBP may be likely dominated. The results demonstrated that the IBP adsorption decreased as pH increased from pH= 7 to 10, suggesting that the negative surface of CRG and the anionic IBP may generate an electrostatic repulsion (p*K*a of IBP is 4.91) [164, 165].

For these adsorbents, pH 7 is the pH we used in the next adsorption studies (dose, temperature effect).

- **Acetyl β-CD/NCs and Benzoyl β-CD/NCs**

The adsorption for these adsorbents Acetyl β-CD/NCs and Benzoyl β-CD/NCs showed in Figure 15(c), that the effect of the pH value on the uptake of Ibuprofen from its water by using Acetyl β-CD/NCs and Benzoyl β-CD/NCs increasing to be the optimum pH at pH 7 for both adsorbents and then become almost steady for higher pH values.

So that, the pH value we used in the next adsorption studies (adsorbent dosage, temperature) is pH 7 for these to adsorbents.

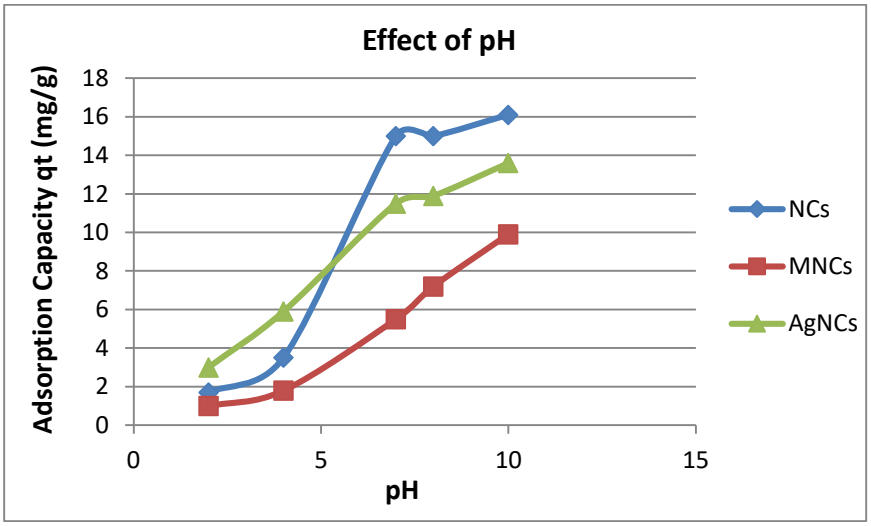

Figure 15(a): Effect of pH on Ibuprofen adsorption by using NCs, MNCs and AgNCs. (C_o= 20 ppm, Temperature= 25°C, adsorbent dosage= 0.05 g, solution Volume= 50 mL, Contact time= 180 min.).

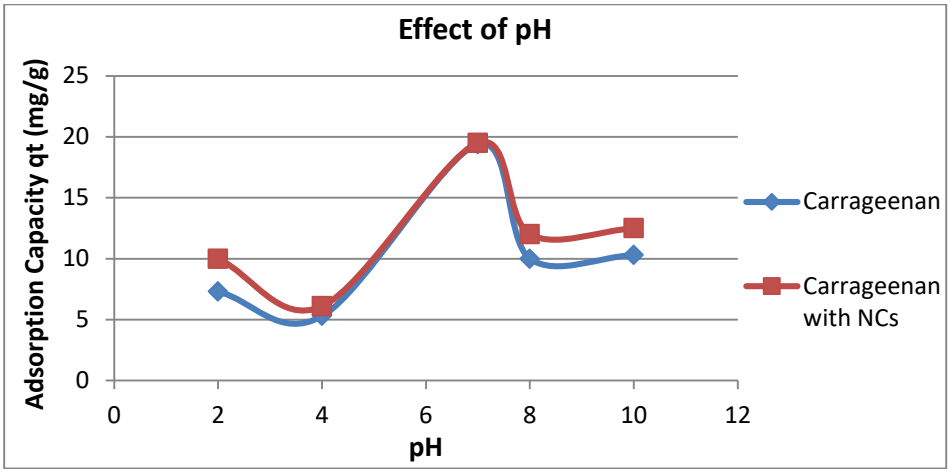

Figure 15(b): Effect of pH on Ibuprofen adsorption by using Carrageenan and Carrageenan composite with NCs. (C_o= 20 ppm, Temperature= 25°C, Contact time= 5 min, adsorbent dosage= 50 mg for both, Volume= 50 mL).

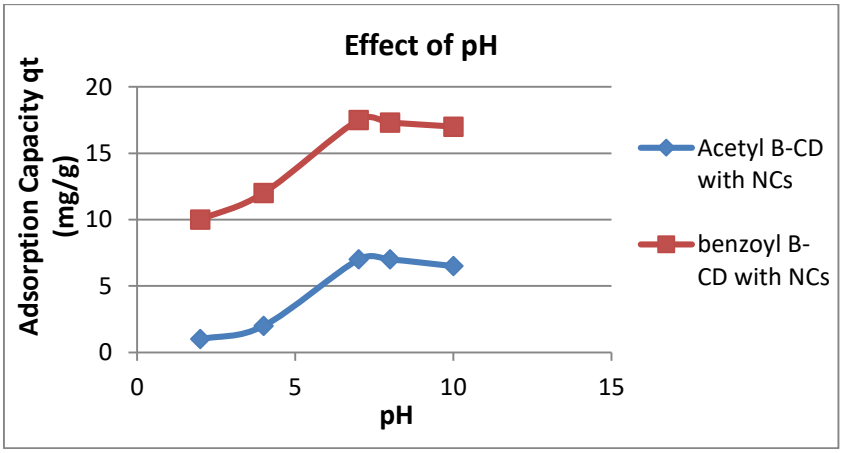

Figure 15(c): The effect of pH on Ibuprofen adsorption by using Acetyl β-Cyclodextrin/NCs and Benzoyl β-Cyclodextrin/NCs. (C_o= 20 ppm, Temperature= 25°C, Contact time= 40min, 5 min respectively, adsorbent dosage= 50 mg for both, Volume= 50 mL).

3.2.4 Effect of temperature on Ibuprofen adsorption

- **NCs, MNCs and AgNCs**

  The effect of temperature on the uptake of IBP by using (NCs, MNCs and AgNCs) was studied at (10.7 -50^{o}C) as shown in Figure 16(a). This figure shows that in general the % removal of IBP increases with increasing the temperature to some extent, at pH 10 by using 20ppm IBP concentration at constant time as determined in section 3.2.1. Increasing the temperature above the room temperature has slight influence on increasing the adsorption capacity of the new modified surface. The increasing of the amount of IBP adsorbed with increasing the temperature may caused by the increasing in the rate of IBP molecules diffusion of neighboring the interfaces and internal pores of the adsorbent [166]. The most responsible for the increase in porosity is increasing in temperature and how much the adsorbent have pore volume.

  The maximum adsorption was achieved at about 35^{o}C. This indicates that the adsorption of IBP on (NCs, MNCs and AgNCs) follows endothermic process.

  In this experiment, we have choose to used 35^{o}C in the other adsorption study by using NCs, MNCs, AgNCs.

- **Carrageenan, Carrageenan/NCs, Acetyl β-CD/NCs and Benzoyl β-CD/NCs**

  For using these adsorbents, we can observe in Figures 16(b) and (c), the amount of adsorption capacity of Ibuprofen from its water has the highest

values at normal temperature (25°C), at pH 7 using 20ppm Ibuprofen at constant time for each adsorbents as determined in section 3.2.1, which indicate efficient results for use these adsorbents in wastewater treatment plant for removal of emerging pollutants, that the heating doesn't needed, so it's a cost-effective adsorbents.

We used the normal temperature in the next adsorption experiment (adsorbent dosage effect) by using CRG, CRG/NCs, Acetyl β-CD/NCs and Benzoyl β-CD/NCs

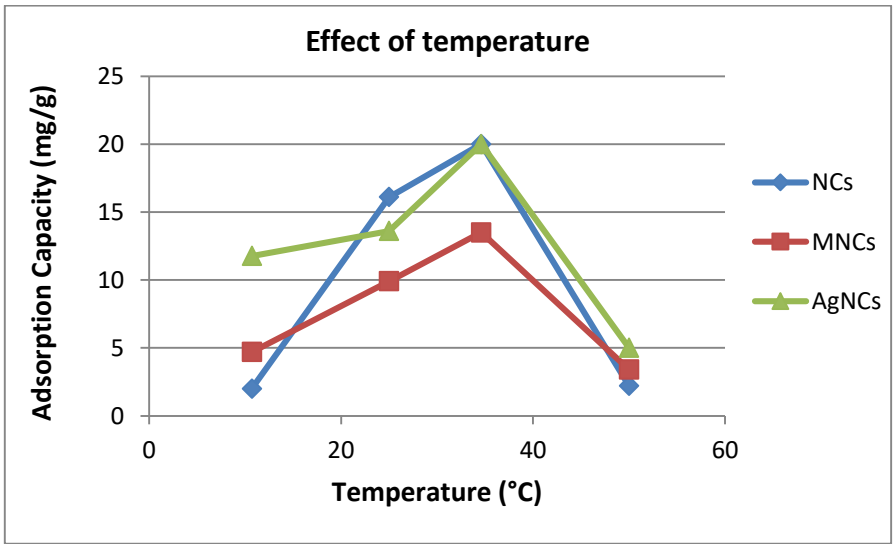

Figure 16(a): Effect of temperature on Ibuprofen adsorption by using NCs, MNCs, AgNCs adsorbents. (C_o= 20 ppm, time= 180 min, pH= 10, adsorbent dose= 0.05 g, solution Volume= 50 mL).

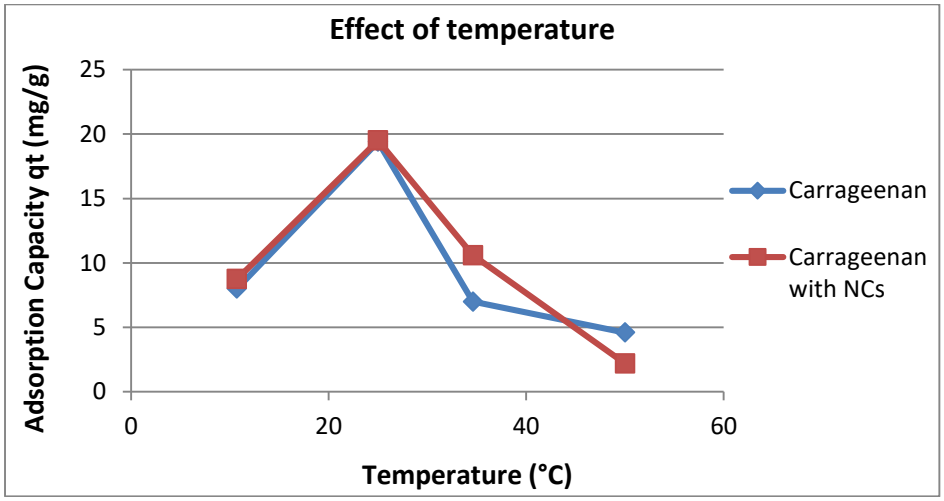

Figure 16(b): Show the effect of different temperature on Ibuprofen adsorption by using Carrageenan and Carrageenan composite with NCs. (C_o= 20 ppm, time= 5 min, pH= 7, adsorbent dose= 0.05 g for both, solution Volume= 50 mL).

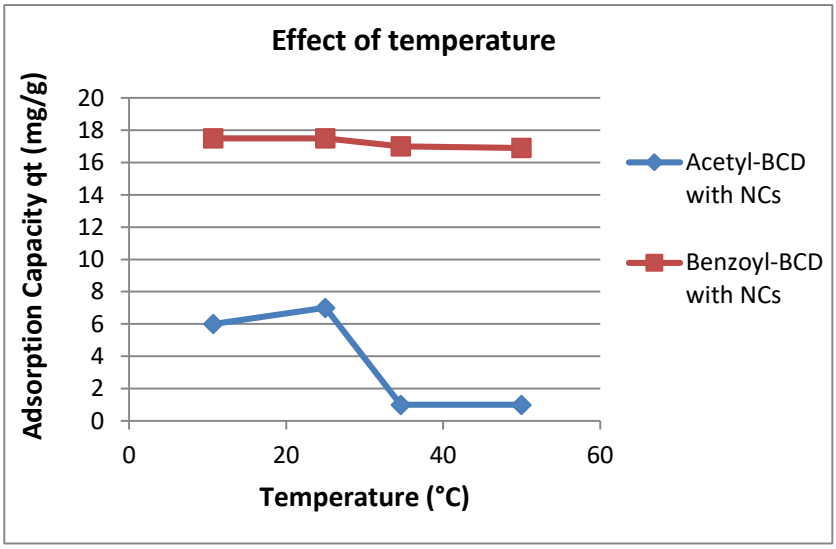

Figure 16(c): Effect of different temperature on Ibuprofen adsorption by using Acetyl β-Cyclodextrin/NCs and Benzoyl β-Cyclodextrin/NCs. (C_o= 20 ppm, Contact time= 40min, 5 min respectively, pH= 7, adsorbent dosage= 50 mg for both, Volume= 50 mL).

3.2.5 Effect of amount of adsorbent

In this experiment study the effect of dose of adsorbent on Ibuprofen removal on the adsorbents surfaces, different experiments were done using different dose of adsorbent substrates ranging between 5–75 mg as shown in Fig.17(a), (b) and (c).

- **NCs, MNCs and AgNCs**

  This experiment was studied using 20 mg/L solution of IBP and pH of 10 at 35 ºC for 180min of contact time. From the figure 17(a) we can see the adsorption efficiency increases as the dose increased specially till it reached 50mg for NCs and AgNCs, and for Magnetic Nanocellulose have a very high results of the amount of adsorption at 5mg dosage, reach about 98.5% removal efficiency, which considered better adsorption efficiency than other modified cellulose in case of comparing the adsorption cost. This can be explained by the vacant sites available.

  So that, we chose 50 mg for each NCs and AgNCs, and 5 mg for MNCs adsorbents.

- **Carrageenan, Carrageenan/NCs**

  This experiment was studied using 20 mg/L solution of IBP and pH of 7 and normal temperature 25°C for 5 min of contact time with adsorbents. From the figure 17(b) we can observe the adsorption efficiency reached the top efficient values when 25 mg used for both adsorbents, in which reached 98%, 98.2% respectively of removal efficiency. Also, at 50 both samples (CRG, CRG/NCs) showed the same percentage of removal

which means the vacant sites are almost saturated with IBP. For this reason, we chose 25 mg of adsorbent dosage.

- **Acetyl β-CD/NCs and Benzoyl β-CD/NCs**

  Adsorption experiment for these adsorbents Acetyl β-CD/NCs and Benzoyl β-CD/NCs was studied using 20 mg/L solution of Ibuprofen and pH 7 at normal temperature (25°C) for about 40 and 5 min. respectively of adsorption contact time. We can see the adsorption efficiency from the Fig. 17(c), the IBP have very effective results with each adsorbent at 5 mg adsorbents dosage, reach about 79.8%, 98.2% of removal efficiency respectively, and we can consider it as very efficient adsorption method, specially the using of Benzoyl β-CD/NCs adsorbent.

  The removal efficiency (% Removal) was calculated using the equation:

$$Removal\ efficiency(\%) = \left[\frac{(C_o - C_f)}{C_o}\right] \times 100 \qquad (3.1)$$

Where, C_o is the concentration of Ibuprofen in the sample solution before treatment and C_e is the concentration of Ibuprofen in the sample solution after treatment. Removal efficiency also can be calculated using absorbance of Ibuprofen in the sample solution before treatment C_o and absorbance of Ibuprofen in the sample solution after treatment C_f.

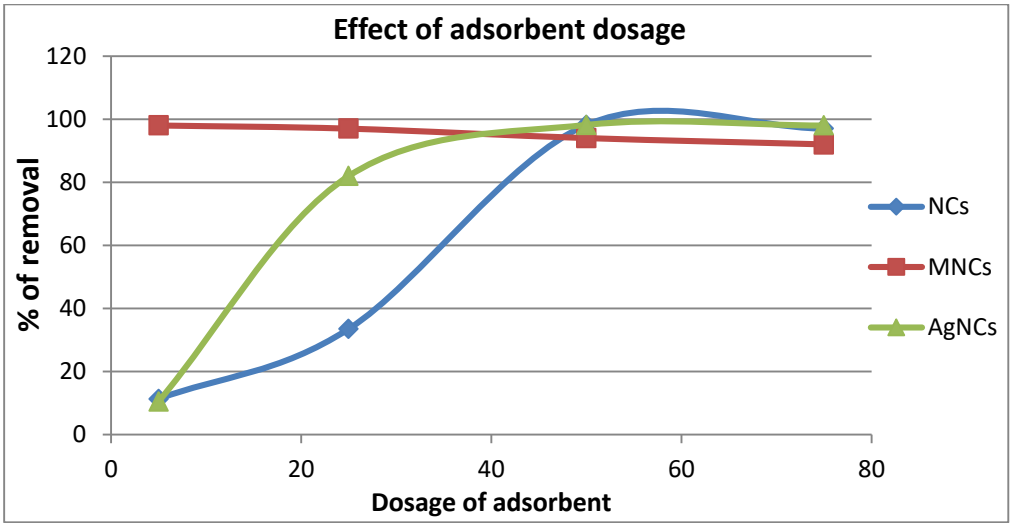

Figure 17(a): Effect of amount of adsorbent on the removal of Ibuprofen by NCs, MNCs and AgNCs. (Temperature= 35°C, time= 180 min., pH= 10, IBP concentration= 20 mg/L, solution Volume= 50 mL).

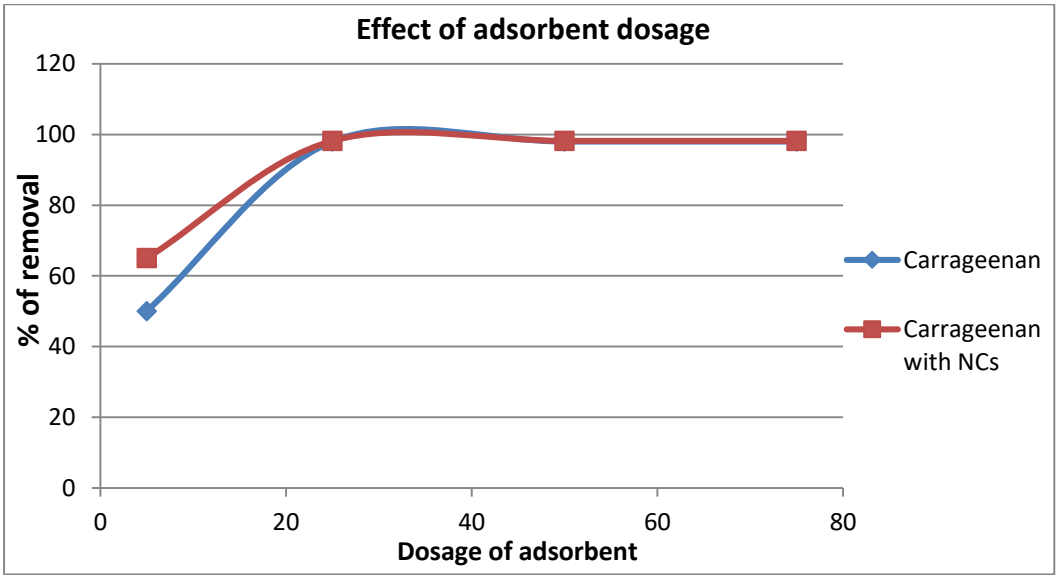

Figure 17(b): Effect of amount of adsorbent on the removal of Ibuprofen by using CRG and CRG composites with NCs. (Temperature= 25°C, time= 5 min., pH= 7, IBP concentration= 20 mg/L, solution Volume= 50 mL).

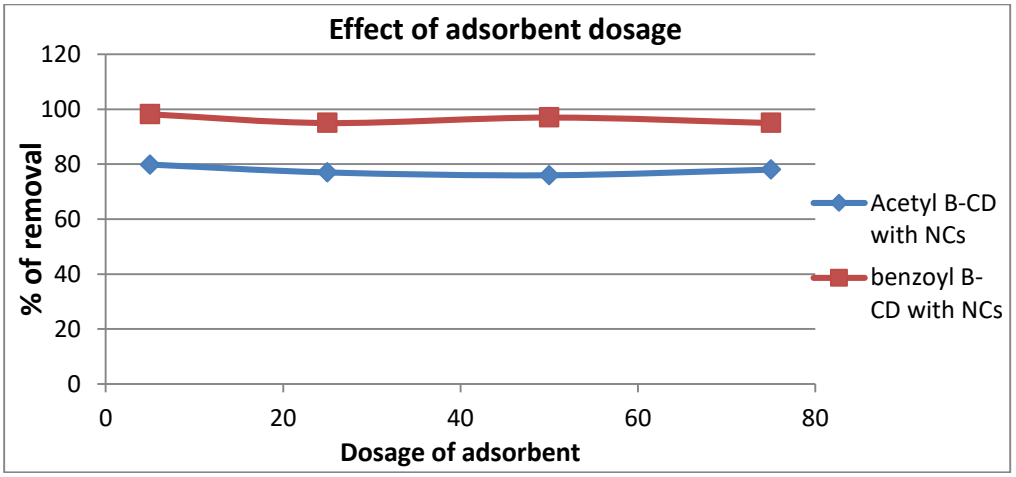

Figure 17(c): Effect of amount of adsorbent on the removal of Ibuprofen by using Acetyl β-Cyclodextrin/NCs and Benzoyl β-Cyclodextrin/NCs. (Temperature= 25ºC, time= 40, 5 min. respectively, pH= 7, IBP concentration= 20 mg/L, solution Volume= 50 mL).

The results of all the optimized parameters seems that the discussed adsorption method was environmentally friendly as most of water have pH 7 (except cellulose derivatives) and the temperature in the range of 273–283 K, also considered somehow as economically efficient that it need from 5min to 3hrs of contact time for IBP with adsorbents and very little amount of adsorbents (50mg) for adsorption process for IBP solution volume 50mL.

3.3 Adsorption isotherm of Ibuprofen

The adsorption isotherm was identified by determined constant values, which represent the surface features and affinity of the adsorbent and can also be used to find the equilibrium adsorption capacities [168].To have an idea about the adsorption equilibrium between the the adsorbents surfaces which is (Cs, NCs, MNCs, CRG, CRG/NCs, Acetyl β-CD/NCs and Benzoyl β-CD/NCs) and concentration of IBP in liquid phase; the two adsorption

isotherm models were used in our study, the Langmuir and Freundlich models. These two isotherm models are the most common adsorption models.

3.3.1 Langmuir Adsorption Isotherm

Langmuir adsorption isotherm is a type of kinetic principle which describes the monolayer adsorption of adsorbate on the solid without interaction between the IBP molecules adsorbed [169].It consider that the adsorbate molecules can accumulate on one localized pore without lateral interaction between the adsorbed molecules, even on the nearby sites. Furthermore, it indicates that after equilibrium there is no further adsorption could be occurs. So, based on this assumptions, the Langmuir expressed by the following equation:

$$\frac{C_e}{Q_e} = \frac{1}{q_{max}} C_e + \frac{1}{q_{max} K_L} \qquad (3.2)$$

Where:

C_e: the equilibrium concentration of adsorbate (IBP) (mg/L)

q_e: the amount of IBP adsorbed per unit mass of adsorbent (Cs, NCs, MNCs, CRG, CRG/NCs, Acetyl β-CD/NCs and Benzoyl β-CD/NCs) at equilibrium (mg/g)

q_{max}: it is defined by the theoretical maximum monolayer adsorption capacity of each adsorbents (mg /g), K_L: the Langmuir isotherm constant (L /mg).

The values of q_m and K_L were find from the slope and intercept of the Langmuir plot of C_e/q_e versus C_e. From Langmuir plots shown in Figures 18

(1, 2 and 3) amount adsorbed for monolayer formation (q_{max}), Langmuir adsorption-desorption equilibrium constant (K_L) and regression constant (R^2) were determined and values are shown in table 3.1(a, b and c), table 3.2(a and b) and table 3.3 (a and b).

From Langmuir isotherm we can also predict if the adsorption is favourable or unfavourable by using this equation (3.3) the dimensionless constant separation factor in

$$R_L = \frac{1}{1 + K_L C_0} \qquad (3.3)$$

Where C_o is the initial concentration of adsorbate and K_L is the Langmuir constant. If the value of R_L is greater than 1 that means the adsorption is unfavourable. And when $0 < RL < 1$ it would be favourable and if $R_L = 1$ describes linear adsorption.

- **NCs, MNCs and AgNCs adsorbents:**

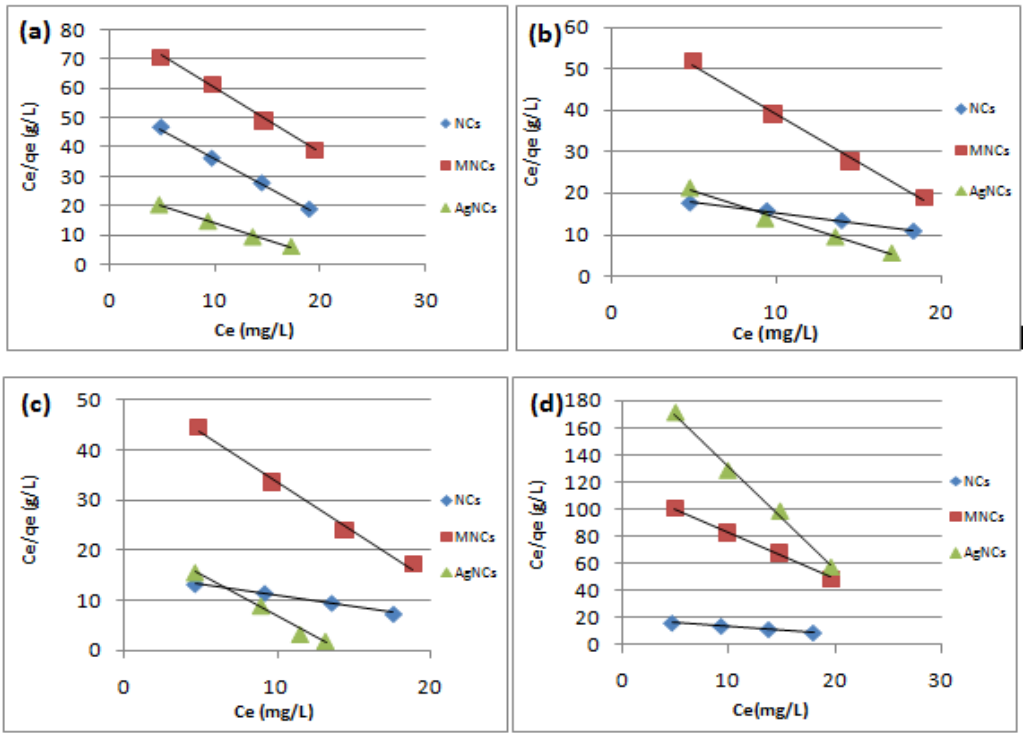

Figure 18.1: Langmuir plot for Ibuprofen adsorption on (NCs and MNCs, AgNCs). Temperature= (a)10ºC, (b) 25ºC,(c) 35ºC, (d) 50ºC , pH= 2, time= 180 min., Volume= 50 mL, adsorbent dosage= 0.05 g.

Table 3.1 (a): Langmuir isotherm model parameters and correlation coefficient for adsorption of Ibuprofen on NCs at 10, 25, 35 and 50° C.

Model	Parameter	Temperature(°C)			
		10	25	35	50
Langmuir isotherm (NCs)	q_{max}(mg/g)	503	416.3	450.1	312.2
	K_L (L/mg)	0.35	0.249	0.293	0.260
	R_L	0.125	0.167	0.146	0.161
	R^2	0.998	0.993	0.994	0.998

Table 3.1 (b): Langmuir isotherm model parameters and correlation coefficient for adsorption of IBP on MNCs at 10, 25, 35 and 50 C°.

Model	Parameter	Temperature(C°)			
		10	25	35	50
Langmuir isotherm (MNCs)	q_{max}(mg/g)	455.5	401.5	421.9	328.2
	K_L (L/mg)	0.280	0.221	0.265	0.203
	R_L	0.151	0.184	0.158	0.197
	R^2	0.996	0.995	0.992	0.997

Table 3.1 (c): Langmuir isotherm model parameters and correlation coefficient for adsorption of IBP on AgNCs at 10, 25, 35 and 50 C°.

Model	Parameter	Temperature(C°)			
		10	25	35	50
Langmuir isotherm (AgNCs)	q_{max}(mg/g)	643.9	601.3	543.11	196.2
	K_L (L/mg)	0.576	0.530	0.470	0.370
	R_L	0.079	0.086	0.096	0.119
	R^2	0.995	0.989	0.989	0.995

- **Carrageenan and Carrageenan/NCs**

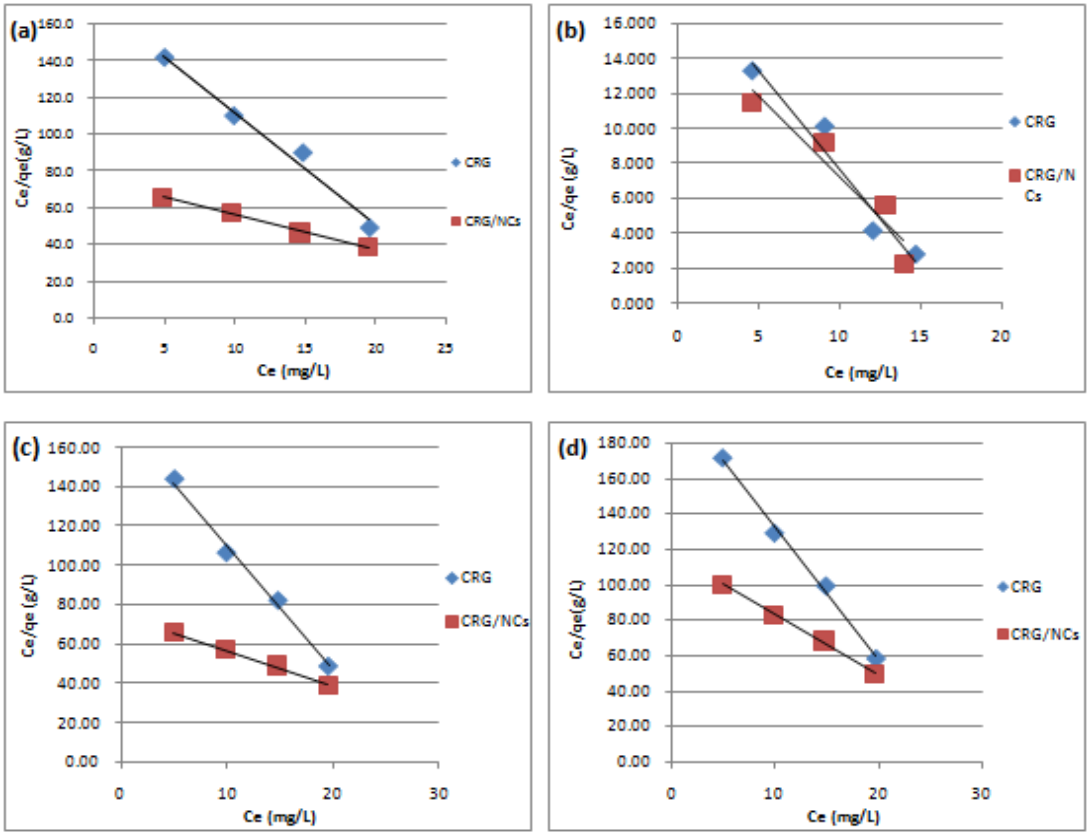

Figure 18.2: Langmuir plot for Ibuprofen adsorption on (Carrageenan and Carrageenan/NCs). Temperature= (a)10^{o}C, (b) 25^{o}C,(c) 35^{o}C, (d) 50^{o}C , pH= 2, time= 5 min., Volume= 50 mL, adsorbent dosage= 0.05 g.

Table 3.2 (a): Langmuir isotherm model parameters and correlation coefficient for adsorption of Ibuprofen on Carrageenan at 10, 25, 35 and 50° C.

Model	Parameter	Temperature(°C)			
		10	25	35	50
Langmuir isotherm (CRG)	q_{max}(mg/g)	160	536.9	150	130.2
	K_L (L/mg)	0.153	0.31	0.15	0.138
	R_L	0.246	0.138	0.25	0.265
	R^2	0.982	0.970	0.994	0.995

Table 3.2 (b): Langmuir isotherm model parameters and correlation coefficient for adsorption of IBP on CRG/NCs at 10, 25, 35 and 50 C°.

Model	Parameter	Temperature(C°)			
		10	25	35	50
Langmuir isotherm (CRG/NCs)	q_{max}(mg/g)	405.5	672.4	221.9	122.2
	K_L (L/mg)	0.298	0.549	0.205	0.177
	R_L	0.143	0.083	0.196	0.22
	R^2	0.994	0.97	0.997	0.997

- **Acetyl β-CD/NCs and Benzoyl β-CD/NCs**

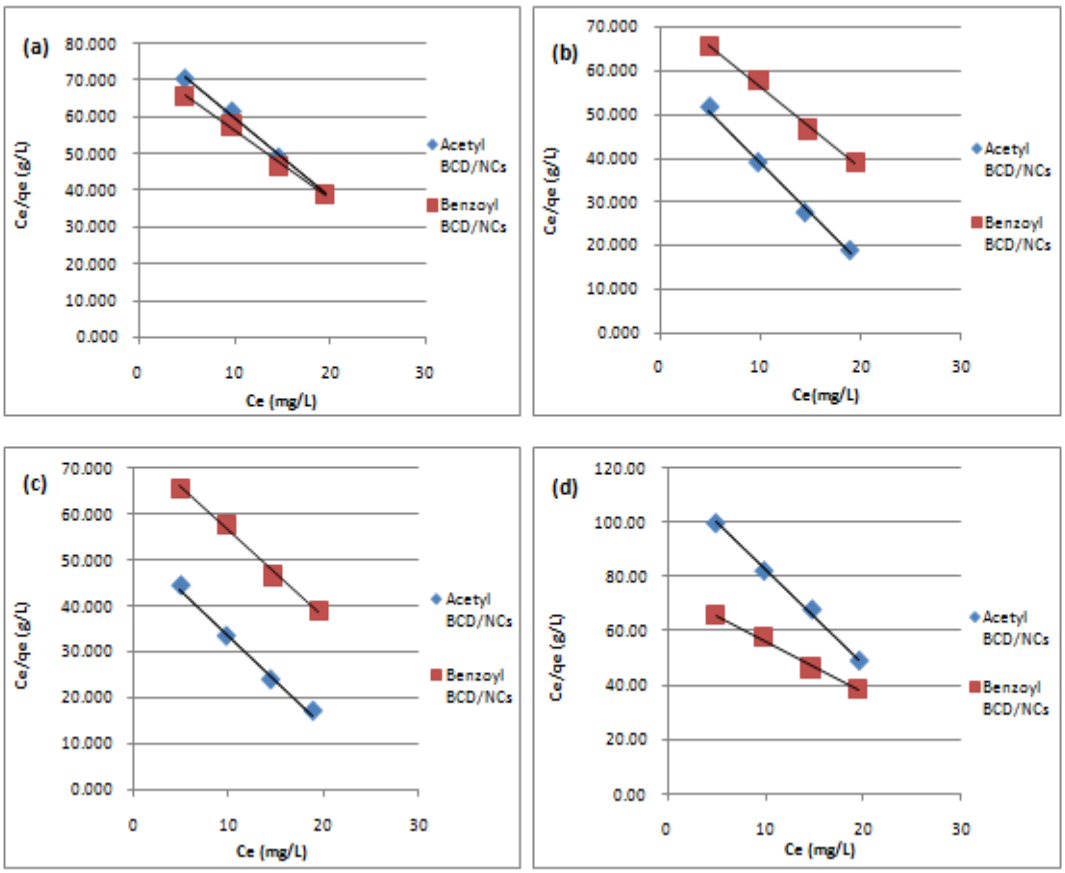

Figure 18.3: Langmuir plot for Ibuprofen adsorption on (Acetyl βCD/NCs and Benzoyl βCD/NCs). Temperature= (a)10ºC, (b) 25ºC,(c) 35ºC, (d) 50ºC , pH= 2, time= 40 min.,5min respectively, Volume= 50 mL, adsorbent dosage= 0.05 g.

Table 3.3 (a): Langmuir isotherm model parameters and correlation coefficient for adsorption of Ibuprofen on Acetyl βCD/NCs at 10, 25, 35 and 50° C.

Model	Parameter	Temperature(°C)			
		10	25	35	50
Langmuir isotherm (Acetyl βCD/NCs)	q_{max}(mg/g)	446.7	411.9	431.2	303.1
	K_L (L/mg)	0.287	0.253	0.281	0.220
	R_L	0.148	0.165	0.151	0.185
	R^2	0.996	0.995	0.992	0.997

Table 3.3 (b): Langmuir isotherm model parameters and correlation coefficient for adsorption of IBP on Benzoyl βCD/NCs at 10, 25, 35 and 50 C°.

Model	Parameter	Temperature(C°)			
		10	25	35	50
Langmuir isotherm (Benzoyl βCD/NCs)	q_{max}(mg/g)	417.5	602.9	241.1	172.2
	K_L (L/mg)	0.348	0.491	0.237	0.199
	R_L	0.125	0.092	0.174	0.200
	R^2	0.994	0.979	0.997	0.997

3.3.2. Freundlich model Isotherm

Freundlich model includes interaction between the Ibuprofen molecules adsorbed in which includes heterogeneous surface energies system and given by Eq.3.4 :

$$q_e = K_F C_e^{1/n} \tag{3.4}$$

The linear form of this equation can be written as:

$$\ln q_e = \ln K_F + \frac{1}{n} \ln C_e \tag{3.5}$$

Where K_F (L /mg) is the Freundlich isotherm constant, n is constant relating to adsorption intensity, If values of 1/n is below one it indicates a normal adsorption and If n value is between 1-10, this suggested a favorable sorption process [170].

To determine the constants n and K_F, the linear form of the equation may be used to plot a scheme of $\ln(q_e)$ vs. $\ln(C_e)$ as shown in the following Figures 19 (1, 2, 3)

- **NCs, MNCs and AgNCs**

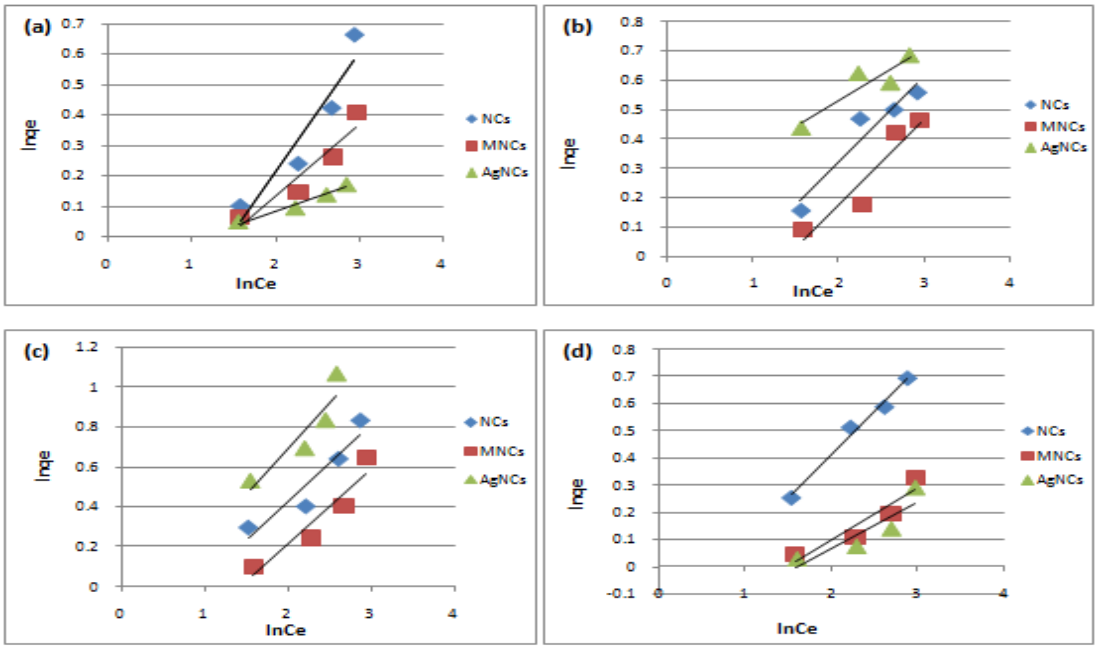

Figure 19.1: Freundlich plot for IBP adsorption on (NCs, MNCs and AgNCs). Temperature= (a)10°C, (b) 25°C,(c) 35°C, (d) 50°C , pH= 2, time= 180 min., Solution Volume= 50 mL, adsorbent dose= 0.05 g.

Freundlich constants K_F , 1/n and regression constant (R^2) were determined and values for all adsorbents are shown in table 3.4 (a, b and c), table 3.5 (a, b) and table 3.6 (a, b)

Table 3.4 (a): Freundlich isotherm model parameters and correlation coefficient for adsorption of IBP on NCs at 10, 25, 35 and 50 C°.

Model	Parameter	Temperature(C°)			
		10	25	35	50
Freundlich isotherm (NCs)	1/n	0.391	0.294	0.398	0.318
	K_F (L/mg)	30.33	14.01	34.12	9.77
	R^2	0.896	0.918	0.887	0.986

Table 3.4 (b): Freundlich isotherm model parameters and correlation coefficient for adsorption of IBP on MNCs at 10, 25, 35 and 50 C°.

Freundlich isotherm (MNCs)	1/n	0.233	0.295	0.372	0.172
	K_F (L/mg)	28.21	61.5	33.11	16.28
	R^2	0.898	0.895	0.899	0.874

Table 3.4 (c):Freundlich isotherm model parameters and correlation coefficient for for adsorption of IBP on AgNCs at 10, 25, 35 and 50 C°.

Freundlich isotherm (AgNCs)	1/n	0.188	0.175	0.45	0.172
	K_F (L/mg)	6.68	6.05	7.92	16.28
	R^2	0.97	0.844	0.833	0.794

- **Carrageenan and Carrageenan/NCs**

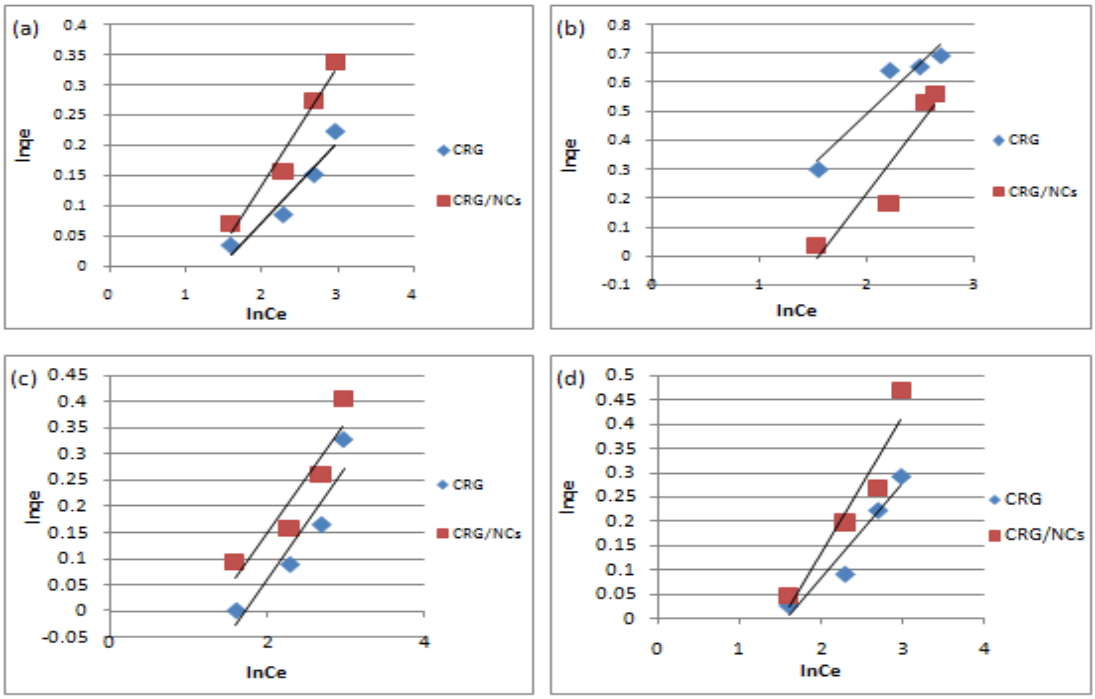

Figure 19.2: Freundlich plot for IBP adsorption on (Carrageenan and Carrageenan/NCs). Temperature= (a)10ºC, (b) 25ºC,(c) 35ºC, (d) 50ºC , pH= 2, time= 5 min., Volume= 50 mL, adsorbent dosage= 0.05 g.

Table 3.5 (a): Freundlich isotherm model parameters and correlation coefficient for adsorption of IBP on CRG at 10, 25, 35 and 50 C°.

Model	Parameter	Temperature(C°)			
		10	25	35	50
Freundlich isotherm (CRG)	1/n	0.132	0.348	0.219	0.305
	K_F (L/mg)	18.3	7.7	43.8	21.11
	R^2	0.924	0.915	0.875	0.926

Table 3.5 (b): Freundlich isotherm model parameters and correlation coefficient for adsorption of IBP on CRG/NCs at 10, 25, 35 and 50 C°.

Freundlich isotherm (CRG/NCs)	1/n	0.194	0.481	0.211	0.28
	K_F (L/mg)	12.42	29.96	19.8	38.71
	R^2	0.962	0.881	0.868	0.91

- **Acetyl β-CD/NCs and Benzoyl β-CD/NCs**

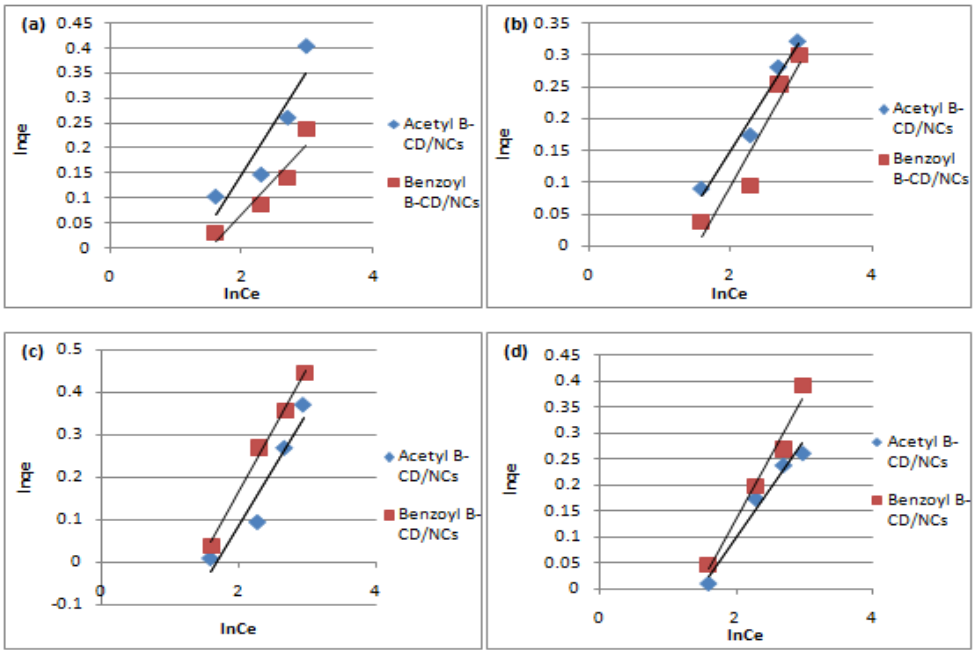

Figure 19.3: Freundlich plot for IBP adsorption on (Acetyl βCD/NCs and Benzoyl βCD/NCs). Temperature= (a)10ºC, (b) 25ºC,(c) 35ºC, (d) 50ºC , pH= 2, time= 40 min., 5min respectively, Volume= 50 mL, adsorbent dosage= 0.05 g.

Table 3.6 (a): Freundlich isotherm model parameters and correlation coefficient for adsorption of Ibuprofen on Acetyl βCD/NCs at 10, 25, 35 and 50° C.

Model	Parameter	Temperature(C°)			
		10	25	35	50
Freundlich isotherm (Acetyl βCD/NCs)	1/n	0.205	0.176	0.268	0.188
	K_F (L/mg)	14.46	17.4	61.4	28.5
	R^2	0.833	0.971	0.92	0.971

Table 3.6 (b): Freundlich isotherm model parameters and correlation coefficient for adsorption of IBP on Benzoyl βCD/NCs at 10, 25, 35 and 50 C°.

Freundlich isotherm (Benzoyl βCD/NCs)	1/n	0.14	0.198	0.291	0.237
	K_F (L/mg)	9.33	20.28	60.3	22.9
	R^2	0.889	0.904	0.993	0.974

- **All parameters and correlation coefficient of Langmuir, Freundlich shown bellow in table 3.7 (a, b and c), table 3.8 (a, b) and table 3.9 (a, b)**

- **NCs, MNCs and AgNCs**

Table 3.7 (a): Parameters and correlation coefficient of Langmuir, Freundlich for adsorption of IBP on NCs at 10, 25, 35 and 50 C°.

Model	Parameter	Temperature(°C)			
		10	25	35	50
Langmuir isotherm (NCs)	q_{max}(mg/g)	503	416.3	450.1	312.2
	K_L (L/mg)	0.35	0.249	0.293	0.260
	R_L	0.125	0.167	0.146	0.161
	R^2	0.998	0.993	0.994	0.998
Freundlich isotherm (NCs)	1/n	0.44	0.37	0.35	0.35
	K_F (L/mg)	14. 51	22.62	25.7	30.32
	R^2	0.986	0.986	0.990	0.982

Table 3.7 (b): Parameters and correlation coefficient of Langmuir, Freundlich and for adsorption of IBP on MNCs at 10, 25, 35 and 50°C.

Model	Parameter	Temperature(°C)			
		15	30	35	50
Langmuir isotherm (Magnetic NCs)	q_{max}(mg/g)	455.5	401.5	421.9	328.2
	K_L (L/mg)	0.280	0.221	0.265	0.203
	R_L	0.151	0.184	0.158	0.197
	R^2	0.996	0.995	0.992	0.997
Freundlich isotherm (Magnetic NCs)	1/n	0.233	0.295	0.372	0.172
	K_F (L/mg)	28.21	61.5	33.11	16.28
	R^2	0.898	0.895	0.899	0.874

Table 3.7 (c): Parameters and correlation coefficient of Langmuir, Freundlich and for adsorption of IBP on AgNCs at 10, 25, 35 and 50°C.

Model	Parameter	Temperature(°C)			
		10	25	35	50
Langmuir isotherm (AgNCs)	q_{max}(mg/g)	643.9	601.3	543.11	196.2
	K_L (L/mg)	0.576	0.530	0.470	0.370
	R_L	0.079	0.086	0.096	0.119
	R^2	0.995	0.989	0.989	0.995
Freundlich isotherm (AgNCs)	1/n	0.188	0.175	0.45	0.172
	K_F (L/mg)	6.68	6.05	7.92	16.28
	R^2	0.97	0.844	0.833	0.794

- **CRG and CRG/NCs**

Table 3.8 (a): Parameters and correlation coefficient of Langmuir, Freundlich for adsorption of IBP on CRG at 10, 25, 35 and 50 C°.

Model	Parameter	Temperature(°C)			
		10	25	35	50
Langmuir isotherm (CRG)	q_{max}(mg/g)	160	536.9	150	130.2
	K_L (L/mg)	0.153	0.31	0.15	0.138
	R_L	0.246	0.138	0.25	0.265
	R^2	0.982	0.970	0.994	0.995
Freundlich isotherm (CRG)	1/n	0.132	0.348	0.219	0.305
	K_F (L/mg)	19.3	7.7	43.8	21.11
	R^2	0.924	0.915	0.875	0.926

Table 3.8 (b): Parameters and correlation coefficient of Langmuir, Freundlich and for adsorption of IBP on CRG/NCs at 10, 25, 35 and 50°C.

Model	Parameter	Temperature(°C)			
		10	25	35	50
Langmuir isotherm (CRG/NCs)	q_{max}(mg/g)	405.5	672.4	221.9	122.2
	K_L (L/mg)	0.298	0.549	0.205	0.177
	R_L	0.143	0.083	0.196	0.22
	R^2	0.994	0.97	0.997	0.997
Freundlich isotherm (CRG/NCs)	1/n	0.194	0.481	0.211	0.28
	K_F (L/mg)	12.42	29.96	19.8	38.71
	R^2	0.962	0.881	0.868	0.91

- **Acetyl β-CD/NCs and Benzoyl β-CD/NCs**

Table 3.9 (a): Parameters and correlation coefficient of Langmuir, Freundlich for adsorption of IBP on Acetyl β-CD/NCs at 10, 25, 35 and 50 C°.

Model	Parameter	Temperature(°C)			
		10	25	35	50
Langmuir isotherm (Acetyl β-CD/NCs)	q_{max}(mg/g)	446.7	411.9	431.2	303.1
	K_L (L/mg)	0.287	0.253	0.281	0.220
	R_L	0.148	0.165	0.151	0.185
	R^2	0.996	0.995	0.992	0.997
Freundlich isotherm (Acetyl β-CD/NCs)	1/n	0.205	0.176	0.268	0.188
	K_F (L/mg)	14.46	17.4	61.4	28.5
	R^2	0.833	0.971	0.92	0.971

Table 3.9 (b): Parameters and correlation coefficient of Langmuir, Freundlich and for adsorption of IBP on Benzoyl β-CD/NCs at 10, 25, 35 and 50°C.

Model	Parameter	Temperature(°C)			
		10	25	35	50
Langmuir isotherm (Benzoyl β-CD/NCs)	q_{max}(mg/g)	417.5	602.9	241.1	172.2
	K_L (L/mg)	0.348	0.491	0.237	0.199
	R_L	0.125	0.092	0.174	0.200
	R^2	0.994	0.979	0.997	0.997
Freundlich isotherm (Benzoyl β-CD/NCs)	1/n	0.14	0.198	0.291	0.237
	K_F (L/mg)	9.33	20.28	60.3	22.9
	R^2	0.889	0.904	0.993	0.974

The Langmuir and Freundlich isotherms for the adsorption of Ibuprofen on each adsorbent, at pH =2 and different temperatures, were fitted to the experimental data as summarized in tables 3.7, 3.8 and 3.9

Based on the value of R^2, Langmuir isotherm was selected. To adjust the data into the Langmuir adsorption isotherm, the value R^2 should be 0.87–1, indicating that the experimental data fits strongly into the individual regression.

In the current study, all the R^2 values satisfied this condition and greater values of R^2 were found in Langmuir adsorption isotherm, that all fitting parameters in all the cases, the experimental results were fitted better to the Langmuir model as the correlation coefficient of the Langmuir graph ($R^2 \geq$ 0.97) were show much higher values than the values obtained for the fitting of the Freundlich model. while the values of 1/n (0.13 – 0.481) which indicates high adsorption intensity, this suggesting that all the functional groups of Ibuprofen are homogeneously spread over the outer porous surfaces of adsorbents. And we can have confirmed that by similar results for Ibuprofen removal using Activated Carbon [171].

3.4 Adsorption kinetics of Ibuprofen

The adsorption of IBP on the adsorbent surfaces were kinetically studied for each adsorbent at four different concentrations of 50 ppm, 100 ppm, 150 ppm and 200 ppm. The experimental data were dynamically fitted to the pseudo-first and pseudo-second orders and the model of intra particle diffusion of adsorbate as equations (3.6 -3.8):

For pseudo-first order equation:

$$\ln(q_e - q_t) = \ln q_e - \left(\frac{K1}{2.303}\right) t \qquad (3.6)$$

For pseudo second-order equation:

$$\frac{t}{q_t} = \frac{1}{q_e} t + \frac{1}{K_2 q_e^2} \quad (3.7)$$

The intraparticle diffusion model equation is

$$q_t = K_{id}\, t^{1/2} + Z \quad (3.8)$$

where q_e and q_t are uptake capacity (mg/g) at equilibrium and time t (min), respectively, K_1 is the rate constant of pseudo-first-order (1/min), K_2 is the equilibrium rate constant of pseudo-second-order (g /mg.min). The K_{id} is the intra-particle diffusion rate constant (mg/ g.min$^{1/2}$) while Z defined as the boundary layer thickness (mg/ g) [172]. The values of all these parameters are presented in tables 3.10 (a, b, c), table 11(a, b), table 12 (a, b) and Figs 20(1, 2, 3) and 21(1, 2, 3). The value of K_1 was obtained by plotting ln(q_e – q_t) vs. time; meanwhile K_2 and q_e where established from the slope and the intercept of plotting t/qt vs. t. While K_{id} and Z obtained from plotting q_t vs. $t^{1/2}$, and the values of R^2 were compared.

It was obviously shown that the adsorption of Ibuprofen onto the adsorbents surfaces follow the pseudo-second order as the values of the correlation coefficients reach $R^2 \geq 0.997$. The coefficients of determination (R^2) of the pseudo-first order fitted showed a very unfavourable results, suggesting that this model did not adapt to the experimental data.

Other indication also came from the values of qe_{cal}, in which ibuprofen sorption at equilibrium determined using pseudo-first and pseudo-second order rate equations, was confronted with the experimental values, qe_{exp}. Suggesting that the adsorption system of IBP on the adsorbent samples were

followed and described by the pseudo-second-order because the qe_{cal} is very closer to qe_{exp} in pseudo-second order in contrast of the calculated first-order qe that give too low values compared with experimental one see Tables 3. (10, 11, 12) and Fig. 21(1, 2, 3).

This meaning that the second -order kinetics is higher compared to other models for Ibuprofen adsorption on these adsorbents.

The pseudo-second-order constant k_2 values which determined at concentration 200 was higher than that at concentration 50 meaning that the Ibuprofen adsorption at concentration 200 need more dose of adsorbents than at concentration 50. As a consequence, the adsorbents has higher affinity for IBP at lower concentrations.

Decreasing of the pseudo second order rate constant values (k_2) as following order: Acetyl β-CD/NCs >CRG/NCs >CRG >NCs >AgNCs >MNCs >Benzoyl β-CD/NCs, it may related to the mesoporosity of the adsorbents structure, as the slowest IBP adsorption kinetic have higher micropore volume [173, 174].

- **Pseudo first order**

▪ **NCs, MNCs, AgNCs**

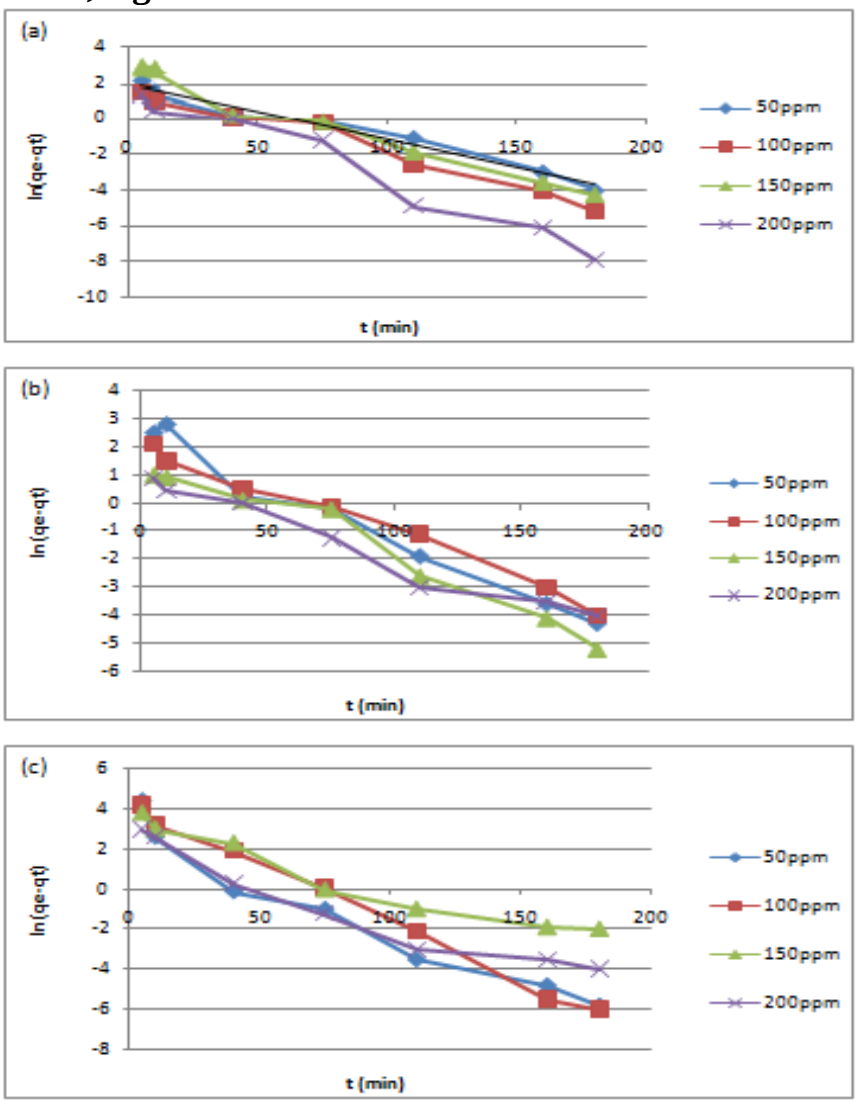

Figure 20.1: Pseudo first order sorption kinetics of IBP on (a) NCs, (b) MNCs and (c) AgNCs. (Temperature= 25ºC, pH= 10, Solution volume= 50 mL, adsorbent dosage= 0.1 g).

- **CRG, CRG/NCs**

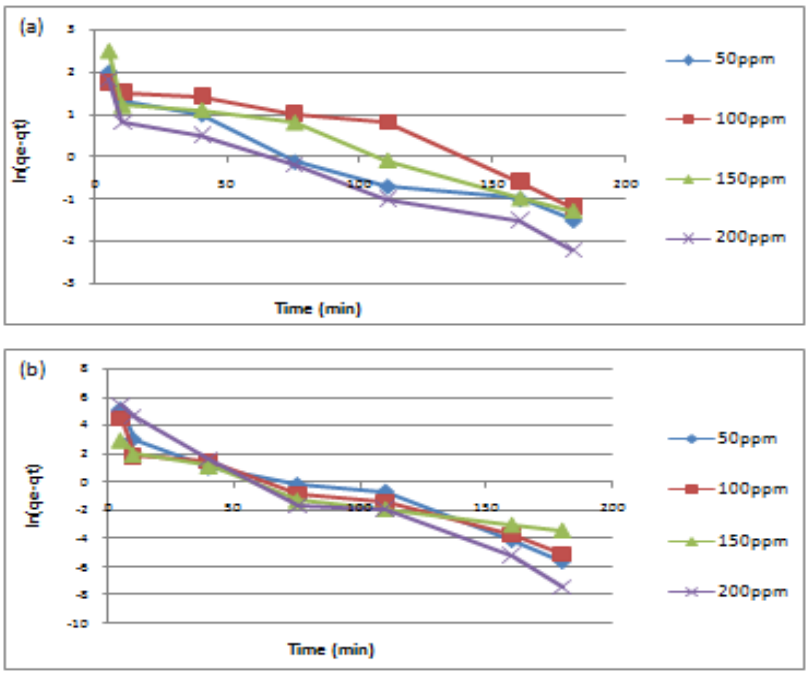

Figure 20.2: Pseudo first order sorption kinetics of IBP on (a) CRG, (b) CRG/NCs.

(Temperature= 25°C, pH= 7, Solution volume= 50 mL, adsorbent dosage= 0.1 g)

- **Acetyl β-CD/NCs and Benzoyl β-CD/NCs**

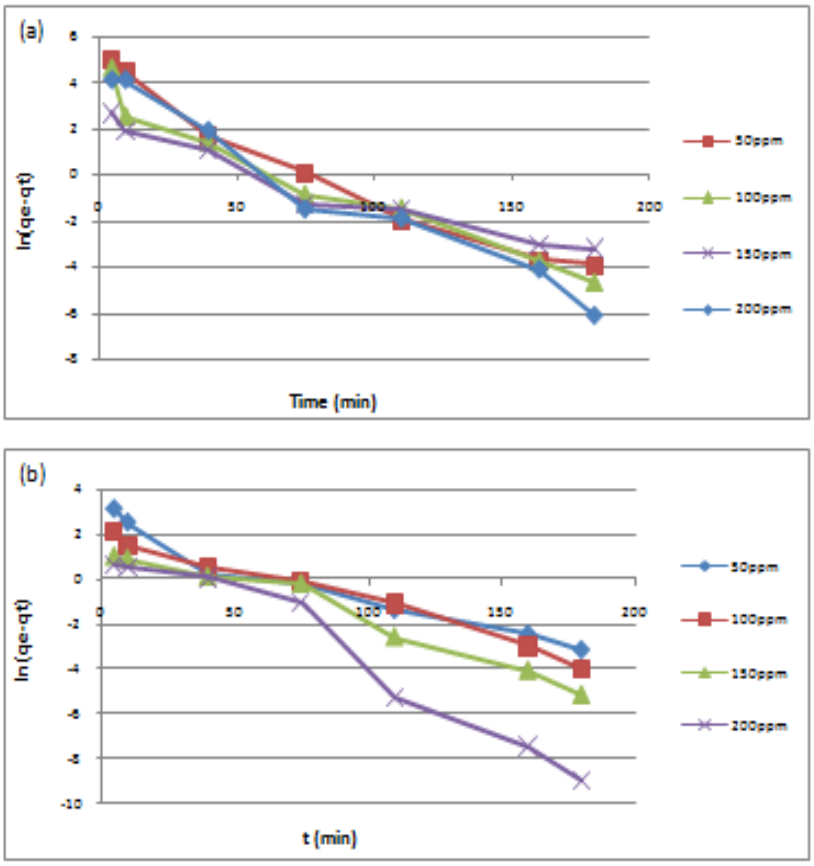

Figure 20.3: Pseudo first order sorption kinetics of IBP on (a) Acetyl βCD/NCs, (b) Benzoyl βCD/NCs. (Temperature= 25°C, pH= 7, Solution volume= 50 mL, adsorbent dosage= 0.1 g)

- **Pseudo second order**

▪ **NCs, MNCs and AgNCs**

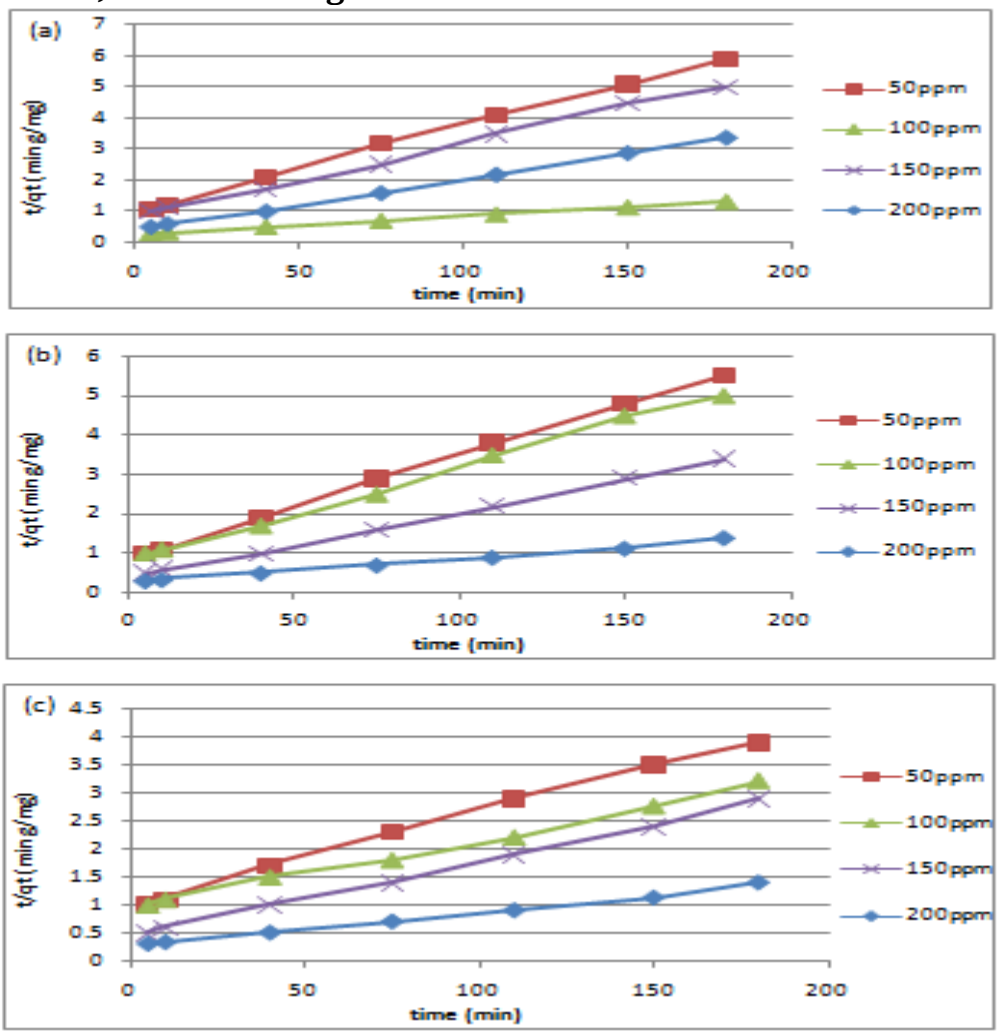

Figure 21.1: Pseudo second order adsorption kinetics of IBP on (a)NCs, (b) MNCs and (c) AgNCs). (Temperature= 25ºC, pH= 10, solution Volume= 50 mL, adsorbent dose= 0.1 g)

- **CRG and CRG/NCs**

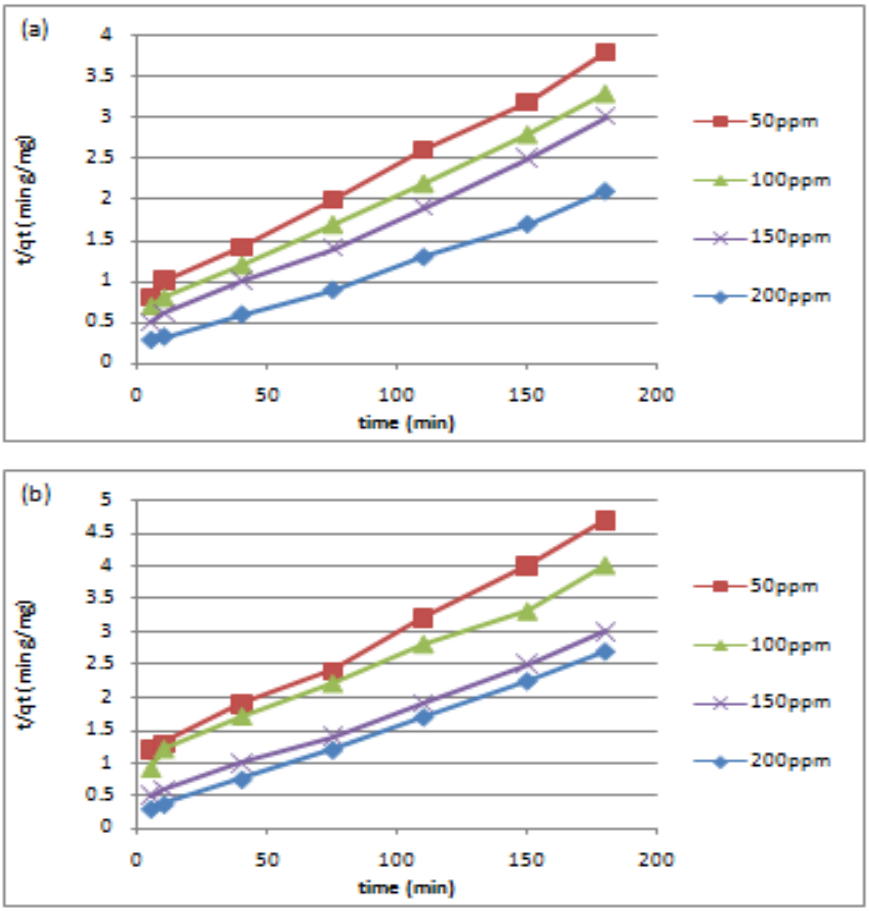

Figure 21.2: Pseudo second order adsorption kinetics of IBP on (a) CRG, (b) CRG/NCs. (Temperature= 25ºC, pH= 7, Solution volume= 50 mL, adsorbent dosage= 0.1 g)

- **Acetyl β-CD/NCs and Benzoyl β-CD/NCs**

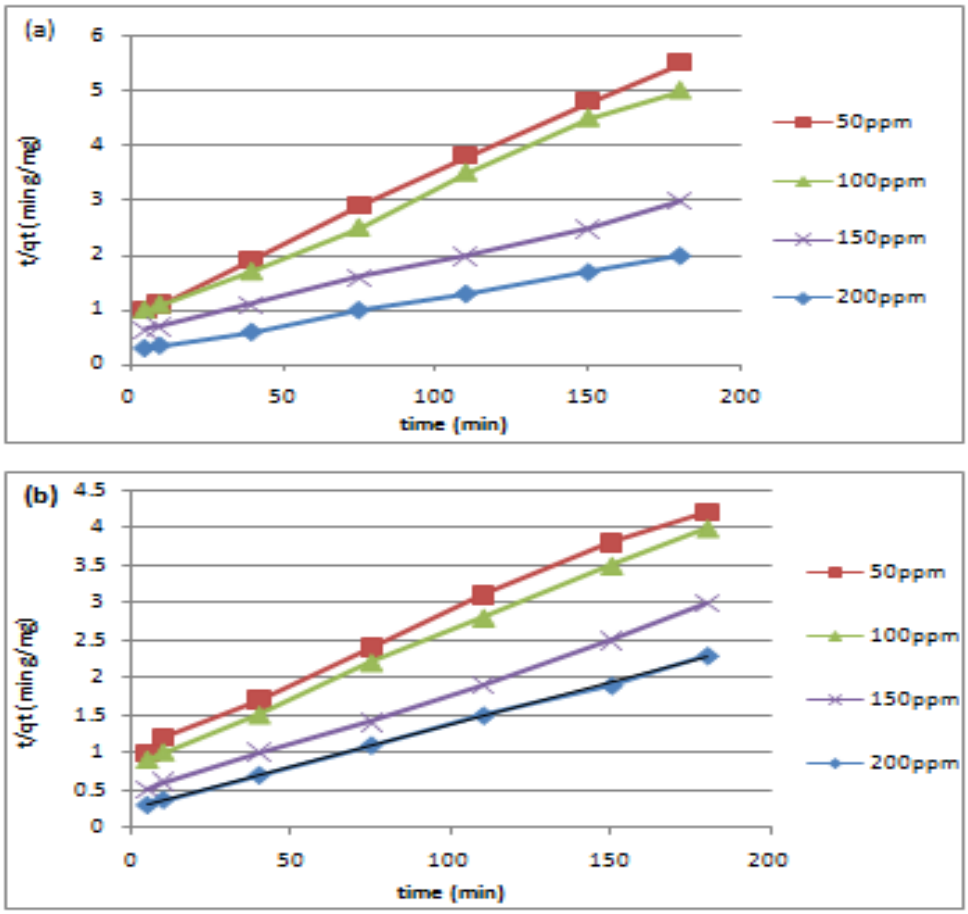

Figure 21.3: Pseudo second order adsorption kinetics of IBP on (a) Acetyl β-CD/NCs and (b) Benzoyl β-CD/NCs. (Temperature= 25°C, pH= 7, Solution volume= 50 mL, adsorbent dosage= 0.1 g)

- **NCs, MNCs and AgNCs**

Table 3.10 (a) Pseudo first and second orders kinetic model parameters for IBP adsorption on NCs at 25ºC.

C_0 (mg/L)	q_e (exp) (mg/g)	Pseudo-first -order model		
		K_1 (min^{-1})	q_{cal}(mg/g)	R^2
50	36.67	0.0389	20.13	0.977
100	49.24	0.0411	12.49	0.976
150	61.94	0.0691	33.40	0.972
200	82.22	0.053	22.1	0.965
C_0 (mg/L)	q_e (exp) (mg/g)	Pseudo-second -order model		
		K_2 (g/mg.min)	q_{cal}(mg/g)	R^2
50	36.67	0.0071	35.79	0.998
100	49.24	0.0627	48.82	1
150	61.94	0.0211	62.7	0.998
200	82.22	0.0758	83.29	0.999

Table 3.10 (b) Pseudo first and second orders kinetic model parameters for IBP adsorption MNCs at 25ºC.

C_0 (mg/L)	q_e (exp) (mg/g)	Pseudo-first -order model		
		K_1 (min^{-1})	q_{cal}(mg/g)	R^2
50	33.15	0.0399	14.51	0.971
100	66.3	0.0332	17.3	0.975
150	73.23	0.0252	26.79	0.968
200	87.89	0.0464	32.25	0.961
C_0 (mg/L)	q_e (exp) (mg/g)	Pseudo-second -order model		
		K_2 (g/mg.min)	q_{cal}(mg/g)	R^2
50	33.15	0.00701	33.92	0.999
100	66.3	0.00992	65.73	0.998
150	73.23	0.0204	72.19	0.999
200	87.89	0.0399	88.55	0.999

Table 3.10 (c) Pseudo first and second orders kinetic model parameters for IBP adsorption AgNCs at 25ºC.

C_0 (mg/L)	q_e (exp) (mg/g)	Pseudo-first -order model		
		K_1 (min^{-1})	q_{cal}(mg/g)	R^2
50	39.12	0.050	14.92	0.943
100	79.15	0.035	15.34	0.979
150	88.45	0.027	10.7	0.938
200	97.55	0.0520	23.2	0.930
C_0 (mg/L)	q_e (exp) (mg/g)	Pseudo-second -order model		
		K_2 (g/mg.min)	q_{cal}(mg/g)	R^2
50	39.12	$8.8 * 10^{-3}$	37.99	0.997
100	79.15	$9.6 * 10^{-3}$	78.8	0.999
150	88.45	$1.71 * 10^{-2}$	88.01	0.998
200	97.55	$5.7 * 10^{-2}$	96.98	0.999

- **CRG and CRG/NCs**

Table 3.11 (a) Pseudo first and second orders kinetic model parameters for IBP adsorption on CRG at 25ºC.

C_0 (mg/L)	q_e (exp) (mg/g)	Pseudo-first -order model		
		K_1 (min^{-1})	q_{cal}(mg/g)	R^2
50	25.5	0.0299	39.51	0.941
100	37.59	0.0397	22.4	0.921
150	52.9	0.0685	40.87	0.926
200	90.81	0.0490	39.71	0.953
C_0 (mg/L)	q_e (exp) (mg/g)	Pseudo-second -order model		
		K_2 (g/mg.min)	q_{cal}(mg/g)	R^2
50	25.5	0.00563	25.01	0.998
100	37.59	0.00389	36.6	0.999
150	52.9	0.021	53.87	0.999
200	90.81	0.0786	91.92	0.997

Table 3.11 (b) Pseudo first and second orders kinetic model parameters for IBP adsorption CRG/NCs at 25ºC.

C_0 (mg/L)	q_e (exp) (mg/g)	Pseudo-first -order model		
		K_1 (min^{-1})	q_{cal}(mg/g)	R^2
50	40.9	0.0434	15.11	0.951
100	70.98	0.0384	27.3	0.946
150	88.56	0.0274	19.19	0.942
200	90.71	0.0420	28.05	0.967
C_0 (mg/L)	q_e (exp) (mg/g)	Pseudo-second -order model		
		K_2 (g/mg.min)	q_{cal}(mg/g)	R^2
50	40.9	0.00684	42.02	0.997
100	70.98	0.00951	71.13	0.997
150	88.56	0.017	86.09	0.999
200	90.71	0.0917	93.17	0.999

- **Acetyl β-CD/NCs and Benzoyl β-CD/NCs**

Table 3.12 (a) Pseudo first and second orders kinetic model parameters for IBP adsorption on Acetyl β-CD/NCs at 25ºC.

C_0 (mg/L)	q_e (exp) (mg/g)	Pseudo-first -order model		
		K_1 (min^{-1})	q_{cal}(mg/g)	R^2
50	26.92	0.043	10.1	0.943
100	37.81	0.0499	14.7	0.975
150	49.99	0.0705	20.14	0.968
200	69.15	0.061	31.79	0.956
C_0 (mg/L)	q_e (exp) (mg/g)	Pseudo-second -order model		
		K_2 (g/mg.min)	q_{cal}(mg/g)	R^2
50	26.92	0.00701	23.99	0.999
100	37.81	0.00992	39.03	0.998
150	49.99	0.0404	50.79	0.998
200	69.15	0.0989	71.24	0.999

Table 3.12 (b) Pseudo first and second orders kinetic model parameters for IBP adsorption Benzoyl β-CD/NCs at 25ºC.

C_0 (mg/L)	q_e (exp) (mg/g)	Pseudo-first -order model		
		K_1 (min^{-1})	q_{cal}(mg/g)	R^2
50	33.15	0.0399	14.51	0.971
100	66.3	0.0332	17.3	0.975
150	73.23	0.0252	16.79	0.968
200	87.89	0.0464	32.25	0.961
C_0 (mg/L)	q_e (exp) (mg/g)	Pseudo-second -order model		
		K_2 (g/mg.min)	q_{cal}(mg/g)	R^2
50	33.15	0.00713	34.08	0.997
100	66.3	0.00997	67.01	1
150	73.23	0.0165	74.91	0.998
200	87.89	0.0223	88.5	1

As shown in Figures 22(1,2,3) and Tables in the following pages, the intraparticle diffusion plot of the adsorption of ibuprofen on adsorbent samples at different concentrations (50 ppm, 100 ppm, 150 ppm and 200 ppm) were studied using some calculations which was studied by Weber and Morris and the model they proposed using eq.(3.8).

From plotting qt vs. $t^{1/2}$ see Figs.22(1, 2, 3) we can indicate at first the instantaneous adsorption, in which the linear portion passes through the origin indicated that the rate of adsorption is controlled by the intraparticle diffusion. The next stage we suggest that the regression is nearly linear and a plateau but does not passing through the origin, which controlled by some external diffusion, intraparticle diffusion and interaction, the process of the rate limiting was not the only rate limiting mechanism in the adsorption (i.e., the diffusion from the bulk phase to the external surface of the adsorbent is the fastest [175]) [176]. Generally, If the linear portion passes through the

origin, the adsorption process is controlled by intraparticle diffusion, if not, the sorption controlled by both intraparticle diffusion and exterior surface adsorption [177-178].

Also we can obtain the values of K_{id} and Z from the Figures. The values are presented in Tables 13(a, b, c), 14(a, b) and 15(a, b). The final stage also linear and they were describing the gradual adsorption.

We can observe from the tables that by increase of concentration the values Z were increased and also increasing of the potential of internal mass transfer.

- **NCs, MNCs and AgNCs**

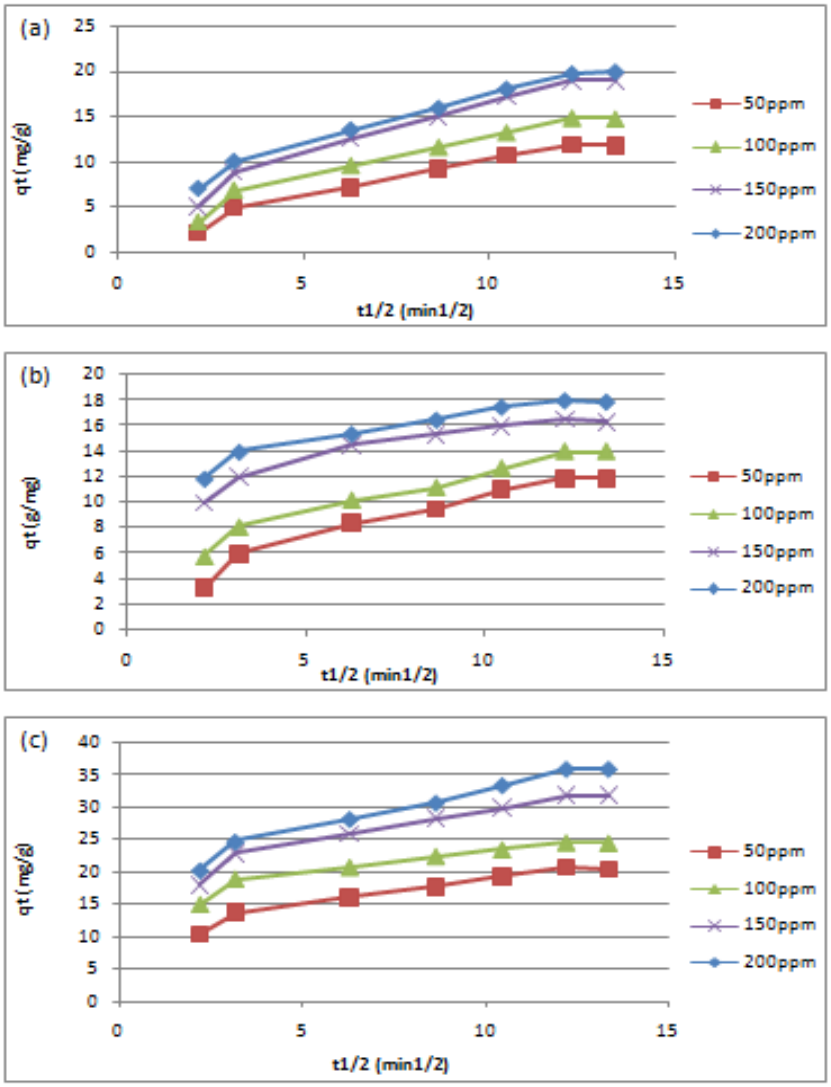

Figure 22.1: The intraparticle diffusion of IBP on (a) NCs, (b) MNCs and (c) AgNCs). (Temperature= 25ºC, pH= 10, solution Volume= 50 mL, adsorbent dose= 0.1 g).

Table 3.13(a)Intraparticle diffusion for various initial concentrations of Ibuprofen by NCs

C_0 (mg /L)	Intraparticle diffusion model	
	K_{id}	Z
50	0.829	1.628
100	0.954	2.904
150	1.192	4.211
200	1.123	5.802

Table 3.13(b) Intraparticle diffusion for various initial concentrations of Ibuprofen by MNCs

C_0 (mg /L)	Intraparticle diffusion model	
	K_{id}	Z
50	0.72	3.046
100	0.694	5.26
150	0.534	10.06
200	0.504	11.81

Table 3.13(c) Intraparticle diffusion for various initial concentrations of Ibuprofen by AgNCs

C_0 (mg /L)	Intraparticle diffusion model	
	K_{id}	Z
50	0.845	10.18
100	0.751	15.37
150	1.136	17.9
200	1.326	19.27

- **CRG and CRG/NCs**

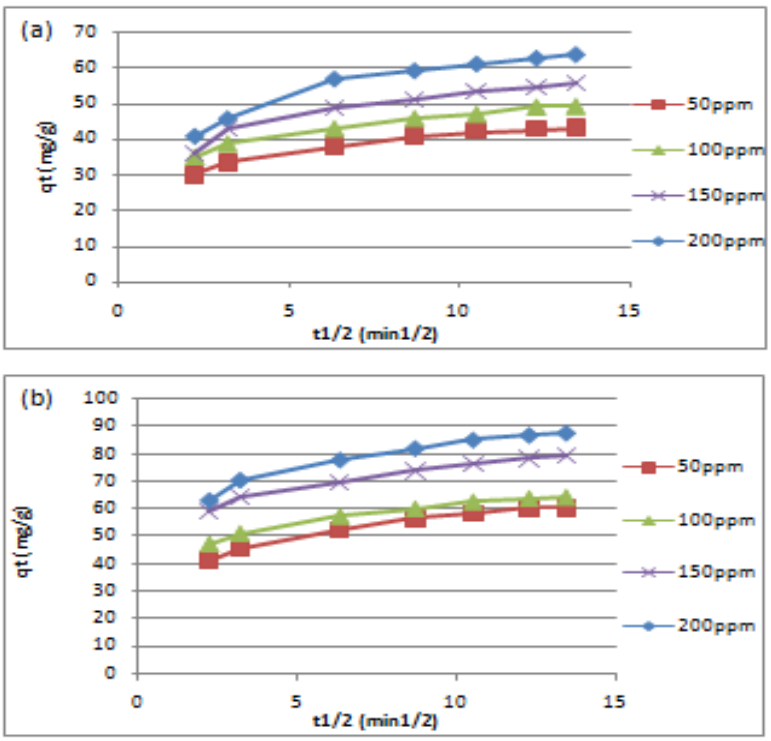

Figure 22.2: The intraparticle diffusion of IBP on (a) CRG, (b) CRG/NCs. (Temperature= 25°C, pH= 7, Solution volume= 50 mL, adsorbent dosage= 0.1 g).

Table 3.14(a)Intraparticle diffusion for various initial concentrations of Ibuprofen by CRG

C_0 (mg /L)	Intraparticle diffusion model	
	K_{id}	Z
50	1.124	29.53
100	1.2	34.3
150	1.567	36.34
200	1.928	40.03

Table 3.14(b) Intraparticle diffusion for various initial concentrations of Ibuprofen by CRG/NCs

C_0 (mg /L)	Intraparticle diffusion model	
	K_{id}	Z
50	1.674	39.92
100	1.487	46.18
150	1.761	57.41
200	2.05	62.52

- **Acetyl β-CD/NCs and Benzoyl β-CD/NCs**

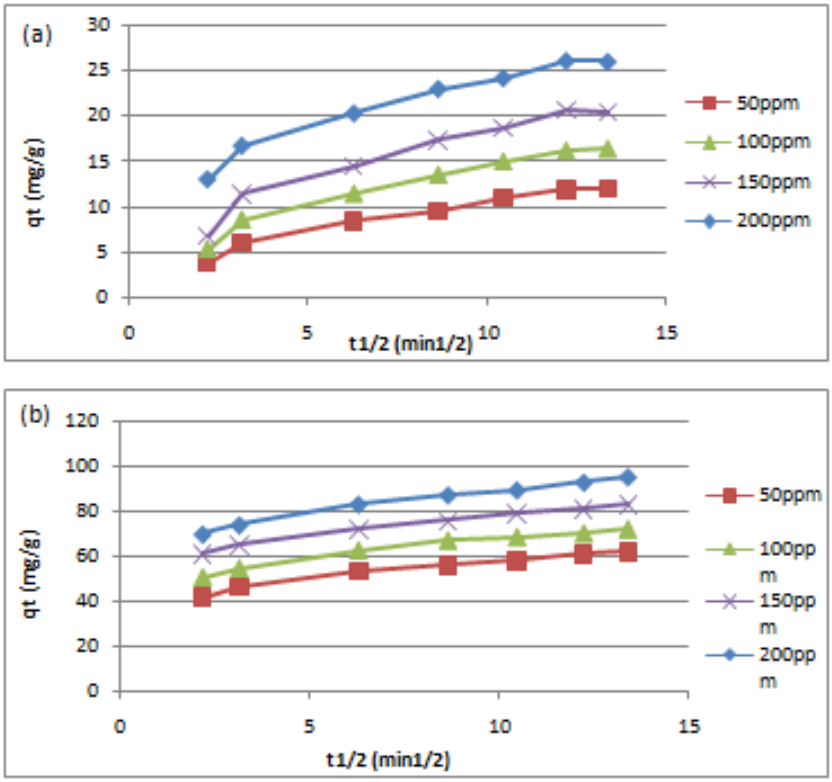

Figure 22.3: The intraparticle diffusion of IBP on (a) Acetyl β-CD/NCs and (b) Benzoyl β-CD/NCs. (Temperature= 25ºC, pH= 7, Solution volume= 50 mL, adsorbent dosage= 0.1 g).

Table 3.15(a)Intraparticle diffusion for various initial concentrations of Ibuprofen by Acetyl β-CD/NCs.

C_0 (mg /L)	Intraparticle diffusion model	
	K_{id}	Z
50	0.699	3.3
100	0.943	4.7
150	1.147	6.478
200	1.109	12.38

Table 3.15(b) Intraparticle diffusion for various initial concentrations of Ibuprofen by Benzoyl β-CD/NCs

C_0 (mg /L)	Intraparticle diffusion model	
	K_{id}	Z
50	1.687	40.79
100	1.809	49.52
150	1.857	59.24
200	2.16	67.64

3.5 Adsorption Thermodynamics parameters at equilibrium

The parameters of thermodynamic were appropriately determined to obtain knowledge about changing of the Gibbs free energy, entropy and enthalpy for the adsorption of IBP using different adsorbents, we obtain the thermodynamics parameters like (K) the equilibrium rate constant (L/g), (ΔG^0) the Gibbs free energy (J/mol), (ΔH^0) the standard enthalpy (J/mol), (ΔS^0) the standard entropy (J/mol.K) using different ranges of temperatures T(K) and perfect gas constant R (J/K.mol). All of these parameters were studied using Van't Hoffs equations (eq.3.10 and 3.11) [179].

$$\ln K_d = \frac{\Delta S}{R} - \frac{\Delta H}{RT} \qquad (3.10)$$

$$\Delta G^0 = -RT\ LnK_d \qquad (3.11)$$

The values of LnK_d were plotted against 1/T (see figs. 23, 24, 25), The plots showed good correlation coefficient values for IBP ($R^2 \geq 0.97$). The slopes and intercept will give us the values of ΔG, ΔS^0 and ΔH^0. The values are shown in Tables (3.16, 3.17, 3.18). The negative ΔG values, implying the spontaneous nature and feasibility of the adsorption process of IBP on the different adsorbents [180] and the free energy increased as the temperature increased indicate that better adsorption when temperature is increased [181].

From the following tables, the ΔS^0 shows positive values which denote that the randomness was increased at the interface of the solid/solution in the adsorption process of IBP on adsorbents, probably due to the competitive adsorption between IBP and solvent molecules (water and methanol) [182], as it considered an important factor that the chemical affinity of IBP adsorption towards adsorbents and water molecules, as the hydrophobicity of this emerging pollutant increased, the affinity toward adsorbents surfaces also increased. So, the chemistry of adsorbents surface have an important role [173].The positive value of ΔH suggested that the uptake of IBP was endothermic in nature [176]. As there is two types of adsorption, chemisorptions and physical adsorption, the ΔG values are in the range -1 to -13 kJ/mol, which suggesting that the sorption are mainly physical [176, 183].

- **NCs, MNCs and AgNCs**

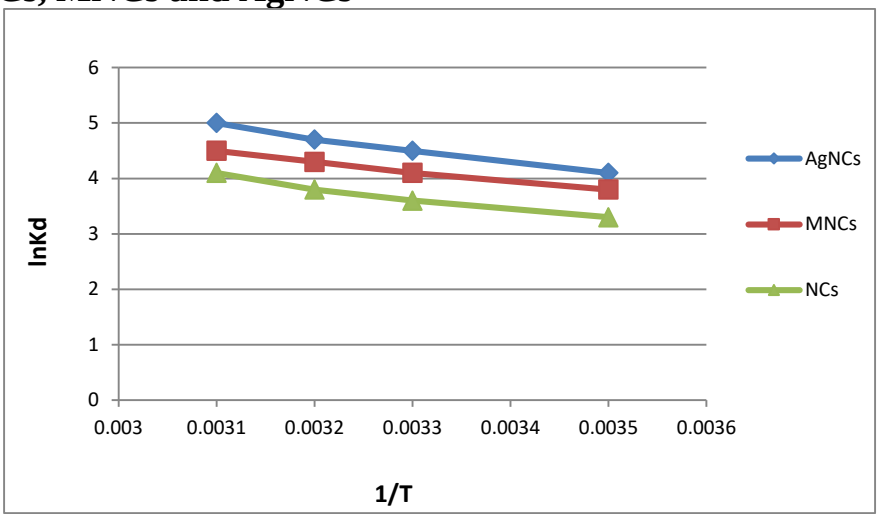

Figure 23: Plot of lnK_d versus 1/T for thermodynamic parameters of IBP adsorption on (NCs, MNCs and AgNCs). (pH= 10, time= 60 min., Solution volume= 20 mL, adsorbent dose= 0.075 g).

Table 3.16(a) Thermodynamic factors for the adsorption of IBP onto NCs ($C_\circ$ = 30 ppm, pH = 10 , t = 60 min, adsorbent dose = 75 mg.

Temperature (K)	ΔG° (KJ/mol)	ΔH° (KJ/mol)	ΔS° (J/K.mol)
283	-7.76	16.1	83.6
298	-8.91		
308	-9.73		
323	-11.01		

Table 3.16(b) Thermodynamic factors for the adsorption of IBP onto MNCs ($C_\circ$ = 30 ppm, pH = 10, t = 60 min ,adsorbent dose = 75 mg.

Temperature (K)	ΔG° (KJ/mol)	ΔH° (KJ/mol)	ΔS° (J/K.mol)
283	-8.94	14.48	82.15
298	-10.15		
308	-11.01		
323	-12.08		

Table 3.16(c) Thermodynamic factors for the adsorption of IBP onto AgNCs ($C_\circ$ = 30 ppm, pH = 10, t = 60 min ,adsorbent dose = 75 mg.

Temperature (K)	ΔG° (KJ/mol)	ΔH° (KJ/mol)	ΔS° (J/K.mol)
283	-9.64	18.29	97.9
298	-11.14		
308	--12.03		
323	-13.42		

- **CRG and CRG/NCs**

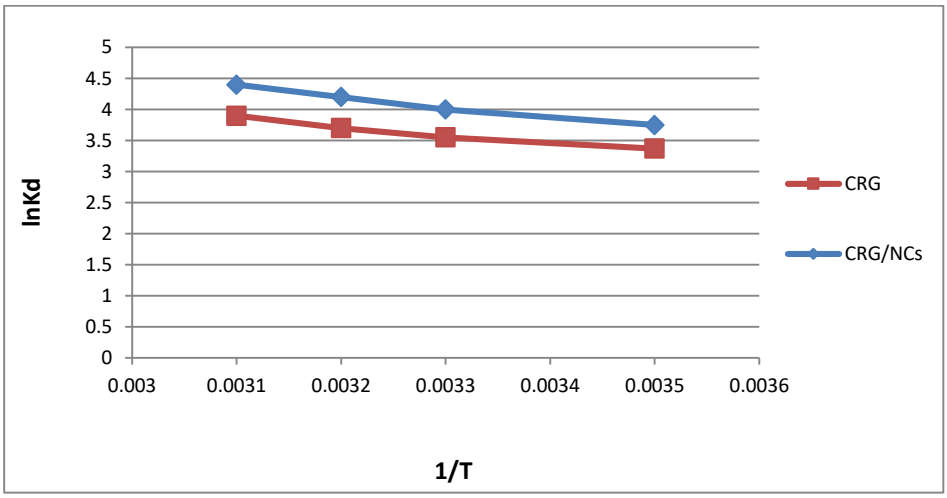

Figure 24: Plot of $\ln K_d$ versus 1/T for thermodynamic parameters of IBP adsorption on (CRG and CRG/NCs). (pH= 7, time= 30 min., Solution volume= 20 mL, adsorbent dose= 0.075 g)

Table 3.17(a) Thermodynamic factors for the adsorption of IBP onto CRG ($C_\circ$ = 30 ppm, pH = 7, t = 30 min ,adsorbent dose = 75 mg.

Table 3.17(b) Thermodynamic factors for the adsorption of IBP onto CRG/NCs ($C_\circ$ = 30 ppm, pH = 7, t = 30 min ,adsorbent dose = 75 mg.

Temperature (K)	ΔG° (KJ/mol)	ΔH° (KJ/mol)	ΔS° (J/K.mol)
283	-8.82	13.41	77.93
298	-9.91		
308	-10.75		
323	-11.81		

- Acetyl β-CD/NCs and Benzoyl β-CD /NCs

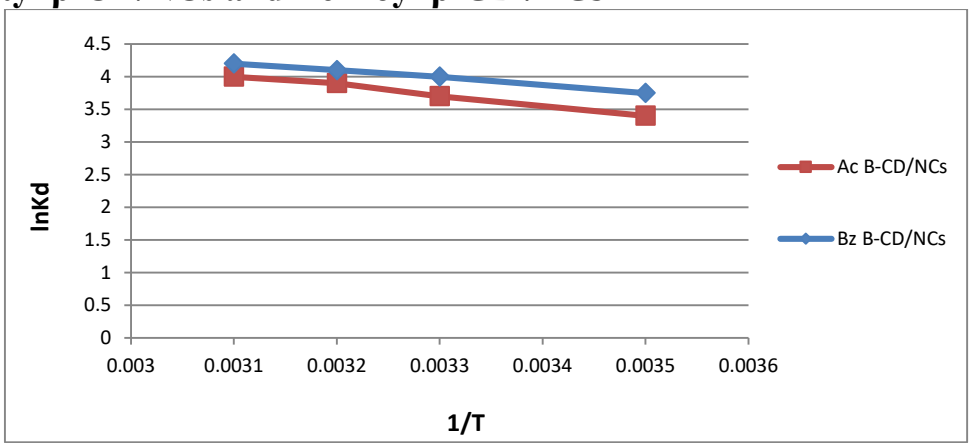

Figure 25: Plot of $\ln K_d$ versus 1/T for thermodynamic parameters of IBP adsorption on (Acetyl β-CD/NCs and Benzoyl β-CD /NCs). (pH= 7, time= 30 min., Solution volume= 20 mL, adsorbent dose= 0.075 g)

Table 3.18(a) Thermodynamic factors for the adsorption of IBP onto Acetyl β-CD/NCs ($C_\circ$ = 30 ppm, pH = 7, t = 30 min, adsorbent dose = 75 mg.

Temperature (K)	ΔG° (KJ/mol)	ΔH° (KJ/mol)	ΔS° (J/K.mol)
283	-7.99	12.82	73.17
298	-9.16		
308	-9.98		
323	-10.74		

Table 3.18 (b) Thermodynamic factors for the adsorption of IBP onto Benzoyl β-CD /NCs ($C_\circ$ = 30 ppm, pH = 7, t = 30 min, adsorbent dose = 75 mg.

Temperature (K)	ΔG° (KJ/mol)	ΔH° (KJ/mol)	ΔS° (J/K.mol)
283	-8.82	9.37	64.08
298	-9.91		
308	-10.49		
323	-11.27		

3.6 Recovery of IBP and reusability of the adsorbents

This part of experiment was done to see how many times we can use the adsorbents and see their efficiencies. In this study, we repeat the experiment for 4 times using the same adsorbents. Figure 26, plots the percent removal efficiency of Ibuprofen adsorbed through four sequential cycles, in which the results presented in the following table 3.19. From the whole cycles there is no noticeable decreasing in the amount of adsorption. Furthermore, this will enhance the industrial application to avoid another pollution during the wastewater treatment.

Table 3.19: Percentage of IBP removal by the regenerated adsorbent compared with a fresh one at (Temperature= 35ºC and pH= 10 for NCs, MNCs and AgNCs, Temperature=25ºC and pH= 7 for other adsorbents, Solution volume= 50 mL, adsorbent dose= 0.1 g)

Recycle time	1	2	3	4
NCs (IBP removal efficiencies, %)	97.9	97.5	94.3	93.2
MNCS (IBP removal efficiencies, %)	98	96	95	90.8
AgNCs (IBP removal efficiencies, %)	98.2	96.8	96.6	95.5
CRG (IBP removal efficiencies, %)	98.1	94.4	90	81
CRG/NCs (IBP removal efficiencies, %)	98.2	94.9	91.6	90.9
Acetyl β-CD/NCS (IBP removal efficiencies, %)	79.1	76.8	73.1	70
Benzoyl β-CD/NCs (IBP removal efficiencies, %)	98.2	95.1	91.8	91.6

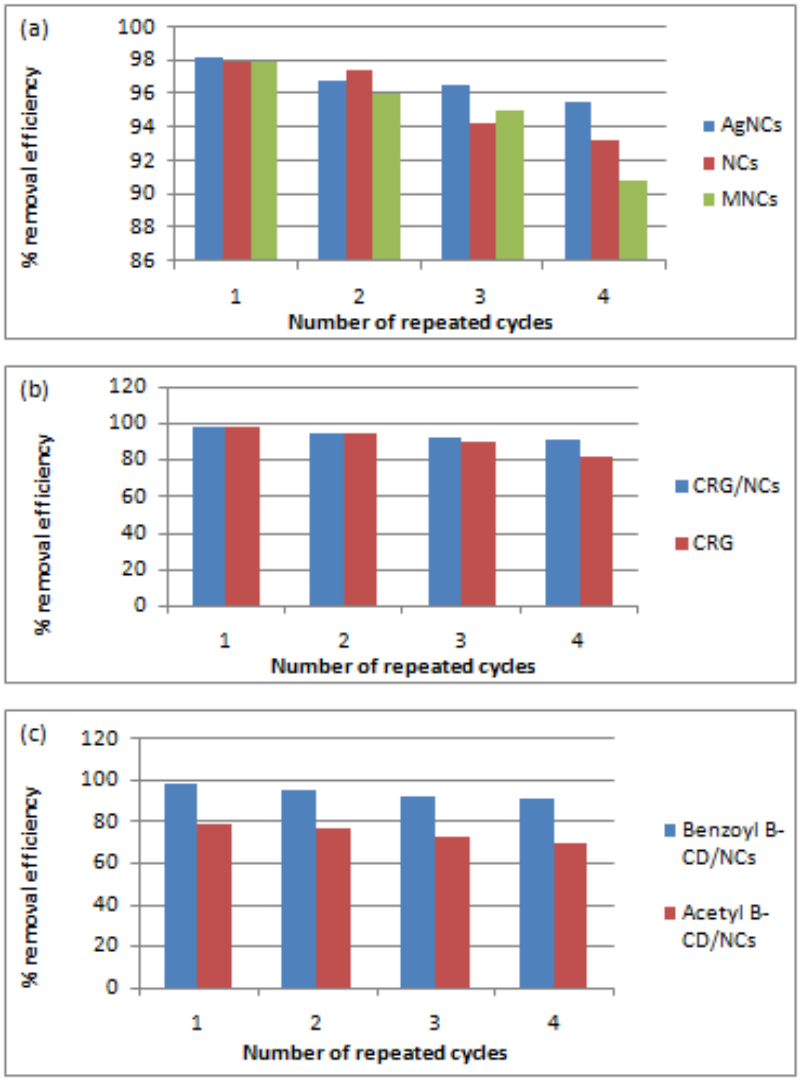

Figure 26: plots the percent removal efficiency of Ibuprofen adsorbed by (a) NCs, MNCs and AgNCs (b) CRG and CRG/NCs, (c) Acetyl β-CD/NCs and Benzoyl β-CD/NCs through four repeated cycles.

The results and the studies show that, the tendency of these polymers, NCs, the prepared MNCs, AgNCs, Carrageenan (CRG), CRG composite with NCs, Acetyl β-CD/NCs and Benzoyl β-CD/NCs, for extracting Ibuprofen (IBP) from water were evaluated. The polymers NCs, AgNCs, Carrageenan/NCs Benzoyl β-CD/NCs showed excellent extraction efficiency toward IBP. At the same time the MNCs, CRG showed very good

extraction efficiency for adsorbate, meanwhile the Acetyl β-CD/NCs give an acceptable tendency for IBP. The thermodynamic studies revealed a spontaneous adsorption of IBP at different temperatures.

Possible interaction between Ibuprofen and absorbent (CNC) is shown in the following figure (27). The figure shows possible H-bonding between cellulose and ibuprofen. As shown in the figure, Ibuprofen has a carboxyl group and each repeat unit of cellulose has three hydroxyl groups. Ibuprofen shall be held into the cellulose matrix.

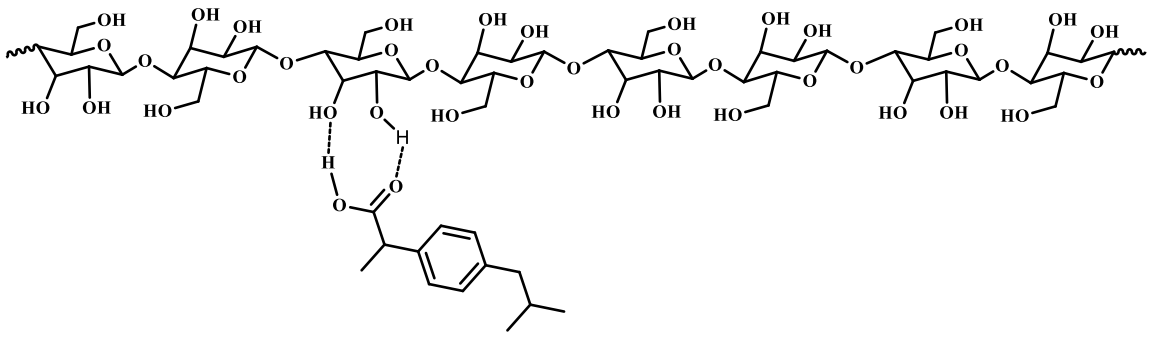

Figure 27: A representative structure showing the interaction between CNC and IBP

Conclusions

In this study, the potentialities of three mainly types of adsorbents were studied as adsorbents for Ibuprofen removal from aqueous solution. The first is cellulose derivatives; cellulose nanocrystalline (CNC), magnetic cellulose nanocrystalline (MNCs) and silver cellulose nanocrystalline (AgNCs). The cellulosic part of the olive Industry Solid Waste (OISW) was extracted and purified then converted to cellulose nanocrystalline. Cellulose nanocrystalline was then converted to magnetic cellulose nanocrystalline by reacting it with solution of $FeC_{l3}.6H_2O$ and $FeSO_4.7H_2O$. Also, the cellulose nanocrystalline converted to silver cellulose nanocrystalline by reacting with solution of $AgNO_3$ and $NaBH_4$. The second adsorbents is Carrageenan (CRG) materials compared with CRG composites with cellulose nanocrystalline. Final adsorbents were prepared using beta cyclodextrin (β-CD), it was converted to Acetyl β-CD by reacting with solution of triethyl amine and acetyl chloride, also the β-CD converted to Benzoyl β-CD by reacting with triethyl amine and benzoyl chloride solution, then these two prepared adsorbents were composites with CNC. The cellulose nanocrystalline, Acetyl β-CD and Benzoyl β-CD were analyzed by using IR.

The ability of the adsorbent samples to extract IBP as an emerging pollutant from wastewater was evaluated. Results showed that NCs, AgNCs, Carrageenan/NCs Benzoyl β-CD/NCs has a better efficiency toward IBP relative MNCs and CRG, but the Acetyl β-CD/NCs showed good efficiency. The studied of time contact of adsorbents with adsorbate shows high efficient removal at 180 min for the first type of adsorbent, and 5min for CRG,

CRG/NCs and Benzoyl β-CD/NCs which is very fast adsorption efficiency, and 40min of time contact for Acetyl β-CD/NCs. The other results show that, the adsorption efficiency increases as the dosage increased for each NCs and AgNCs till reached 50mg, and 25mg adsorbent dose from MNCs, CRG and CRG/NCs, for the Acetyl and Benzoyl β-CD/NCs 5mg is better dosage. which can be explained by the availability of vacant sites and the unsaturation of adsorption sites. The highest efficiency of the three cellulosic materials toward IBP was at pH 10, and 35°C. Meanwhile, the other adsorbents (CRG, CRG/NCs, Acetyl and Benzoyl β-CD/NCs) showed best adsorption at normal pH and normal temperature (pH 7, 25°C). Here, the Langmuir isotherm model shown better indicating results, so that the adsorption mechanism followed this model. Both pseudo-first-order and the second-pseudo-order kinetics were plotted and studied and founded the correlation coefficients (R^2) was higher for the pseudo second order than that for the pseudo-first-order which reached more than 0.997 for all adsorbent samples used in this work. Moreover, we found that the experimental q_e values for the pseudo-second-order were closer to the calculated one than that for pseudo-first-order, indicating that the adsorption process of IBP on the surfaces of adsorbent samples were followed and described by the pseudo second order model.

The ΔS^0 value for the adsorption process found to be positive in all cases, indicating that the randomness at the solid/solution interface increased during adsorption process, Meanwhile, the ΔH^0 values were also positive for all adsorbent samples due to their endothermic nature. For study of the free

energies for the adsorbents it was show a negative values indicating the spontaneously nature of the sorption process by using various temperatures.

- Novelty of Work:

In fact, the strong novelty of this research is this is the first research in which the Acetyl β-Cyclodextrins, Benzoyl β-Cyclodextrins and Carrageenan polymers have been used as adsorbents to extract pharmaceuticals from wastewater. The composites of the polymers synthesis as extraction adsorbents, specially that we use a very important and hazard class of environmental pollutants as emerging drugs, provides an extra novelty to this work.

References

[1] Javaid Akhtar, Nor Aishah Saidina Amin & Khurram Shahzad 2015***: A review on removal of pharmaceuticals from water by adsorption***, **Desalination and Water Treatment**

[2] Desireddy Harikishore Kumar Reddy 2017, ***Water Pollution Control Technologies***, Jeonbuk, **Republic of Korea Encyclopedia of Sustainable Technologies**, Volume 4.

[3] Bradford A. 2015, ***Pollution Facts & Types of Pollution***, Mar. 10, **Live Science Contributor**

[4] Meritxell Gros, Mira Petrovi´c , Dami´a Barcel´o, 2006, ***Development of a multi-residue analytical methodology based on liquid chromatography–tandem mass spectrometry (LC–MS/MS) for screening and trace level determination of pharmaceuticals in surface and wastewaters***, Spain, **Talanta** 70 678–690.

[5] K. Mogolodi Dimpe, Philiswa N. Nomngongo 2016, ***Current sample preparation methodologies for analysis of emerging pollutants in different environmental matrices***, **Trends in Analytical Chemistry** 82 199–207.

[6] Fella Kermiche, Houria Berrebah and Mohamed Reda Djebar, 2016, ***Toxicological effects of drugs (Diclofenac, Ibuprofen, mixture) and Hormesis on a non-target organism: Paramecium sp***, **Journal of Entomology and Zoology Studies**; 4(5): 187-191.

[7] Prasanna Reddy Battu and MS Reddy, 2009, ***RP-HPLC Method for Simultaneous Estimation of Paracetamol and Ibuprofen in Tablets***, **Asian J. Research Chem.** 2(1): Jan.-March.

[8] Joss A, Zabczynski S, Gobel A, Hoffman B, Lffler D, McArdell CS, Ternes TA, Thomsen A, Siegrist H, 2006, ***Biological degradation of pharmaceuticals in municipal wastewater treatment: proposing a classification scheme***. **Water Res** 40:1686–1696.

[9] H. Ozaki, 2004, "***Rejection of micropollutants by membrane filtration," in Proceedings of the Regional Symposium on Membrane Science and Technology***, **Johor**, Malaysia.

[10] M. R. Servos, D. T. Bennie, B. K. Burnison et al., 2005, "***Distribution of estrogens, 17β-estradiol and estrone, in Canadian municipal wastewater treatment plants***" **Science of the Total Environment**, vol. 336, no. 1–3, pp. 155–170.

[11] Mestre, A. S.; Pires, J.; Nogueira, J. M. F.; Parra, J. B.; Carvalho, A. P.; Ania, C.O., 2009, ***Waste-derived activated carbons for removal of ibuprofen from solution: Role of surface chemistry and pore structure***, **Bioresource Technology**, 100(5), 1720-1726

[12] T. Urase and T. Kikuta, 2005, "***Separate estimation of adsorption and degradation of pharmaceutical substances and estrogens in the activated sludge process***" **Water Research,** vol. 39, no. 7, pp. 1289–1300.

[13] Martin J. Hilton, Kevin V. Thomas, 2003, ***Determination of selected human pharmaceutical compounds ineffluent and surface water***

samples by high-performance liquid chromatography–electrospray tandem mass spectrometry, **Journal of Chromatography** A, 1015 129–14.

[14] Seo, P. W. et al., 2016, ***Adsorptive Removal of Pharmaceuticals and Personal Care Products from Water with Functionalized Metal-organic Frameworks: Remarkable Adsorbents with Hydrogen-bonding Abilities***. **Sci. Rep**. 6, 34462; doi: 10.1038/srep34462).

[15] Esplugas, S., Bila, D. M., Krause, L. G. T. & Dezotti, M, 2007, ***Ozonation and advanced oxidation technologies to remove endocrine disrupting chemicals (EDCs) and pharmaceuticals and personal care products (PPCPs) in water effluents***. J. **Hazard. Mater**. 149,631–642

[16] Klavarioti, M., Mantzavinos, D. & Kassinos, D., 2009, ***Removal of residual pharmaceuticals from aqueous systems by advanced oxidation processes***. **Env. Int.** 35, 402–417

[17] Rashed MN., 2013 Jan. 30 ***Adsorption Technique for the Removal of Organic Pollutants from Water and Wastewater, Organic Pollutants Monitoring,*** **Risk and Treatment**. Prof. M. Nageeb Rashed (Ed.).

[18] Sanna Hokkanen, Amit Bhatnagar, Mika Sillanpaa 2016, ***A review on modification methods to cellulose-based adsorbents to improve adsorption capacity,*** **Water Research** 91 156-173.

[19] Sullivan 1997, A. C. O. **Cellulose**, 173–207.

[20] Azizi Samir, M. A. S.; Alloin, F., 2005; Dufresne, **A. Biomacromolecules**, 6, 612–626.

[21] Nishiyama, Y. J., 2009, **Wood Sci**., 55, 241–249.

[22] Dae-Young Kim, Yoshiharu Nishiyama, Masahisa Wada & Shigenori Kuga 2001 Jan, ***High-yield carbonization of cellulose by sulfuric acid impregnation***, **Cellulose** 8: 29–33.

[23] Martınez-Sanz, Marta., Pettolino, Filomena., Flanagan, Bernadine, Gidley, Michael J., & Gilbert Elliot P., ***Structure of cellulose microfibrils in mature cotton fibres***. **Carbohydrate Polymers**.

[24] David William O'Connell, Colin Birkinshaw, Thomas Francis O'Dwyer, 2008: ***Review Heavy metal adsorbents prepared from the modification of cellulose*** **Bioresource Technology** 99 6709–6724.

[25] Nathalie Lavoine, Isabelle Desloges, Alain Dufresne, Julien Bras, 2012, ***Microfibrillated cellulose – Its barrier properties and applications in cellulosic materials: A review***, **Carbohydrate Polymers** 90 735– 764.

[26] Dieter Klemm, Brigitte Heublein, Hans-Peter Fink and Andreas Bohn, 2005, ***Cellulose***: ***Fascinating Biopolymer and Sustainable Raw Material***, **Angew. Chem. Int. Ed.,** 44, 3358 – 3393.

[27] Moon, Robert J.; Martini, Ashlie; Nairn, John; Simonsen, John; and Youngblood, Jeffrey, 2011, "***Cellulose nanomaterials review: structure, properties and nanocomposites***" **Birck and NCN Publications**. Paper 769.

[28] Varshney V.K., Naithani S., 2011, ***Chemical Functionalization of Cellulose Derived from Nonconventional Sources. In: Kalia S., Kaith B., Kaur I. (eds) Cellulose Fibers: Bio- and Nano-Polymer Composites***. **Springer**, Berlin, Heidelberg

[29] L. Brinchia, F. Cotanaa, E. Fortunatib, J.M. Kenny, 2013, ***Production of nanocrystalline cellulose from lignocellulosic biomass: Technology and applications***, **Carbohydrate Polymers** 94 154– 169.

[30] Neto, Wilson Pires Flauzino., Mariano, Marcos., Silva, Ingrid Souza Vieira da., Silv´erio, Hudson Alves., Putaux, Jean-Luc., Otaguro, Harumi., Pasquini, Daniel., & Dufresne, Alain. 2016, ***Mechanical properties of natural rubber nanocomposites reinforced with high aspect ratio cellulose nanocrystals isolated from soy hulls***. **Carbohydrate Polymers**

[31] Ng H-M, Sin LT, Tee T-T, Bee S-T, Hui D, Low C-Y, Rahmat AR, 2015, ***Extraction of cellulose nanocrystals from plant sources for application as reinforcing agent in polymers***, **Composites Part B**.

[32] Mariano Pracella, Md. Minhaz-Ul Haque , Debora Puglia, 2014, ***Morphology and properties tuning of PLA/cellulose nanocrystals bionanocomposites by means of reactive functionalization and blending with PVAc***, **Polymer** 1-9.

[33] J. Theron, J.A.Walker, and T.E, 2008. ***Cloete Nanotechnology and Water Treatment: Applications and Emerging Opportunities***, **Critical Reviews in Microbiology**, 34:43–69.

[34] Chirayil CJ., Lovely Mathew L., Thomas S., 2014, ***Review of Recent Research in Nano Cellulose Preparation From Different Lignocellulosic Fibers*** ,**Rev .Adv. Mater. Sci**, Vol. 37: 20-28.

[35] Garcia de Rodriguez, N. L. 2006; Thielemans, W.; Dufresne, A, ***Sisal Cellulose Whiskers Reinforced Polyvinyl Acetate Nanocomposites,*** **Cellulose,** 13, 261–270.

[36] Wang, B.; Sain 2007, **M. Compos. Sci. Technol**., 67, 2521–2527.

[37] Bai, W.; Holbery, J.; Li, K, 2009. **Cellulose**, 16, 455–465.

[38] Siqueira G, Bras J, Dufresne A, 2010. ***Cellulosic bionanocomposites: a review of preparation, properties and applications***. **Polymers**; 2(4):728–65.

[39] Hernán Charreau, María L. Foresti and Analía Vázquez, 2013, ***Nanocellulose Patents Trends: A Comprehensive Review on Patents on Cellulose Nanocrystals***, ***Microfibrillated and Bacterial Cellulose,*** **Nanotechnology**, 7, 56-80.

[40] Hamad, W. Front 2006. **Chem. Eng. Res**., 84, 513–519.

[41] Salas, C.; Nypelö, T.; Rodriguez-Abreu, C.; Carrillo, C.; Rojas, O.J. 2014. ***Nanocellulose properties and applications in colloids and interfaces. Curr. Opin.*** **Colloid Interface Sci**., 19, 383–396.

[42] Emmanuel Abu-Danso, Varsha Srivastava, Mika Sillanpaa, Amit Bhatnagar, 2017, ***Pretreatment assisted synthesis and characterization of cellulose nanocrystals and cellulose nanofibers***

from absorbent cotton, **International Journal of Biological Macromolecules** 353.

[43] Siqueira, G., Bras, J., Dufresne, A. 2010, ***Cellulosic bionanocomposites: a review of preparation, properties, and applications***. **Polymers** 2:728-765.

[44] Michael T. Postek, Robert J. Moon, Alan W. Rudie and Michael A. Bilodeau 2013, **Production And Applications Of Cellulose Nanomaterials**

[45] Wei Li, Xin Zhao, Shouxin Liu, 2013, ***Preparation of entangled nanocellulose fibers from APMP and its magnetic functional property as matrix.*** **Carbohydrate Polymers** 94 278– 285.

[46] Moraisa J., Rosa M., Filho M., Nascimentoa L., Diego Magalhães do Nascimento D., Cassale A., 2013, ***Extraction and characterization of nanocellulose structures from raw cotton linter***, **Carbohydrate Polymers**, Vol. 91(1): 229–235.

[47] Jindrayani Nyoo Putro, Alfin Kurniawan, Suryadi Ismadji, Yi-Hsu Ju, 2017, ***Nanocellulose based biosorbents for wastewater treatment: Study of isotherm, kinetic, thermodynamic and reusability***, **Environmental Nanotechnology, Monitoring and Management.**

[48] J. Lamaming, R. Hashim, O. Sulaiman, C.P. Leh, T. Sugimoto, N.A. Nordin, 2015, ***Cellulose nanocrystals isolated from oil palm trunk,*** **Carbohydrate polymers**, 127 202-208.

[49] A.K. Mishra, 2014, **Nanocomposites in Wastewater Treatment**, Pan Stanford.

[50] Ali Reza Mahdavian, Monir Al-Sadat Mirrahimi, 2010, "***Efficient separation of heavy metal cations by anchoring polyacrylic acid on superparamagnetic magnetite nanoparticles through surface modification***", **Chemical Engineering Journal**, 159, 264.

[51] Mustafa Ozmen, Keziban Can, Gulsin Arslan, Ali Tor, Yunus Cengeloglu, Mustafa Ersoz, 2010, "***Adsorption of Cu(II) from aqueous solution by using modified Fe3O4 magnetic nanoparticles***", **Desalination,** 254, 162.

[52] Saeid Zarei, Mahmood Niad, Hossein Raanaei, 2017, ***The removal of mercury ion pollution by using Fe3O4-nanocellulose: Synthesis, characterizations and DFT studies***, **Journal of Hazardous Materials**.

[53]: Chia C H, Zakaria S, & Bguyen K L, Abdullah M., 2008. ***Utilisation of unbleached kenaf fibers for the preparation of magnetic paper***. **Industrial crops and products**, vol. 28, No.3, PP. 333-339, ISSN. 1011-1344.

[54] Hokkanen S., Repo E., Loub S., Sillanpää M., 2015, ***Removal of arsenic(V) by magnetic nanoparticle activated microfibrillated cellulose***, **Chemical Engineering Journal**,Vol. 260: 886–894.

[55] X. Sun, L. Yang, Q. Li, J. Zhao, X. Li, X. Wang, H. Liu, 2014, ***Amino-functionalized magnetic cellulose nanocomposite as adsorbent for removal of Cr(VI): synthesis and adsorption studies,*** **Chem. Eng. J.** 241 175–183.

[56] Y. Benmassaoud, M.J. Villaseñor, R. Salghi, S. Jodeh, M. Algarra, M. Zougagh, Á. Ríos, 2017, ***Magnetic/non-magnetic argan press cake nanocellulose for the selective extraction of sudan dyes in food samples prior to the determination by capillary liquid chromatography***, **Talanta** 166 63–69.

[57] M.H. Beyki, M. Bayat, F. Shemirani, 2016, ***Fabrication of core-shell structured magnetic nanocellulose base polymeric ionic liquid for effective biosorption of Congo red dye***, **Bioresour. Technol**. 218 326–334.

[58] Feras Abujaber, Mohammed Zougagh, Shehdeh Jodeh, Ángel Ríos, 2018, ***Magnetic cellulose nanoparticles coated with ionic liquid as a new material for the simple and fast monitoring of emerging pollutants in waters by magnetic solid phase extraction***, **Microchemical Journal** 137 490–495.

[59] Quang Huy Tran, Van Quy Nguyen and Anh-Tuan Le, 2013, ***Silver nanoparticles: synthesis, properties, toxicology, applications and perspectives***, **Adv. Nat. Sci.: Nanosci. Nanotechnol**. 4 033001 (20pp).

[60] M. Abu-Saied, E. Hafez, T. Taha, K.A. Khalil, 2014, ***Bionanosilver-poly (methyl 2-methylpropenoate) electrospun nanofibre as a potent antibacterial against multidrug resistant bacteria***, **International Journal of Nanoparticles** 7(3-4) 190-202.

[61] J.S. Devi, B.V. Bhimba, 2013, ***Biogenic synthesis by Gracilaria corticata for efficient production of biocompatible silver***

nanoparticles and its applications, International **Journal of Nanoparticles** 6(4) 312-323.

[62] P. Prema, S. Lakshmi Priya, G. Rameshkumar, 2012, ***Bio-based and chemical mediated fabrication of silver nanoparticles and evaluation of their potential antimicrobial activity–a comparative view***, **International Journal of Nanoparticles** 5(4) 338-357.

[63] N. Durán, P.D. Marcato, O.L. Alves, G.I. De Souza, E. Esposito, 2005, ***Mechanistic aspects of biosynthesis of silver nanoparticles by several Fusarium oxysporum strains***, **Journal of nanobiotechnology** 3(1) 8.

[64] Evan M. Hetrick and Mark H. Schoenfisch, 2006, ***Reducing implant-related infections: active release strategies***, **Chem. Soc. Rev.,** 35, 780–789.

[65] Catalina Marambio-Jones, Eric M. V. Hoek, 2010, ***A review of the antibacterial effects of silver Nanomaterials and potential implications for human health and the environment***, **J Nanopart Res** 12:1531–1551.

[66] Z.-M. Xiu, J. Ma, and P. J. J. Alvarez, 2011, "***Differential effect of common ligands and molecular oxygen on antimicrobial activity of silver nanoparticles versus silver ions***," **Environmental Science and Technology**, vol. 45, no. 20, pp. 9003–9008.

[67] Z.-M. Xiu, Q.-B. Zhang, H. L. Puppala, V. L. Colvin, and P. J. J. Alvarez, 2012, "***Negligible particle-specific antibacterial activity of silver nanoparticles***," **Nano Letters**, vol. 12, no. 8, pp. 4271–4275.

[68] E. Fortunatia, I. Armentano, Q. Zhouc, A. Iannonia, E. Saino, L. Visai, L.A. Berglund, J.M. Kenny, 2012, ***Multifunctional bionanocomposite films of poly(lactic acid), cellulose nanocrystals and silver nanoparticles***, **Carbohydrate Polymers** 87 1596– 1605.

[69] E. Fortunati, M. Peltzer, I. Armentano, A. Jiménez, J.M. Kenny, 2013, ***Combined effects of cellulose nanocrystals and silver nanoparticles on the barrier and migration properties of PLA nano-biocomposites,*** **Journal of Food Engineering** 118 117–124.

[70] He Liu, Dan Wang, Zhanqian Song, Shibin Shang, 2011, ***Preparation of silver nanoparticles on cellulose nanocrystals and the application in electrochemical detection of DNA hybridization***, **Cellulose** 18:67–74.

[71] Arcot R. Lokanathan, Khan Mohammad Ahsan Uddin, Orlando J. Rojas and Janne Laine, 2014, ***Cellulose Nanocrystal-Mediated Synthesis of Silver Nanoparticles: Role of Sulfate Groups in Nucleation Phenomena***, **Biomacromolecules**, 15, 373−379.

[72] Liou, Polly., Nayigiziki, Francois Xavier., Kong, Fanbin., Mustapha, Azlin., & Lin, Mengshi. 2016, ***Cellulose Nanofibers Coated with Silver, Nanoparticles as a SERS Platform for Detection of Pesticides in Apples***. **Carbohydrate Polymers.**

[73] M. Jalili Tabaii, G. Emtiazi, 2018, ***Transparent nontoxic antibacterial wound dressing based on AgNPs/bacterial cellulose nano composite synthesized by tripolyphosphate***, **Journal of Drug Delivery Science and Technology**

[74] Massimo Di Rosa, 1972, ***Biological properties of carrageenan***, **J. Plzavm. Phavrnac.**, 24, 89-102.

[75] Srinivas Janaswamy, Rengaswami Chandrasekaran, 2002, ***Effect of calcium ions on the organization of iota-carrageenan helices: an X-ray investigation***, **Carbohydrate Research** 337 523–535.

[76] Myslabodski, D. E., Stancioff, D., & Heckert, R. A. 1996, ***Effect of acid hydrolysis on the molecular weight of kappa carrageenan by GPC-LS.*** **Carbohydrate Polmers**, 31, 83–92.

[77] Anders Karlssona, Satish K. Singh, 1999, ***Acid hydrolysis of sulphated polysaccharides. Desulphation and the effect on molecular mass,*** **Carbohydrate Polymers** 38 7–15.

[78] Hideki Nakashima, Yasuji Kido, Nobuyuki Kobayashi, Yoshinobu Motoki, Michael Neushul and Naoki Yamamoto, 1987, ***Purification and Characterization of an Avian Myeloblastosis and Human Immunodeficiency Virus Reverse Transcriptase Inhibitor, Sulfated Polysaccharides Extracted From Sea Algae***, **Antimicrobial Agents And Chemotherapy**, P. 1524-1528.

[79] Christopher J. Morris, ***Carrageenan-Induced Paw Edema in the Rat and Mouse***, **Methods in Molecular Biology**, vol. 225: Inflammation Protocols.

[80] Zia, K.M.; Tabasum, S.; Nasif, M.; Sultan, N.; Aslam, N.; Noreen, A.; Zuber, M, 2017, ***A review on synthesis, properties and applications of natural polymer based carrageenan blends and composites.*** **Int. J. Biol.Macromol**. 96, 282–301.

[81] Nanaki, S.G.; Kyzas, G.Z.; Tzereme, A.; Papageorgiou, M.; Kostoglou, M.; Bikiaris, D.N.; Lambropoulou, D.A, 2015. ***Synthesis and characterization of modified carrageenan microparticles for the removal of pharmaceuticals from aqueous solutions.*** **Colloids Surf. B Biointerfaces**, 127, 256–265.

[82] L.M. Duizer' And O.H. Campanella And G.R.G. Barnes, Sensory, 1998, ***Instrumental And Acoustic Characteristics Of Extruded Snack Food Products***, **Journal Of Texture Studies** 29 397-41 1.

[83] M. A. García, M. N. Martino and N. E. Zaritzky, 2001, ***Composite starch-based coatings applied to strawberries (Fragaria ananassa),*** **Nahrung/Food** 45 No. 4, pp. 267- 272.

[84] Kimiko Makino, Rie Idenuma, Tomokazu Murakami, Hiroyuki Ohshima, 2001, ***Design of a rate- and time-programming drug release device using a hydrogel: pulsatile drug release from k-carrageenan hydrogel device by surface erosion of the hydrogel***, **Colloids and Surfaces B: Biointerfaces** 20 355–359.

[85] McHugh, D. J. 2003. ***A guide to the seaweed industry: FAO fisheries technical*** paper No. 441 (pp. 61–72). **Rome: FAO.**

[86] Yun-Peng Jiang, Xi-Kun Guo, 2005, ***O-maleoyl derivative of low-molecular-weight k-carrageenan: Synthesis and characterization***, **Carbohydrate Polymers** 61 441–445.

[87] Vanessa Leiria Campo, Daniel Fbio Kawano, Dlson Braz da Silva Jr., Ivone Carvalho, 2009, ***Carrageenans: Biological properties,***

chemical modifications and structural analysis– A review, **Carbohydrate Polymers** 77 167–180.

[88] Önder Pekcan and Özlem Tarı, 2008, ***Cation effect on gel – sol transition of kappa Carrageenan,*** **Polymer Bulletin** 60, 569–579.

[89] Heyraud, A., & Rochas, C. 1982. ***Sulfated oligosaccharides from j-carrageenan and oligogalacturonic acids separation by HPLC*****.** **Journal of Liquid Chromatography**, 5, 403–412.

[90] Rochas, C., Lahaye, M., & Yaphe, W. 1986. ***Sulphate content of carageenan and agar determined by infrared spectroscopy***. **Botanica Marina**, 29, 335–340.

[91] Chiovitti, A., Bacic, A., Craik, D. J., Kraft, G. T., Liao, M.-L., Falshaw, R., et al. 1998. ***A pyruvated carrageenan from Australian specimens of the red alga Sacronema filiforme***. **Carbohydrate Research**, 310, 77–83.

[92] Bulmer, C., Margaritis, A., & Xenocostas, A. 2012. ***Encapsulation and controlled release of recombinant human erythropoietin from chitosan–carrageenan nanoparticles.*** **Current Drug Delivery**, 9, 527–537.

[93]: Pinheiro, A. C., Bourbon, A. I., Medeiros, B. G. D. S., da Silva, L. H. M., da Silva, M. C. H., Carneiro-da-Cunha, M. G., et al. 2012. ***Interactions between kappa-carrageenan and chitosan in nanolayered coatings-Structural and transport properties***. **Carbohydrate Polymers**, 87, 1081–1090.)

[94] Liang Li, Rui Ni, Yang Shao, Shirui Mao, 2014, ***Carrageenan and its applications in drug delivery***, **Carbohydrate Polymers** 103 1– 11.

[95] Jingjing Liu, Xiudan Zhan, Jianbo Wan, Yitao Wang, Chunming Wang, 2015, ***Review for carrageenan-based pharmaceutical biomaterials: Favourable physical features versus adverse biological effects***, **Carbohydrate Polymers** 121 27–36.

[96] Mohd Aiman Hamdan, Fatmawati Adam, Khairatun Najwa Mohd Amin, 2018, ***Investigation of Mixing Time on Carrageenan-Cellulose Nanocrystals (CNC) Hard Capsule for Drug Delivery Carrier,*** **International Journal of Innovative Science and Research Technology**, Volume 3, Issue 1.

[97] Myrsini Papageorgiou, Stavroula G. Nanaki, George Z. Kyzas, Christina Koulouktsi, Dimitrios N. Bikiaris and Dimitra A. Lambropoulou, 2017, ***Novel Isocyanate-Modified Carrageenan Polymer Materials: Preparation, Characterization and Application Adsorbent Materials of Pharmaceuticals***, **Polymers**, 9, 595.

[98] P. S. Lau, N. F. Y. Tam & Y. S. Wong, 1997, ***Wastewater Nutrients (N and P) Removal by Carrageenan and Alginate Immobilized Chlorella Vulgaris***, **Environmental Technology**, 18:9, 945-951.

[99] Diana G´omez Mart´ınez, Mats Stading, Anne-Marie Hermansson, 2013, ***Viscoelasticity and microstructure of a hierarchical soft composite based on nano-cellulose and κ-carrageenan***, **Rheol Acta**.

[100] Siti Zarina, Ishak Ahmad, 2015, ***Biodegradable Composites Films based on κ-carrageenan Reinforced by Cellulose Nanocrystal from***

Kenaf Fibers, Carrageenan-CNC Films, **BioResources** 10(1), 256-271.

[101] Siti Zarina Zakuwan, Ishak Ahmad, and Nazaruddin Ramli, 2013, ***Preparation of hybrid nano biocomposite κ-carrageenan/cellulose nanocrystal/ nanoclay***, **AIP Conference Proceedings** 1571, 738.

[102] Lokesh R. Rane, Niranjan R. Savadekar, Pravin G. Kadam, and Shashank T. Mhaske, 2014, ***Preparation and Characterization of K-Carrageenan/Nanosilica Biocomposite Film***, **Journal of Materials**, 1- 8 pages.

[103] Gholami, M., Vardini, M. T., and Mahdavinia, G.R., 2015, ***Investigation of the effect of magnetic particles on the Crystal Violet adsorption onto a novel nanocomposite based on rmkappa-carrageenan-g-poly (methacrylic acid)***, **Carbohydrate Polymers**.

[104] Ali Pourjavadi, Malihe Doulabi, Mohadese Doroudian, 2013, ***Adsorption characteristics of malachite green dye onto novel kappa-carrageenan-g-polyacrylic acid/TiO2–NH2 hydrogel nanocomposite***, **J IRAN CHEM SOC**.

[105] adsorptionOsman Duman, Sibel Tunc , Tülin Gürkan Polat, Bahar Kancı Bozoglan, 2016, ***Synthesis of magnetic oxidized multiwalled carbon nanotube- κ-carrageenan-Fe3O4nanocomposite adsorbent and its application in cationic Methylene Blue dye***, **Carbohydrate Polymers** 147 79–88.

[106] Ana M. Salgueiro, Ana L. Daniel-da-Silva, Ana V. Girao, Paula C. Pinheiro, Tito Trindade, 2013, ***Unusual dye adsorption behavior of j-***

carrageenan coated superparamagnetic nanoparticles, **Chemical Engineering Journal** 229 276–284.

[107] Gholam Reza Mahdavinia, Ali Baghban, Samira Zorofi, Abdolhossein Massoudi, 2014, ***Kappa-Carrageenan Biopolymer-Based Nanocomposite Hydrogel and Adsorption of Methylene Blue Cationic Dye from Water***, J**. Mater. Environ. Sci.** 5 (2) 330-337.

[108] Szejtli, J. 1989, **Trends Biotechnol**., 7, 170–174.

[109] Szejtli J. 2004, **Pure Appl Chem**; 76(10): 1825-1845.

[110] E.M. Martin Del Valle, 2004, ***Cyclodextrins and their uses: a review***, **Process Biochemistry** 39 1033–1046.

[111] Schardinger F.Zentralbl 1911**Bakteriol Parasitenk Abt II**;29: 188-197.

[112] Dass, C. R.; Jessup, W. J. 2000, **Pharm. Pharmacol**. 52, 731–761.

[113] Kaneto Uekama, Fumitoshi Hirayama, and Tetsumi Irie, 1998, ***Cyclodextrin Drug Carrier Systems***, **Chem. Rev.** 98, 2045-2076.

[114] Jansook P, Ogawa N, Loftsson T, 2010, ***Cyclodextrins: structure, physicochemical properties and pharmaceutical applications***, **International Journal of Pharmaceutics.**

[115] Qi ZH, Hedges AR. ***Use of cyclodextrins for flavours. In: Ho CT, Tan CT, Tong CH (Eds.), 1995, Flavour technology: Physical chemistry, modification and process. ACS symposium series 610, Washington DC,*** **American Chemical Society**, pp. 231-243.

[116] L.A. Hergert, G.M. Escandar, 2003, ***Spectrofluorimetric study of the ß-cyclodextrin_/ibuprofen complex and determination of ibuprofen in pharmaceutical preparations and serum***, **Talanta** 60 235-246.

[117] Laura Jurecskaa, Péter Dobosya, Katalin Barkácsa, Éva Fenyvesib, Gyula Záray, 2014, ***Characterization of cyclodextrin containing nanofilters for removal of pharmaceutical residues***, **Journal of Pharmaceutical and Biomedical Analysis** 98 90–93.

[118] Guohao Yuan, Mayakrishnan Prabakaran, Sun Qilong, JungSoon Lee, Ill-Min Chung, Mayakrishnan Gopiraman, Kyung-Hun Song, Ick Soo Kim, 2016, ***Cyclodextrin functionalized cellulose nanofiber composites for the faster adsorption of toluene from aqueous solution***, **Journal of the Taiwan Institute of Chemical Engineers** 1–7.

[119] D. Shi, T. Mei, Q. Chen, F. Duan & M. Chen, 2015, ***Preparation and adsorption properties of laponite–cyclodextrin complex***, **Materials Research Innovations,**19:sup9, S9-157-S9-161.

[120] Jianxin Chen, Yunping Pu, Zhongbin Wang, Jian Han, Yunlong Zhong, Kaili Liu, 2017, ***Synthesis of a novel nanosilica-supported poly -cyclodextrin sorbent and its properties for the removal of dyes from aqueous solution***, **Colloids and Surfaces A: Physicochemical and Engineering Aspects**

[121] Giampiero Bettinettia, Paola Murab, Maria Teresa Fauccib, Milena Sorrentia, Massimo Setti, 2002, ***Interaction of naproxen with noncrystalline acetyl b- and acetyl g-cyclodextrins in the solid and***

liquid state, **European Journal of Pharmaceutical Sciences** 15 21–29

[122] Cao Yujuan, Lu Runhua, 2009, ***Influence of substituted groups on the binding ability of benzoyl-modified β-cyclodextrins***, **Spectrochimica Acta Part** A 74 892–895.

[123] P. Leonard, S. Hearty, J. Brennan et al., 2003, "***Advances in biosensors for detection of pathogens in food and water***," **Enzyme and Microbial Technology**, vol. 32, no. 1, pp. 3–13.

[124] P. H. Gleick, P. I. , 1993 for S. in D., ***Environment, and Security, and S. E. Institute, Water in Crisis: A Guide to the World's Fresh Water Resources***, **Oxford University Press**.

[125] D. Seckler, D. Molden, and R. Sakthivadivel, 2003, **The Concept of Efficiency inWater Resources Management and Policy**.

[126] M. T. Amin, A. A. Alazba, and U.Manzoor, 2014, ***A Review of Removal of Pollutants from Water/Wastewater Using Different Types of Nanomaterials,*** **Advances in Materials Science and Engineering**, 24 pages.

[127] Miège, C., Choubert, J.-M., Ribeiro, L., Eusèbe, M., Coquery, M., 2009. ***Le devenir des résidus pharmaceutiques dans les stations d'épuration d'eaux usées. Une synthèse de la littérature***. **Technique Science et Méthode** 11, 75–94.

[128] Zuccato, E., Calamari, D., Natangelo, M., Fanelli, R., 2000. ***Presence of therapeutic drugs in the environment.*** **Lancet** 355, 1789–1790.

[129] Jin-Lin Liu, Ming-Hung Wong, 2013, ***Pharmaceuticals and personal care products (PPCPs): A review on environmental contamination in China,*** **Environment International** 59208–224.

[130] G. Massmann, U. Dünnbier, T. Heberer, T. Taute, 2008, **Chemosphere** 71 1476.

[131] M. Gros, M. Petrovic, D. Barcelo, 2009, **Analytical Chemistry** 81 898.

[132] J. Feitosa-Felizzola, B. Temime, S. Chiron, 2007, **Journal of Chromatography** A 1164 95.

[133] A. Garcia-Ac, P.A. Segura, C. Gagnon, S. Sauvé, 2009, **Journal of Environmental Monitoring** 11 830.

[134] Rebeca Lopez-Serna, Sandra Pérez, Antoni Ginebreda, Mira Petrovic, Damià Barcel, 2010, ***Fully automated determination of 74 pharmaceuticals in environmental and waste waters by online solid phase extraction–liquid chromatography-electrospray–tandem mass spectrometry***, **Talanta** 83 410–424.

[135] Barceló, D. & López, M. 2008, ***Contaminación y calidad química del agua: el problema de los contaminantes emergentes***. ***Panel Científico – Técnico de seguimiento de la política de aguas.*** **Fundación de Nueva Cultura del Agua.**

[136] Tiphanie Deblondea, Carole Cossu-Leguille, Philippe Hartemann, 2011***, Emerging pollutants in wastewater: A review of the literature,*** **International Journal of Hygiene and Environmental Health** 214 442– 448.

[137] José Rivera-Utrilla, Manuel Sanchez-Polo a, Marya Angeles Ferro-Garcia a, یGonzalo Prados-Joya a, Raol Ocampo-Pérez, 2013, ***Pharmaceuticals as emerging contaminants and their removal from water. A review*,** **Chemosphere.**

[138] Henrry Saúl Delgado Ortega, Barcelona, 2016, **Análisis De La Exposición De Compuestos Emergentes En Varios Escenarios De Usos Del Agua**, pages 49-50.

[139] Rhys E. Green, Ian Newton, Susanne Shultz, Andrew A. Cunningham, Martin Gilbert, Deborah J. Pain And Vibhu Prakash, 2004, ***Diclofenac poisoning as a cause of vulture population declines across the Indian subcontinent,*** **Journal of Applied Ecology** 41, 793–800.

[140] Kümmerer, K. 2010. ***Pharmaceuticals in the environment.*** **Annual Review of Environment and Resources,** 35(1), 57-75.

[141]: **Encyclopedia Britannica Online**. 2012***, Ibuprofen***.

[142]: **Hawthorne Parmecuticals**, 2005, ***REPREXAIN (hydrocodone bitartrate, ibuprofen) tablet, film coated*.**

[143] Richardson, S. D. 2007. ***Water analysis: Emerging contaminants and current issues. National Exposure Research Laboratory***, **U.S. Environmental Protection Agency**, Athens, Georgia, 4295-4324.

[144] Zuccato, E.; Castiglioni, S.; Fanelli, R.; Reitano, G.; Bagnati, R.; Chibrando, C., Calamari, D. 2006. ***Pharmaceuticals in the environment in italy: Causes, occurrence, effects and control***. **ESPR – Environ Sci & Pollut Res**, 13(1).

[145] Roizman, T. 2011. **Ibuprofen side effects with longterm use.**

[146] Ncibi MC., 2008, ***Applicability of some statistical tools to predict optimum adsorption isotherm after linear and non-linear regression analysis***, **Journal of Hazardous Materials**, Vol. 153: 207–212.

[147] Sylvester O. Adejo and Mbanefo M. Ekwenchi., 2014***, Proposing a new empirical adsorption isotherm known as Adejo-Ekwenchi isotherm***, **Journal of Applied Chemistry**, Vol. 6(5): 66-71.

[148] Foo KY. and B.H. Hameed BH., 2010, ***Insights into the modeling of adsorption isotherm systems,*** **Chemical Engineering Journal**, Vol. 156, : 2-10.

[149] Chen X., 2015, ***Modeling of Experimental Adsorption Isotherm Data***, **Information**, Vol. 6: 14-22.

[150] Dada A., Olalekan A., Olatunya A., Dada O., 2012, ***Langmuir, Freundlich, Temkin and Dubinin – Radushkevich Isotherms Studies of Equilibrium Sorption of Zn^{+2} unto phosphoric acid modified Rice Husk,*** **IOSR Journal of Applied Chemistry**, Vol. 3 (1): 38-45.

[151] Qiu H., Lv L., Pan B., Zhang Q., Zhang W., 2009, ***Critical Review in Adsorption Kinetic Models,*** **Journal of Zhejiang University Science** A., Vol. 10: 716-724.

[152] He J., Hong S., Zhang L., Gan F., Ho Y., 2010, ***Equilibrium and Thermodynamic Parameters of Adsorption of Methylene Blue onto Rectorite***, **Fresenius Environmental Bulletin,** Vol. 19: 2651-2656.

[153] Sridev D., Rajendran K., 2009, Synthesis and Optical Characteristics of ZnO Nanocrystals, Bulletin of Materials Science, Vol. 32: 165-168.

[154] Ferrari L, Kaufmann J, Winnefeld F, Plank J., 2010, ***Interaction of cement model systems with superplasticizers investigated by atomic force microscopy, zeta potential, and adsorption measurements*, J Colloid Interface Sci.**, Vol. 347 (1): 15-24.

[155] BAI Y., BARTKIEWICZ B., 2009, ***Removal of Cadmium from wastewater using ion exchange resin amberjet 1200H columns***, **Polish J. of Environ. Stud.** Vol. 18(6): 1191-1195.

[156] Agrawal A., Sahu K., 2006***, Kinetics and isotherm studies of cadmium adsorption on manganese nodule residue***, **Journal of Hazardous Materials,** Vol. 137 (2): 915–924.

[157] Ugurlu M., Gurses A., Acıkyıldız M., 2008, ***Comparison of textile dyeing effluent adsorption on commercial activated carbon and activated carbon prepared from olive stone by $ZnCl_2$ activation***, **Microporous and Mesoporous Materials**, Vol. 111 (1–3): 228–235.

[158] Elmolla E., Chaudhuri M., 2009, ***Improvement of biodegradability of synthetic amoxicillin wastewater by Photo-Fenton process***, **World Applied Science Journal**, Vol.5 (special issue for environment): 53-58

[159] Tan I., Hameed B., Ahmad A., 2007, ***Equilibrium and Kinetic studies on basic dye adsorption by oil palm fiber activated carbon***, **Chemical Engineering Journal**, Vol. 127(1–3): 111–119.

[160] Ho Y., Malarvizhi R., Sulochann N., 2009, ***Equilibrium Isotherm Studies of Methylene Blue Adsorption onto Activated Carbon***

Prepared from Delonix regia Pods, **Journal of Environmental Protection Science**, Vol. 3: 111 – 116.

[161] EL Boujaady H.,MourabetM.,Bennani-ZiatniM.,Abderrahim T., 2013, ***Adsorption/desorption of Direct Yellow 28 on an apatitic phosphate: Mechanism, Kinetic and thermodynamic studies***, **Journal of the Association of Arab Universities for Basic and Applied Sciences**, Vol. 16: 64-73.

[162] Vitz J., ErdmengerT., Haensch C., Schubert US., 2009, ***Extended dissolution studies of cellulose in imidazolium based ionic liquids, Green Chemistry, Vol. 11 (3): 417-424.***

[163] Hamed O., Jodeh S., Al-Hajj N., Abo-Obeid A., Hamed E.M., Fouad Y., 2015, Cellulose acetate from biomass waste of olive industry, **Journal of Wood Science**, Vol.61 (1): 45-52.

[164] AnirudhanT.S, Rejeena S.R, Binusree j., 2013, ***Adsorptive separation of Myoglobin from aquous solution using iron oxide magnetic nanoparticles modified with functionalized nanocrystalline cellulose***, **J. Chem. Eng.** Vol.58: 1329 – 1339.

[165]: Vadivelan V., Kumar K.V, 2005***, Equilibrium, kinetics, mechanism, and process design for the sorption of methylene blue onto rice husk***, **J. Coll. Interface Sci**. Vol.286: 90–100.

[166] S. K. Behera, S. Y. Oh, H. S. Park, 2012, ***Sorptive removal of ibuprofen from water using selected soil minerals and activated carbon***, **Int. J. Environ. Sci. Technol**. 9:85–94.

[167] Lindqvist N, Tuhkanen T, Kronberg L, 2005. ***Occurrence of acidic pharmaceuticals in raw and treated sewages and in receiving waters***. **Water Res**; 39(11):2219–28.

[168] Priya Banerjee, Pinaki Das, Aisha Zaman, Papita Das, 2016, ***Application of Graphene Oxide nanoplatelets for adsorption of Ibuprofen from aqueous solutions: Evaluation of process kinetics and thermodynamics***, **Process Safety and Environment Protection**

[169] He J., Hong S., Zhang L., Gan F., Ho Y., 2010, ***Equilibrium and Thermodynamic Parameters of Adsorption of Methylene Blue onto Rectorite***, **Fresenius Environmental Bulletin**, Vol. 19: 2651-2656.

[170] Zainal IG, 2010, ***Biosorption of Cr(VI) from aqueous solution using new adsorbent: equilibrium and thermodynamic study***. **E J Chem** 7: S488–S494.

[171] Dada A., Olalekan A., Olatunya A., Dada O., 2012, ***Langmuir, Freundlich, Temkin and Dubinin – Radushkevich Isotherms Studies of Equilibrium Sorption of Zn+2 unto phosphoric acid modified Rice Husk***, **IOSR Journal of Applied Chemistry**, Vol. 3 (1): 38-45.

[172] A.S. Mestre, J. Pires, J.M.F. Nogueira, A.P. Carvalho, 2007, ***Activated carbons for the adsorption of ibuprofen***, **Carbon** 45 1979–1988.

[173] Vimonses V., Lei S.M, Jin B., Chow C.W.K, Saint C., 2009, ***Adsorption of congo Red by three Australian kaolins***, **Applied Clay Science**. Vol.43 (3–4): 465–472.

[174] S. Álvarez-Torrellas, A. Rodríguez, G. Ovejero, J. García, 2016, ***Comparative adsorption performance of ibuprofen and tetracycline from aqueous solution by carbonaceous materials***, **Chemical Engineering Journal** 283 936–947.

[175] Ana S.Mestre, JoãoPires, José M.F.Nogueira, Jose B.Parra, Ana P.Carvalho, Conchi O.Ania, 2009, ***Waste-derived activated carbons for removal of ibuprofen from solution: Role of surface chemistry and pore structure,*** **Bioresource Technology**, Volume 100, Issue 5, Pages 1720-1726.

[176] Ruhul Amin Reza, M. Ahmaruzzaman, Asim K. Sil and Vinod Kumar Gupta, 2014, ***Comparative Adsorption Behavior of Ibuprofen and Clofibric Acid onto Microwave Assisted Activated Bamboo Waste***, **Ind. Eng. Chem. Res.** 53, 9331−9339.

[177] Hanen Guedidi, Laurence Reinert, Yasushi Soneda, Nizar Bellakhal, Laurent Duclaux, 2017, ***Adsorption of ibuprofen from aqueous solution on chemically surface-modified activated carbon cloths***, **Arabian Journal of Chemistry** 10, S3584–S3594.

[178] Jun Wang, Haibo Li, Chendong Shuang, Aimin Li, Cheng Wang, Yu Huang, 2015, ***Effect of pore structure on adsorption behavior of ibuprofen by magnetic anion exchange resins***, **Microporous and Mesoporous Materials** 210 94-100.

[179] Qi Tao, Zhaoyi Xu, Jiahong Wang, Fengling Liu, Haiqing Wan, Shourong Zheng, 2010, ***Adsorption of humic acid to aminopropyl***

functionalized SBA-15, **Microporous and Mesoporous Materials**, Volume 131, Issues 1–3, Pages 177-185.

[180] Ayla Özer, Gönül Akkaya, Meral Turabik, 2005, ***The biosorption of Acid Red 337 and Acid Blue 324 on Enteromorpha prolifera: The application of nonlinear regression analysis to dye biosorption***, **Chemical Engineering Journal**, Volume 112, Issues 1–3, Pages 181-190.

[181] Ferraria L., Kaufmam J., Winnefeld F., Plank J., 2010, ***Interaction of cement model systems with superplasticizers investigated by atomic force microscopy, zeta potential, and adsorption measurements***, **Journal of Colloid and Interface Science**, Vol. 347 (1): 15–24.

[182] Sandip Mondal, Kiran Bobde, Kaustav Aikat, Gopinath Halder, 2016, ***Biosorptive uptake of ibuprofen by steam activated biochar derived from mung bean husk: Equilibrium, kinetics, thermodynamics, modeling and eco-toxicological studies***, **Journal of Environmental Management** 182 581-594.

[183] Ying Yu a, Yuan-Yi Zhuang, Zhong-Hua Wang, Ming-Qiang Qiu, 2004, ***Adsorption of water-soluble dyes onto modified resin***, **Chemosphere** 54 425–430.

جامعة النجاح الوطنية

كلية الدراسات العليا

استخلاص متبقيات الأدوية من المحاليل المائية باستخدام ثلاثة أنواع من الممتزات

إعداد

ياسمين أكرم خالد ظاهر

إشراف

أ.د. شحدة جودة

د. عثمان حامد

قدمت هذه الأطروحة استكمالاً لمتطلبات درجة الماجستير في الكيمياء بكلية الدراسات العليا في جامعة النجاح الوطنية في نابلس، فلسطين.

2018

استخلاص متبقيات الأدوية من المحاليل المائية باستخدام ثلاثة انواع من الممتزات

إعداد

ياسمين أكرم خالد ظاهر

إشراف

أ.د. شحدة جودة

د.عثمان حامد

الملخص

استخدم ثلاث أنواع مختلفة من المبلمرات في استخراج الايبوبروفين (IBP) من المحاليل المائية، السليلوز حيث تم تحويله إلى نانو سليلوز (CNC).وCNC المصنع تم تحويله إلى نانوسليلوز المغناطيسي (MCNC) والى نانو سليلوز الفضة. أما المبلمرات الأخرى فهي مادتي الكارجينان وبيتا-سايكلودكسترين CRG and β-CD ، حيث تم تحويل ال β-CD إلى Acetyl β-CDو أيضا Benzoyl β-CD وتم المقارنة بينهما. وقد تم تشخيص النانو سيليولوز وβ-CD المصنعة عن طريق FTIR. تم حساب قدرة المبلمرات المصنعة على استخراج الايبوبروفين (IBP) من الماء ومقارنته مع بعضها. أظهرت المبلمرات كفاءة استخلاص ممتازة نحو IBP فيما اظهر ال Acetyl β-CD ميل مقبول لاستخلاصه. تم رصد خمسة متغيرات وتقييمها أثناء عملية الاستخراج: الوقت، والpH، ودرجة الحرارة، والجرعة، والتركيز. تم دراسة الديناميكا الحرارية لادمصاص المواد جميعها، كل منهم يتبعLangmuir isothermوpseudo –second– order. وكشفت الدراسات الحرارية الطابع التلقائي للادمصاص في درجات حرارة مختلفة.